

**CYTOCHROME C PURIFICATION WITH SURFACE
IMPRINTED BACTERIAL CELLULOSE NANOFIBERS**

**YÜZEY BASKILANMIŞ BAKTERİYEL SELÜLOZ
NANOFİBERLER İLE SİTOKROM C SAFLAŞTIRILMASI**

EMEL TAMAHKAR IRMAK

PROF. DR. ADİL DENİZLİ

Supervisor

Submitted to Graduate School of Science and Engineering of Hacettepe University
as a Partial Fulfillment to the Requirements
for the Award of the Degree of Doctor of Philosophy
In Bioengineering

2014

This work named '**Cytochrome c Purification with Surface Imprinted Bacterial Celulose Nanofibers**' by EMEL TAMAHKAR IRMAK has been approved as a thesis for the Degree of **DOCTOR OF PHILOSOPHY IN BIOENGINEERING** by the below mentioned Examining Committee Members.

Prof. Dr. Adil DENİZLİ
Head and Supervisor



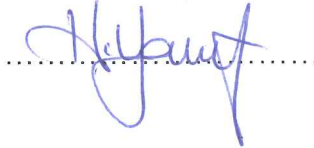
Prof. Dr. Serap ŞENEL
Member



Prof. Dr. F. Sema BEKTAŞ
Member



Prof. Dr. Handan YAVUZ ALAGÖZ
Member



Assist. Prof. Dr. Fatma YILMAZ
Member



This thesis has been approved as a thesis for the Degree of **DOCTOR OF PHILOSOPHY IN BIOENGINEERING** by Board of Directors of the Institute for Graduate Studies in Science and Engineering.

Prof. Dr. Fatma SEVİN DÜZ
Graduate School of Science and
Engineering

ETHICS

In this thesis study, prepared in accordance with the spelling rules of Graduate School of Science and Engineering of Hacettepe University,

I declare that

- all the information and documents have been obtained in the base of the academic rules
- all audio-visual and written information and results have been presented according to the rules of scientific ethics
- in case of using other works, related studies have been cited in accordance with the scientific standards
- all cited studies have been fully referenced
- I did not do any distortion in the data set
- and any part of this thesis has not been presented as another thesis study at this or any other university.

19/12/2014



EMEL TAMAHKAR IRMAK

ÖZET

YÜZEY BASKILANMIŞ BAKTERİYEL SELÜLOZ NANOFİBERLER İLE SİTOKROM C SAFLAŞTIRILMASI

Emel TAMAHKAR IRMAK

Doktora, Biyomühendislik Anabilim Dalı

Tez Danışmanı: Prof. Dr. Adil DENİZLİ

İkinci Tez Danışmanı: Prof. Dr. Tülin KUTSAL

Aralık 2014, 93 sayfa

Bu çalışmada, sitkrom c saflaştırma ve tanıma işlemleri için yüzey baskılama yöntemi ile sitokrom c baskılanmış bakteriyel selüloz (Cyt c-MIP) nanofiberler hazırlanmıştır. N-metakriloil L-histidin metil ester (MAH) monomeri spesifik tanıma bölgeleri oluşturmak için sentezlenmiştir. MAH monomeri ile bakır (II) iyonu arasında kompleks oluşumundan sonra metal iyon koordinasyon etkileşimleri kullanılarak MAH-Cu(II) monomeri ve sitokrom c hedef molekülleri ile önkomples hazırlanmıştır. Cyt c-MIP nanofiberler farklı % toplam monomer oranlarında, farklı monomer/hedef molekül molar oranlarında ve farklı polimerizasyon sürelerinde hazırlanmıştır. Cyt c-MIP nanofiberler ATR-FTIR, SEM ve temas açısı ölçümleri ile karakterize edilmiştir. Adsorplanan protein moleküllerinin polimer yapıdan desorpsiyonu için 1 M NaCl çözeltisi kullanılmıştır. Adsorpsiyon çalışmaları pH, sıcaklık ve iyonik şiddete göre gerçekleştirilmiştir ve adsorpsiyon kapasitesi spektrofotometrik olarak analiz edilmiştir. Uygun denge izotermi Langmuir izotermi olarak belirlenmiştir. Bu sistem için hız sınırlayıcı basamağın kimyasal reaksiyon olmasından dolayı yalancı-ikinci derece kinetik modelin bu sisteme daha uygun olduğu belirlenmiştir. Cyt c-MIP nanofiberlerin seçiciliğinin değerlendirilmesi için hedef moleküle benzer yapıda olan sığır serum albumin, hemoglobin, miyoglobin

ve lizozim kullanılmıştır. Metal iyon koordinasyonu etkileşimlerinin spesifik bağlanma bölgeleri hazırlanmasında katkısının olduğu tespit edilmiştir. Bu sonuçlar hedef proteini baskılama işleminin yüksek adsorpsiyon kapasitesi ile başarılı bir şekilde gerçekleştiğini göstermiştir. Cyt c-MIP nanofiberlerin bağlanma özellikleri ayrıca QCM sensör çalışmaları ile de değerlendirilmiştir. Bu kapsamda QCM nanosensörler Cyt c-MIP nanofiberler ile hazırlanmış ve kinetik ve seçicilik çalışmalarında kullanılmıştır. Bu nanosensörler AFM ile karakterize edilmiştir. Bağlanma özelliklerinin belirlenmesi için kinetik ve bağlanma sabiti Scatchard, Langmuir, Freundlich ve Langmuir-Freundlich izotermi ile hesaplanmıştır. Elde edilen sonuçlar kesikli sistemde bağlanma çalışmalarının sonuçları ile örtüşmektedir.

Anahtar kelimeler: Moleküler baskılanmış polimerler, yüzey baskılama, metal-iyon koordinasyonu, protein tanıma, bakteriyel selüloz nanofiberler.

ABSTRACT

CYTOCHROME C PURIFICATION WITH SURFACE IMPRINTED BACTERIAL CELLULOSE NANOFIBERS

Emel TAMAHKAR IRMAK

Doctor of Philosophy, Bioengineering Division

Supervisor: Prof. Dr. Adil DENİZLİ

Co-supervisor: Prof. Dr. Tülin KUTSAL

December 2014, 93 pages

In the present study, cytochrome c imprinted bacterial cellulose (Cyt c-MIP) nanofibers were prepared for the purification and recognition of cytochrome c via surface imprinting approach. N-methacryloyl-L-histidine methyl ester (MAH) was synthesized to create specific binding sites. After the complexation between MAH and chelating metal ion copper(II), the preorganized complex was prepared with MAH-Cu(II) monomer and Cyt c template molecules via metal ion coordination interactions. Cyt c-MIP nanofibers were prepared in the presence of different amounts of %w total monomer, monomer/template ratio and polymerization time. Cyt c-MIP nanofibers were characterized by ATR-FTIR, SEM and contact angle measurements. In order to desorb the adsorbed proteins from the polymer network, 1 M NaCl solution was used. Adsorption studies were performed with respect to pH, temperature and ionic strength and the adsorption capacity was evaluated spectrophotometrically. The suitable equilibrium isotherm was determined as Langmuir isotherm. It was determined that pseudo-second order kinetic model was more suitable to this system referring chemical reaction as a rate limiting step. To evaluate the selectivity of the Cyt c-MIP nanofibers, similar proteins were utilized as non-template proteins, which were bovine serum albumin,

hemoglobin, myoglobin and lysozyme. The metal ion coordination interactions were found to contribute for the fabrication of specific recognition binding sites. The results present the successful imprinting of the template protein with high adsorption capacity. The binding properties of Cyt c-MIP nanofibers were also evaluated with QCM sensor studies. In this context QCM nanosensors were prepared with Cyt c-MIP nanofibers and used for further kinetic and selectivity studies. These nanosensors were characterized by AFM. In order to determine the binding characteristics, kinetic and binding constant were calculated with Scathard, Langmuir, Freundlich and Langmuir-Freundlich isotherms. The results were conformable with the results of batch rebinding studies.

Key words: Molecular imprinted polymers, surface imprinting, metal-ion coordination, protein recognition, bacterial cellulose nanofibers.

ACKNOWLEDGEMENTS

This thesis could not be finished without the help and support of many people who are gratefully acknowledged here. At the very first, I would like to express my deepest gratitude to my supervisor Prof. Dr. Adil Denizli for his patience, encouragement, support and supervision throughout my studies. I am gratefully indebted to him for many valuable discussions that helped me understand my research area better.

I am also gratefully indebted to my co-supervisor Prof. Dr. Tülin Kutsal for encouragement, support and guidance.

I would like to thank to my committee members, Prof. Dr. Serap Şenel, Prof. Dr. F. Sema Bektaş, Prof. Dr. Handan Yavuz Alagöz and Dr. Fatma Yılmaz for their contribution and comments for my thesis.

A special thanks to Gülsu for the discussions, suggestions, her time and especially her friendship. In particular, I would like to thank to Müge and Işık for their help and support. Thanks to all my lab mates, Canan, Seda, Kemal, Fatma, Sevgi, Gizem, Mine, Çiğdem, Dilara, Yeşeren, Monir, Erdoğan, Emin, Aykut, Erkut, Recep, Esmâ, Nilay, Gözde, Ali, Bahar, Iğım, Duygu, Semra, Sabina and Deniz, for their friendship, help and providing nice working environment.

I would like to thank to Prof. Dr. Karsten Haupt for giving me an opportunity to work in his laboratory and for the warm hospitality during my stay in Compiègne. Thanks go to Serena Ambrosini for the contributions in my view of the academic life.

I would like to express my warm thanks to my dear friends Bengi and Eda for their helpful advises, optimistic comments and particularly their friendship.

My greatest thanks go to my family, to my dear mother Fatma and father Ertuğrul who always loved, encouraged and supported me.

Finally, I would like to thank to my dear sister Ebru and my dear husband Sercan for their endless love, understanding and helping me get through the difficult times. To them I dedicated this thesis.

CONTENTS

	<u>Page</u>
ÖZET	i
ABSTRACT	iii
ACKNOWLEDGEMENTS	v
CONTENTS.....	vi
FIGURES	viii
TABLES.....	xi
SYMBOLS AND ABBREVIATIONS	xii
1. INTRODUCTION	1
2. GENERAL INFORMATION	4
2.1. Molecular Imprinting Process	4
2.1. 1. Factors Affecting The Molecular Imprinting Process.....	5
2.1. 2. Template	5
2.1. 3. Functional Monomer.....	5
2.1. 4. Cross-linker	6
2.1. 5. Initiation Method and Temperature	6
2.1. 6. Polymerization Time.....	6
2.1. 7. Solvent	7
2. 1. Types of Molecular Imprinting	7
2.2. 1. Covalent Imprinting	7
2.2. 2. Non-covalent Imprinting	8
2.2. 3. Metal Ion Mediated Molecular Imprinting	8
2. 2. Protein Imprinting	14
2.3. 1. Bulk Imprinting.....	15
2.3. 2. Surface Imprinting	16
2. 3. Affinity Nanofiber Membranes for Protein Recognition	17
2. 4. Bacterial Cellulose.....	25
2. 5. Cytochrome c	27
2. 6. QCM Sensors.....	29
3. EXPERIMENTAL METHOD	32
3. 1. Materials.....	32
3. 2. Preparation of Cyt c-MIP Nanofibers.....	32
3.2. 1. Production of Bacterial Cellulose Nanofibers	32
3.2. 2. Synthesis of N-methacryloyl L-histidine methylester (MAH)	33
3.2. 3. Synthesis of MAH-Cu(II) Metal-chelate Monomer.....	33
3.2. 4. Preorganization of MAH-Cu(II) Monomer with Cyt c	33
3.2. 5. Preparation of Cyt c-MIP Nanofibers.....	34
3. 3. Batch Adsorption Studies	35
3.3. 1. Rebinding Experiments	35
3.3. 2. Selectivity Studies	35
3. 4. Fabrication of QCM Nanosensors	36
3.4. 1. Surface Characterization of QCM Nanosensors	37
3.4. 2. Kinetic Studies with QCM Nanosensors.....	37
3.4. 3. Selectivity Studies of QCM Nanosensors.....	37

4. RESULTS AND DISCUSSION	38
4. 1. Preparation of Surface Imprinted MIP Nanofibers.....	38
4.1.1. Synthesis of MAH-Cu(II) Complex	38
4.1.2. Characterization of Cyt c-MIP nanofibers.....	39
4. 2. Study of Conditions of Polymerization.....	42
4.2. 1. Effect of Monomer/Template Ratio.....	43
4.2. 2. Effect of Total Monomer Ratio.....	44
4.2. 3. Effect of Polymerization Time.....	45
4. 3. Rebinding studies.....	46
4.3. 1. Effect of pH.....	46
4.3. 2. Effect of Temperature.....	47
4.3. 3. Effect of NaCl Concentration.....	48
4. 4. Binding Isotherms.....	49
4. 5. Binding Kinetics.....	53
4. 6. Thermodynamic Analyses	58
4. 7. Selectivity Studies	59
4. 8. QCM Studies	61
4.8. 1. Surface Morphology of QCM nanosensor	62
4.8. 2. Kinetic Studies with Cyt c-MIP QCM nanosensor	63
4.8. 3. Mathematical analysis of Cyt c-MIP QCM sensor data	65
4.8. 4. Equilibrium isotherm models	66
4.8. 5. Selectivity studies.....	68
4.8. 6. Reproducibility.....	70
5. CONCLUSION.....	71
REFERENCES.....	75
APPENDIX.....	89
CURRICULUM VITAE.....	92

FIGURES

Figure 2. 1. Representation of molecular imprinting process.....	5
Figure 2.2. The schematic representation of complexation of TC/Fe ²⁺ /MAA.	9
Figure 2.3. The binding interactions of MIP via a.) H-bonding and b.) Metal ion coordination.....	10
Figure 2.4. Metal coordination between metal ion (Me) and a.) TED and b.) IDA.	11
Figure 2.5. Schematic representation of binding of various bis(imidazole) molecules..	12
Figure 2.6. The schematic presentation of protein imprinting process with metal ion coordination.....	13
Figure 2.7. The representation of MAH-Cu(II)-L-histidine formation.	14
Figure 2.8. Schematic representation of preparation of surface imprinted nanowires.	16
Figure 2.9. Schematic representation of preparation of surface imprinted silica nanoparticles.	17
Figure 2.10. Mass transfer mechanisms through bead (A) and membrane (B)	19
Figure 2.11. Schematic presentation of accessible binding sites of bulk and nanosized MIPs.....	19
Figure 2.12. SEM images of nanofibers having different morphologies. Beaded (a), non-porous (b), core-shell (c), porous (d).....	20
Figure 2.13. SEM images of PVA-PE nanofibers (A), Cibacron Blue F3GA-attached PVA-PE nanofibers.....	22
Figure 2.14. Schematic representation of preparation of electrospun MIP nanofibers using electrospinning equipments.	23
Figure 2.15. SEM images of polypyrrole nanowires.	23
Figure 2.16. Schematic presentation of preparation strategy of MIP nanotube membrane.	24
Figure 2.17. Schematic presentation of fabrication of MIP-PDA nanowires.....	25
Figure 2.18. Schematic presentation of MIP-NPs on the SEM image of PET nanofibers.....	25
Figure 2.19. TEM image of bacterial cellulose ribbon produced by the bacteria...	26
Figure 2.20. SEM image of bacterial cellulose network containing bacteria cells..	26
Figure 2.21. Chemical structure of cellulose.	27

Figure 2.22. Schematic representation of QCM sensor chip.....	30
Figure 2.23. Schematic view of the experimental setup for humidity sensor of QCM with BC nanofibers.	31
Figure 3. 1. Schematic presentation of preparation strategy of Cyt c-MIP QCM nanosensors.....	36
Figure 4. 1. UV-vis spectra of MAH and MAH-Cu(II) complexes.	39
Figure 4. 2. ATR-FTIR spectrum of MAH monomer.....	40
Figure 4. 3. ATR-FTIR spectrum of BC.....	40
Figure 4. 4. ATR-FTIR spectrum of Cyt c-MIP nanofibers.	41
Figure 4. 5. SEM image of Cyt c-MIP nanofibers.....	42
Figure 4. 6. Contact angle measurement of Cyt c-MIP nanofiber.	42
Figure 4. 7. Adsorption capacities of the MIP nanofibers with different monomer/template ratio.	44
Figure 4. 8. Adsorption capacities of MIP nanofibers with different weight ratio of total monomer..	45
Figure 4. 9. Adsorption capacities of MIP nanofibers with different polymerization time.....	46
Figure 4. 10. Effect of pH of adsorption solution on adsorption capacity of MIP nanofibers.....	47
Figure 4. 11. Effect of temperature of adsorption solution on adsorption capacity of MIP nanofibers.	48
Figure 4. 12. Effect of NaCl concentration on adsorption capacity of MIP nanofibers.....	49
Figure 4. 13. Effect of equilibrium concentration Cyt c on adsorption capacity of MIP nanofibers.	50
Figure 4. 14. Langmuir isotherm of MIP nanofibers.	51
Figure 4. 15. Freundlich isotherm of MIP nanofibers.	51
Figure 4. 16. Binding kinetics of MIP nanofibers.....	54
Figure 4. 17. First-order kinetics of adsorption of MIP and NIP nanofibers.....	56
Figure 4. 18. Second-order kinetics of adsorption of MIP and NIP nanofibers.	56
Figure 4. 19. Intraparticle diffusion kinetic model of MIP and NIP nanofibers.....	57
Figure 4. 20. Effect of metal ion coordination and molecular imprinting process on adsorption capacity of Cyt c.	60

Figure 4. 21. The adsorption capacity of cyt c and competing proteins on Cyt c-MIP nanofibers.	61
Figure 4. 22. AFM images of MIP nanofiber QCM chip.....	62
Figure 4. 23. Dynamic response of Cyt c-MIP nanofibers QCM sensors with respect to frequency change.	63
Figure 4. 24. Dynamic response of Cyt c-MIP nanofibers QCM sensors with respect to mass change.	64
Figure 4. 25. The relation between mass shift and cytochrome c concentration...	64
Figure 4. 26. Determination of equilibrium analysis (Scatchard).....	66
Figure 4. 27. Langmuir adsorption model.....	67
Figure 4. 28. Freundlich adsorption isotherm.....	68
Figure 4. 29. Langmuir-Freundlich adsorption isotherm.....	68
Figure 4. 30. Selectivity of Cyt c-MIP QCM sensors.	69
Figure 4.29. Reproducibility of Cyt c-MIP QCM sensors.....	70

TABLES

Table 4. 1. Langmuir and Freundlich parameters of MIP nanofibers	52
Table 4. 2. Comparison of Cyt c adsorption capacities of different adsorbents with MIP nanofibers prepared in this study	52
Table 4. 3. Constants for first and second order kinetic and intraparticle diffusion kinetic model of adsorption of MIP and NIP nanofibers	57
Table 4. 4. Thermodynamic parameters of MIP nanofibers	58
Table 4. 6. Kinetic parameters.	65
Table 4. 7. The equilibrium isotherms	66
Table 4. 8. The parameters of equilibrium isotherms.	67
Table 4. 9. Selectivity of Cyt c-MIP QCM nanosensors to Cyt c and non-template proteins.....	70

SYMBOLS AND ABBREVIATIONS

Symbols

Q Adsorption capacity

Abbreviation

MIP	Molecularly Imprinted Polymer
Cyt c	Cytochrome c
MAH	N-Methacryloyl-L-Histidine Methyl Ester
MAH-Cu(II)	The complex of MAH monomer and cooper(II) ion
MAH-Cu(II)-Cyt c	The complex of MAH monomer, copper(II) ion and Cyt c
Cyt c-MIP	Cytochrome c Imprinted Bacterial Cellulose Nanofibers
UV-Vis	Ultraviolet-Visible Spectroscopy
SEM	Scanning Electron Microscopy
AFM	Atomic Force Microscopy
QCM	Quartz Crystal Microbalance
Cyt c MIP QCM	Cytochrome c Imprinted Quartz Crystal Microbalance Sensor

1. INTRODUCTION

Purification, separation and isolation of proteins are necessary for further developments of bioscience and biotechnology. The purification of proteins is crucial since they possess therapeutic value for diagnosis and treatment. The development of production processes of highly specific materials available to capture proteins requires rapid development of purification systems [1]. There is a growing interest in the development of purification processes to obtain materials with high specificity and capacity. In addition the purification process should be easy-to-apply and cost effective [2].

Molecular recognition refers to the affinity between two or more molecules via various types of interactions. Molecular imprinting is a promising alternative to create highly selective binding sites through polymeric materials via molecular recognition [3]. There are many molecular imprinted polymers (MIPs), which show unique characteristics of this method targeting various types of molecules [4]. The molecule of interest namely a template molecule is surrounded by functional monomers and cross-linkers via covalent, non-covalent or metal ion coordination interactions. After the polymerization takes place, the template molecule is removed from this polymeric structure leaving a specific binding cavity. Surface imprinting is a widely used approach to improve the performance of MIPs by solving the problems of mass transfer limitations and removal of template molecules generally related with traditional molecular imprinting technique [5]. This method is especially significant for imprinting of macromolecules like proteins since mass transfer limitations for these large molecules is an important factor. The creation of thin films onto solid supports is one of the common approaches of surface imprinting method. This strategy enhances rebinding kinetics significantly because of the easy transportation of molecules through the binding sites on the or near the surface of the material. Other important advantage of this method is simple removal of target molecules leaving a large amount of recognition sites onto the solid support. These features are especially significant for macromolecules like proteins. The purification of proteins using this type of materials which have thin films created onto the solid support is feasible regarding to important features explained above [6], [7], [8], [9]. Molecular imprinting via metal ion coordination provides high selectivity and stability. In this context metal ions play a role as a

mediator between template protein and monomer contributing the well-defined orientation of this complex. The utilization of metal ion coordination during molecular imprinting favors the preparation of polymerization process in aqueous environment [10].

Protein purification is generally performed with traditional chromatography, which is packed with beads. In order to avoid the drawbacks of packed beds such as high pressure loss and mass transfer limitations, nanofiber membranes bearing high surface area are powerful alternatives. Nanofibers are typically prepared via electrospinning technology and used in many application areas. Bacterial cellulose (BC) is a biocompatible, thermal and chemically stable material, which is produced by *A. xylinum* bacteria with the presence of only carbon source [11]. Also it is prepared easily without requiring any special device. BC has high purity when synthesized and it does not need any further purification steps after the removal of bacteria cells from the membrane [12].

Cytochrome c is an essential protein for the transportation of electron in respiratory chain of the cell. It is a small and highly stable protein. In recent years, its role in apoptosis process was investigated and it was reported as a therapeutic protein.

In this thesis, surface imprinted cytochrome c nanofibers were prepared onto the surface of bacterial cellulose nanofibers via metal coordination interactions (Cyt c-MIP nanofibers) and used for efficient separation cytochrome c molecules from aqueous solutions. Firstly, N-methacryloyl-L-histidine methylester (MAH) as a metal chelate monomer was synthesized by reaction of methacryloyl chloride and histidine. Then it was preorganized with copper ions to obtain metal chelate monomer, MAH-Cu(II). The ternary complex was prepared with the addition of Cyt c molecules bearing one surface histidine to this MAH-Cu(II) complex and allowed to interact to form stable structure. After polymerization with cross-linker, template molecules were extracted from polymeric structure. The characterization of Cyt c-MIP nanofibers was performed with ATR-FTIR, SEM and contact angle measurements. To determine the optimum conditions of polymerization process, the effects of monomer/template ratio, total monomer ratio and polymerization time were investigated. The adsorption properties of Cyt c-MIP nanofibers were evaluated at different experimental conditions in batch wise system from aqueous solutions. The desorption was achieved with 1 M NaCl solution The suitable

binding equilibrium isotherm was determined as Langmiur isotherm model. Selectivity properties of Cyt c-MIP nanofibers were investigated using bovine serum albumin, hemoglobin, myoglobin and lysozyme as non-template proteins. The binding characteristics of the surface imprinted nanofibers were also examined with QCM sensor studies. QCM nanosensors were prepared via casting Cyt c-MIP and NIP nanofibers onto the chip surface. The results obtained from QCM studies were in conformity with the results of batch rebinding studies.

2. GENERAL INFORMATION

Protein purification processes has been performed for more than 200 years with various kinds of processes such as precipitation, centrifugation, ion-exchange chromatography, affinity chromatography etc. [13]. The purification of proteins is an attractive field since most proteins have therapeutic value regarding to pharmaceutical industry. In order to purify the protein of interest from its mixture, which may contain several hundreds of other proteins, the recognition mechanism between protein and adsorbent material is necessary to develop. Molecular recognition based on lock and key model is a basic process found in nature. It bears affinity interactions between two or more molecules. Molecular imprinting is based on the molecular recognition process is a promising alternative for protein purification with high selectivity [14].

2.1. Molecular Imprinting Process

Molecular imprinting is a technology creating highly specific recognition sites into cross-linked polymer using template molecule as a target. The molecule of interest is allowed to interact with functional monomers either by covalent, non-covalent or metal ion coordination interactions. This template molecule(s)-monomer(s) complex is then preserved via polymerization to create a binding site recognizing the template molecule. After extraction of template molecule from the polymeric material, recognition cavity complementary to template molecule with both functionality and shape is formed (Figure 2.1) [15], [16]. The molecular imprinted polymers (MIPs) are resistant to elevated temperature and pressure, inert to chemicals, stable and cheap [17].

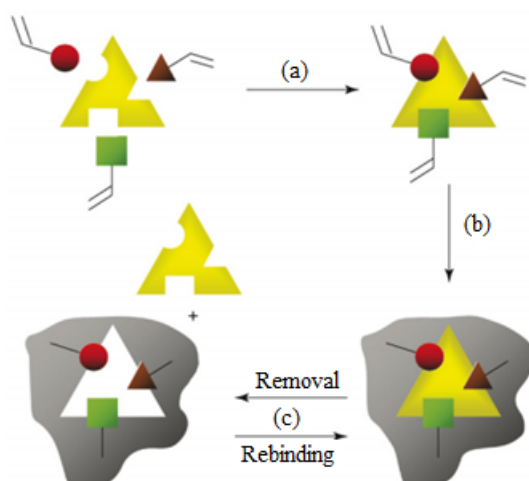


Figure 2. 1. Representation of molecular imprinting process. a.) Pre-polymerization complex of template and functional monomers (red, green and brown) via covalent, non-covalent and metal ion coordination interactions. b.) Polymerization process with cross-linkers. c.) Template (yellow) removal with extraction solvents to create specific binding sites complementary to template molecule Reprinted from ref. [18].

2.1. 1. Factors Affecting The Molecular Imprinting Process

The design of molecular imprinting is a big challenge since the structure depends on many variables such as chemical structure and amount of template, functional monomer, cross linker, solvent, initiator, method of initiation and temperature [19]. Binding characteristics, stability, selectivity and binding kinetics are governed by recognition cavity formed into polymeric structure. In order to obtain high recognition capacity with high selectivity, it is important to optimize these parameters that are explained below [20].

2.1. 2. Template

Molecular imprinting method is applied to various kinds of templates such as metal ions, antibiotics, drugs, sugars, amino acids, peptides, proteins and even cells [21], [22], [23], [24], [25]. The nature of the template will determine the choice of the functional monomers. In order to create a well-defined orientation between functional monomers and template molecule, target should contain functional groups able to interact with monomers. Also it should be stable in the course of polymerization process. In order to provide high selectivity, stability of template is essential to create high fidelity for recognition cavity resulting minimum change of conformational state after rebinding to binding site [26].

2.1. 3. Functional Monomer

Chemical structure of functional monomers is also an issue of major importance for efficient imprinting process since they should interact with template molecule in the right orientation to preserve conformational state of the target [27]. The most frequently used functional monomers are acrylic acid, methacrylic acid, trifluoromethacrylic acid, 4-vinylbenzoic acid, styrene, acrylamide and methyl

methacrylate. The ideal monomer for molecular imprinting is selected due to the strength and chemical structure of the interactions between monomer and template molecules [28].

2.1. 4. Cross-linker

The cross-linkers also serve important role for recognition capability of MIPs providing rigidity of polymer network that is necessary to stabilize the recognition sites [29]. The most common cross-linkers are ethylene glycol dimethacrylate, divinylbenzene, N,N-ethylenebismethacrylamide and trimethylolpropane trimethacrylate. Ideally cross-linkers should not interact with template molecules to avoid non-specific adsorption [30].

2.1. 5. Initiation Method and Temperature

The formation of free radicals is widely used technique for initiation of polymerization of MIP synthesis and usually carried out by thermally and photolytically. Azonitriles are commonly used initiators, which are decomposed by heat or UV light. The ideal initiator should control polymerization degree that is exothermic reaction. The MIPs prepared using photochemical or thermal initiation techniques was utilized for evaluation of enantioselectivity properties. It was found that photolytic method at low temperature achieved better enantioselectivity [31]. Monomer-template complexation is equilibrium-based reaction and depends on temperature. Temperature effect for chiral recognition was investigated using azobisnitriles as initiators with thermal and photolytic methods. It was reported that lower temperatures achieve better enantioseparation [32].

2.1. 6. Polymerization Time

Polymer morphology is directly depended on polymerization time. When it is long, polymer becomes more rigid in structure since prolonged polymerization period allows consuming all the polymerizable double bonds. This may provide defined binding cavities resulting higher selectivity properties. Also it may cause to obtain slow binding kinetics since transport properties of rigid materials are limited. On the other hand, when polymerization time is short, polymer structure becomes loose. It was shown that separation factor increases with increasing polymerization

time when the thermal and UV light source (0.016 W/cm^2) used as an initiation method [33], [34].

2.1. 7. Solvent

Polymer morphology and imprinting process is significantly affected by nature and amount of solvent used in the polymerization procedure. Solvent solubilizes the components of polymerization syrup and provides the stabilization of template-monomer complex, which is important step for imprinting process. Furthermore the porosity of the MIP prepared is strongly depended on solvent, which serves as a porogen. The utilization of appropriate solvent provides the fabrication of high specific surface area that is necessary for high adsorption capacity [35].

2. 1. Types of Molecular Imprinting

The driving forces required for the interaction between template and functional monomer are covalent bonds, non-covalent bonds and metal ion coordination [36]. Molecular imprinting methods prepared using these interactions are explained below.

2.2. 1. Covalent Imprinting

In this type of molecular imprinting procedure, template molecule is copolymerized with functional monomers. After polymerization, covalent bond is cleaved with chemicals leading a fixed cavity with well chemical orientation. The substantial advantage is to create exact-fit recognition sites reducing non-specific interactions and preventing leakage of template molecules because of the formation of stable covalent bonds. The major disadvantage is to use harsh chemicals to chemically cleave the template molecules resulting the possible damage to the imprinted sites [37]. Since cholesterol-imprinted polymers prepared via covalent imprinting method were found to have higher chromatographic separation efficiency of cholesterol than cholesterol-imprinted polymers prepared via non-covalent imprinting method resulting reduced peak broadening and tailing [38]. However covalent bonding gives strong interaction between template and monomer, it has slow rebinding kinetics that is an important issue for rapid separation and purification processes and low template removal.

2.2. 2. Non-covalent Imprinting

To synthesize MIPs via non-covalent imprinting approach, template and functional monomers were pre-organized before polymerization using secondary interactions such as H-bonding, van der Waals interactions and Coulomb forces. The major advantage of non-covalent imprinting is the ability to apply this method for large variety of template molecules. Also it is a direct, easy-to-apply and flexible method. The major disadvantages are the weak complexation of template and monomers and also the formation of heterogeneous binding sites when used excess of functional monomer [39]. Despite water is common solvent for molecular imprinting since many biomolecules have limited solubility in organic media; the recognition capacity is low due to weakness of hydrogen bonds. Also imprinting effect may be weakened in aqueous environment since polar solvents compete with hydrogen bonding interactions [40].

2.2. 3. Metal Ion Mediated Molecular Imprinting

Metal ion coordination with biological molecules is well suited to molecular recognition due to its specificity and stability. In metal ion coordination during imprinting process, metal chelating monomers are pre-organized to metal ion, generally a transition metal ion, which, in turn, coordinates the template molecule. Metal ions are employed as mediator that directs functional monomer and template molecule to establish a high fidelity of imprint with high specificity [41], [42], [43]. Metal ion coordination has higher strength with respect to hydrogen bonding which makes it more stable in water for example, binding energy of the complex of Cu^{2+} and imidazole residue of histidine is 4.8 kcal/mol and it is more than 1 kcal/mol for typical hydrogen bonding interaction [44]. Additionally metal ion coordination is a fast binding process and binding strength can be adjusted by choosing appropriate metal ion for a defined template molecule. Furthermore it is possible to replace the metal ion with another one to enhance the selectivity or use the MIP for different aim [45], [46], [47]. Therefore within this context, metal ion coordination approach has an important potential for preparation of highly specific MIPs in aqueous medium.

The most important step of the preparation of the MIP is the pre-arrangement of the functional monomer, metal ion and template molecule. This ternary complex is then polymerized with cross-linking agents initiated thermally or by UV light. After

polymerization the template molecule is easily removed with appropriate chemicals. In order to use this resultant material with other metal ions, it can be washed with complexing agents such as EDTA to remove all the metal content and then reload the other metal ion [48].

2.2.3. 1. Key Parameters for Metal Ion Coordination

The selection of metal ion is one of the most important parameter to create specific recognition. Template molecule dominates selection of the type of the metal ion used for imprinting process. The type of the metal ion defines binding strength of the template-metal ion-monomer complex and the spatial arrangement of this complexation. In order to obtain high specificity, coordination mode of the metal ion-monomer complex should be determined to guarantee the immobilization of the metal ions in the imprinted matrix. The molecularly imprinted polymers for extraction of tetracyclines -a large family of common antibiotics- from biological fluids was prepared in aqueous medium utilizing Fe^{2+} as mediator and methacrylic acid (MAA) as functional monomer (Figure 2.2) [49]. Different metal ions such as Mg^{2+} , Fe^{2+} and Cu^{2+} were complexed with tetracycline (TC) in the preparation of MIP. It was found that Fe^{2+} could obtain high recognition capacity due to specific coordination interaction between TC and MAA.

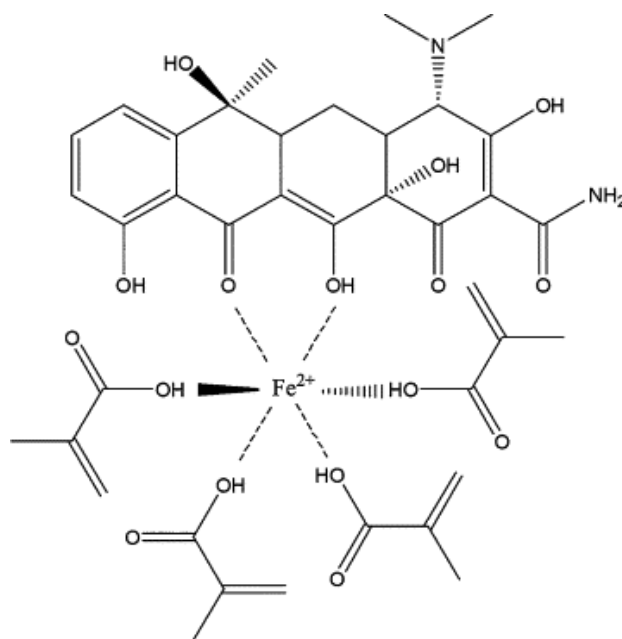


Figure 2.2. The schematic representation of complexation of TC/ Fe^{2+} /MAA. Reproduced from ref. [50].

As mentioned before, the self-assembling of template and monomers is the pre-polymerization step for the fabrication of MIP. Utilizing metal ion as mediator assembles a bridge between template and monomer through coordination bond. (S)-naproxen was complexed with 4-vinylpyridine through coordination with Co^{2+} and thus MIP with high selectivity was prepared [47]. Figure 2.3 shows the schematic presentation of this complex and further the binding of template and monomer via hydrogen bonding. It was shown that the absence of metal ion, which means in that case using hydrogen-bonding interactions, resulted reduced selectivity. The stoichiometry of the complex used was determined with UV spectrum by titrating monomer and template. The optimization of monomer amount is necessary for the design of MIPs. High amount of monomer results low adsorption capacity due to inefficient template removal and low amount of monomer causes incomplete organization of template and monomer. In the same manner, the amount of metal ion plays important role to enhance selectivity. In order to form highly specific recognition sites complementary to template, the stoichiometric amount of metal ion to bridge the specific interaction between template and monomer with high stability is necessary [51].

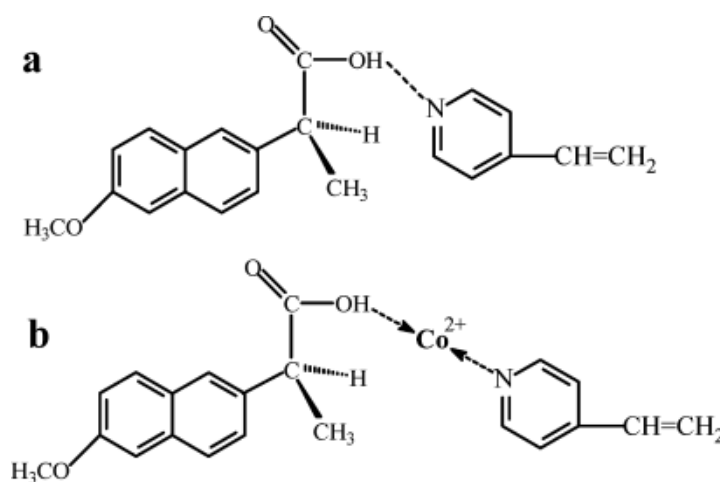


Figure 2.3. The binding interactions of MIP via a.) H-bonding and b.) Metal ion coordination. Reprinted from ref. [52].

The other parameter is the influence of anion used since it may participate in the recognition process. Molecularly imprinted solid phase microextraction fiber was developed to recognize thiabendazole (TBZ) - a kind of fungicide - via the metal coordination interaction. It was found that enrichment properties in aqueous solutions were improved with respect to hydrogen bonding interactions. Four

different copper salts as acetate, sulfate, nitrate and chloride were evaluated with respect to adsorption capacity and copper (II) acetate was found to have the highest adsorption capacity. This demonstrates the effects of anion to the recognition process since it changes the size and shape of the template-metal-monomer complex [53].

2.2.3. 2. Metal Ion Coordination for Bis-imidazole Recognition

Metal ion coordination with its specificity and stability is well-suited procedure for molecular recognition of biological molecules which is exemplified by the chromatographic method namely IMAC (Immobilized Metal Affinity Chromatography) [54]. It has been developed by Porath and protein purification was achieved via binding of electron donor groups on protein surface and metal ion immobilized on the support surface [55]. The amino and carboxyl groups of amino acid participate in the fabrication of metal-amino acid complex. Especially histidine containing peptides form stable complex with metal ions due to metal coordination between metal ion and imidazole side chain of amino acid. The common chelating ligands are iminodiacetic acid (IDA), nitrilotriacetic acid (NTA) and tris carboxymethyl ethylene-diamine (TED) and are shown below (Figure 2. 4).

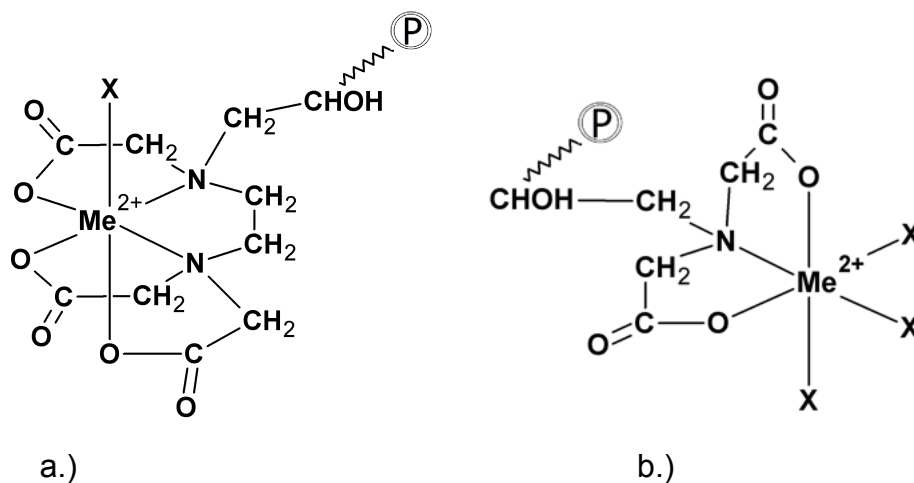


Figure 2.4. Metal coordination between metal ion (Me) and a.) TED and b.) IDA. Reproduced from ref. [56].

The complementarity between metal ion and template molecule forms specific assembly prior to polymerization. After polymerization when template is removed from polymer matrix, there exists a very specific binding cavity complementary to template due to this specific arrangement of functional groups around template

molecule. In order to prepare selective abiotic receptors for 1,4-Bis (imidazol-1-ylmethyl) benzene (2 in Figure 2.5) which is analog of surface histidine bearing proteins, metal chelating monomer Cu(II)-(N-(4-vinylbenzyl)-imino)diacetic acid was pre-organized with template molecule and then polymerized in the presence of cross linking agent [57]. The affinity for molecule 2 was higher than the analog molecules 4,4'-Bis(imidazol-1-ylmethyl) biphenyl (4) and 1-Imidazol-1-ylmethyl)-4-(pyrrol-1-ylmethyl) benzene (6) which contain single imidazole. This bigger affinity may be explained by two point binding mechanism of the template to MIP and it shows that the importance of templating is for distribution of metal ions through the polymer matrix.

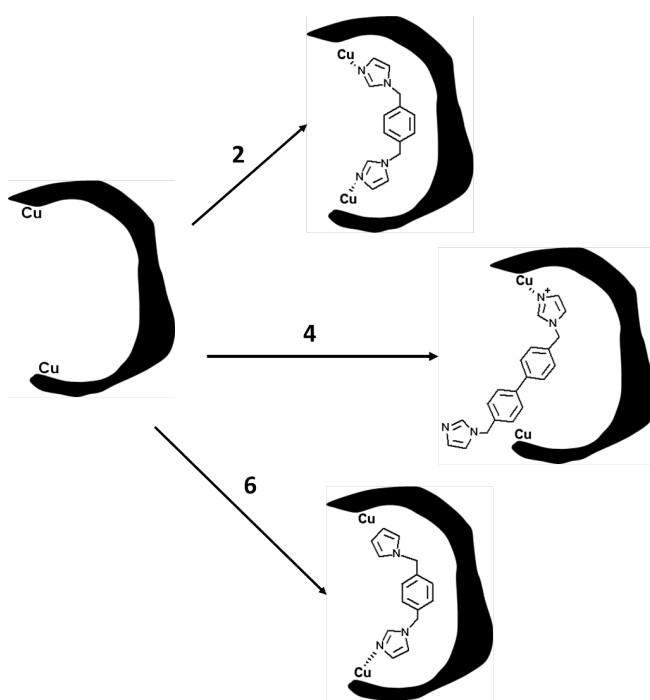


Figure 2.5. Schematic representation of binding of various bis(imidazole) molecules. Reproduced from ref. [58].

2.2.3. 3. Metal Ion Coordination for Amino Acid, Peptide and Protein Recognition

Amino acid imprinted polymers were prepared via metal ion coordination for chiral separation of various amino acids from aqueous solutions [40]. MIPs were prepared with the complex of Cu(II)-N-(4-vinylbenzyl)iminodiacetic acid as a metal chelate monomer and amino acid as a template in the presence of cross linkers. All the MIPs showed high enantioselectivity for the template and also it was

reported that enantioselectivity depends on both size and shape of the side chain of amino acid residue.

Hochuli et al. has been firstly developed a new quadridentate chelating ligand nitrilotriacetic acid (NTA) for protein purification via metal chelate chromatography [59]. It was reported that NTA forms more stable coordination interaction with both Cu(II) and Ni(II) than the interaction of IDA with each of these metals. NTA when complexed with Ni(II) occupies four positions in metal octahedral coordination sphere and leaving two for dipeptide His-Ala interaction [60]. It was achieved selective polymeric receptors to separate between peptide sequence via strong coordination NTA, Ni and His-Ala.

Kempe et al. was first developed metal mediated molecular imprinting procedure for protein imprinting [61]. Molecular imprinted polymers were prepared to recognize ribonuclease A (RNase A) through metal coordination utilizing N-(4-vinyl)-benzyl iminodiacetic acid (VBIDA) as the metal chelating monomer and copper ion as the mediator in the presence of the protein onto methacrylate-derivatized silica particles (Figure 2.6). There has been growing attention in metal mediated protein imprinted polymers [62], [63], [64], [65]. All these studies shows promising properties of metal coordination for the preparation of highly selective MIPs via stable and specific arrangement of metal ions with protein surface for protein separation and recognition.

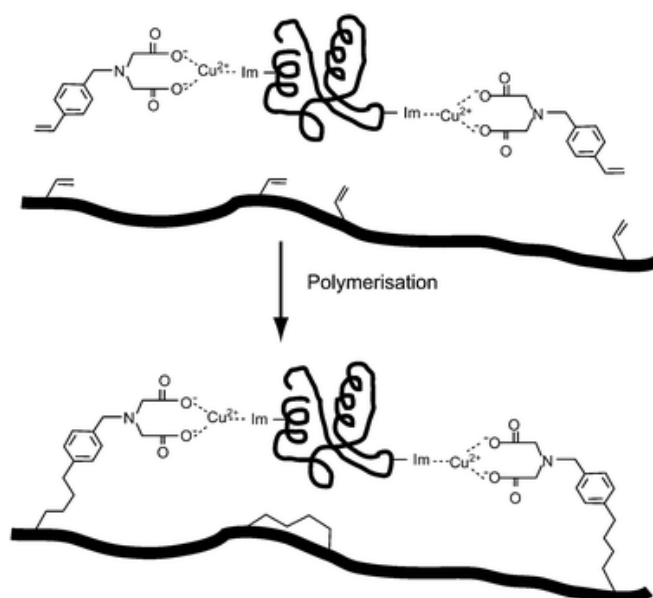


Figure 2.6. The schematic presentation of protein imprinting process with metal ion coordination. Reprinted from ref. [66].

A thermoresponsive macroporous hydrogel for lysozyme recognition was developed via molecular imprinting method based on metal ion coordination between protein and metal ion [62]. N-(4-vinyl)-benzyl iminodiacetic acid (VBIDA) as the metal chelate monomer was pre-organized with Cu(II) as the mediator and lysozyme as the template and then polymerized with N-isopropylacrylamide (NIPAAm) for thermoresponsiveness, acrylamide for mechanical strength and N,N-methylenebisacrylamide for cross-linking. The Lysozyme-MIP prepared via metal ion coordination between VBIDA, Cu(II) and lysozyme demonstrated higher protein recognition than Lysozyme-MIP prepared via electrostatic interactions obtained with pre-organization of VBIDA and protein. Also it was confirmed with selectivity tests that metal ion coordination was important for appropriate positioning of the binding groups around the template molecule.

L-histidine imprinted polymers were developed via metal coordination between Cu(II) as the mediator, L-histidine as the template and N-methacryoyl-(L)-histidine (MAH) as the metal chelating monomer for selective separation of cytochrome c (Cyt c) (Figure 2.7) [65]. The chromatographic separation of cytochrome c and ribonuclease A was also achieved.

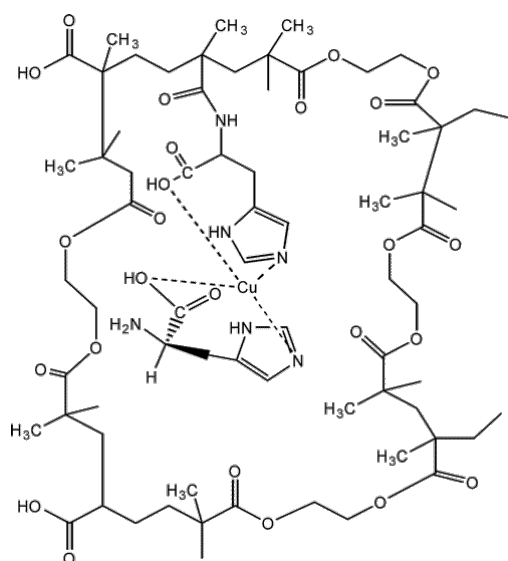


Figure 2.7. The representation of MAH-Cu(II)-L-histidine formation. Reprinted from ref. [67].

2. 2. Protein Imprinting

Specific molecular recognition, which is coordinated primarily by proteins, is the basic phenomenon that controls all the biological processes. The recognition of

proteins with high affinity and selectivity is a big challenge since natural biomacromolecular receptors are not stable for long-term processes and also require high costs. Thus production of artificial recognition elements, which mimic the natural counterparts with high selectivity and capacity, is a great demand requiring cost-effective, robust and reusable alternatives. Synthesis of molecularly imprinted polymers capable of selective recognition of proteins offers great potential providing low cost, easy to prepare and unique recognition properties [68].

There are some obstacles when imprinting proteins, which are largely absent when imprinting of small molecules and these are based on protein properties such as molecular size, complexity, conformational flexibility and solubility. Proteins have large molecular size resulting poor mass transport properties when binding through some MIP monolithic columns, which have dense polymeric structure [69]. Proteins have large number of functional groups over a large surface area. This complex structure should be considered when selecting appropriate functional monomers for protein imprinting process to avoid multiple weak interactions that favor non-specific binding. Also polymerization conditions may cause denaturation of proteins or may change the conformational states since proteins are flexible in nature [70]. Furthermore proteins are water-soluble compounds, which is not compatible with traditional MIP procedure since majority of molecular imprinting processes take place in organic media. The major strategies to synthesize MIPs for selective recognition of proteins are explained below.

2.3. 1. Bulk Imprinting

The principle of bulk imprinting of proteins is to recognize the shape via templating the protein into the polymeric matrix. There are different types of protein-imprinted matrices such as hydrogels, sol-gels, cryogels and monoliths that prepared via bulk imprinting [67], [71], [72], [73]. However bulk imprinting is simple and common method to prepare specific MIPs for protein recognition, the system has major limitation, which is poor accessibility of imprinted cavities. Since easy removal and fast rebinding of templates is the fundamental requirement of any system, the protein imprinting via bulk imprinting method is limited with the control of porosity and pore size of the matrices [5].

2.3. 2. Surface Imprinting

Since imprinted sites are located at the surface or close to the surface of the support material, surface imprinting presents an important alternative to bulk imprinting by improving the mass transfer properties and enhancing template removal of MIPs. The surface imprinted polymers let free access for biomacromolecules such as proteins to binding sites by using specific areas of proteins as a target [74].

One of the common methods to synthesize surface imprinted polymers has two steps; firstly the template is immobilized onto the solid support and lastly the support is dissolved after polymerization with monomers and cross-linkers. This method was used to prepare different types of materials such as nanowires [75] (Figure 2.8) and porous silica beads [76], [77].

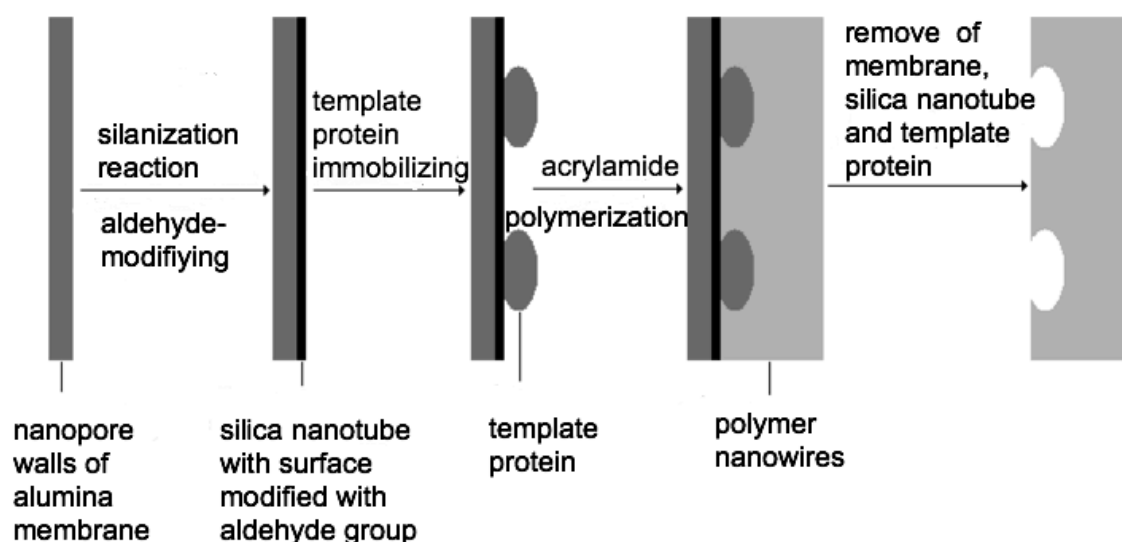


Figure 2.8. Schematic representation of preparation of surface imprinted nanowires. Reprinted from ref. [78].

Nanoporous alumina membrane was used to prepare protein-imprinted nanowires. Firstly alumina membrane surface was modified with aldehyde to immobilize the protein onto surface, then the pores of the membrane was filled with the polymerization medium containing AAm and MBAAm. After the polymerization in the nanopores, the alumina membrane was cleaved resulting protein binding sites on the surface. To show the universality of the procedure, bovine serum albumin,

bovine cytochrome c and horseradish peroxidase were used as template proteins. The surface imprinted nanowires demonstrated higher template protein recognition than the control nanowires for all of the template proteins used.

The other common approach for surface imprinting of proteins is the fabrication of thin films on the suitable substrates. Different types of supports were used such as polypyrrole and polystyrene for the preparation of sensing material and microplates respectively [79], [80]. The template protein is attached onto support material via covalent bonding [81] or self-assembly method [82]. The Lys imprinted matrix was prepared via self-assembly of protein molecules onto vinyl modified silica nanoparticles (Figure 2.9). Then highly dilute mixture of functional monomers and cross-linkers (0.4 w%) were polymerized over the template protein in order to create very thin recognition film onto the silica nanoparticles. To investigate the recognition property of these surface-imprinted silica nanoparticles competitive adsorption experiments containing the template protein (lysozyme) and the competitor protein (cytochrome c) were performed. It was found that MIP nanoparticles showed high selectivity for the template lysozyme against cytochrome c.

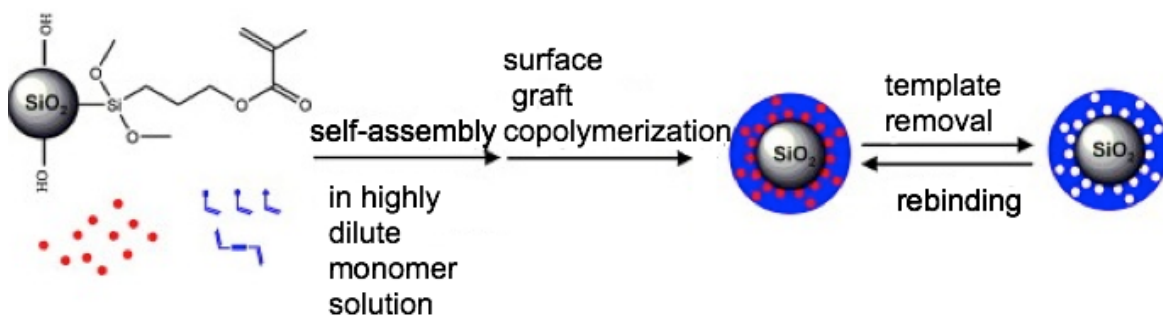


Figure 2.9. Schematic representation of preparation of surface imprinted silica nanoparticles. Reprinted from ref. [83].

2. 3. Affinity Nanofiber Membranes for Protein Recognition

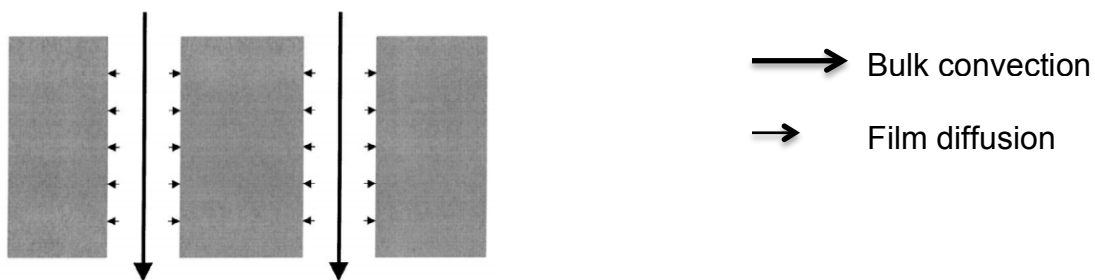
Protein purification is performed traditionally by using packed bed chromatography. However there are some limitations of this method such as high-pressure loss, long operation time and difficult scaling up since mass transfer of protein molecules is carried out with diffusion through the micro channels of

beads, which is packing material in the packed bed. Furthermore it may exist channeling caused by non-homogenous distribution of beads through the column resulting the decrement of column efficiency [84].

Porous membranes are powerful alternatives to avoid these technical limitations of the packed beds. The most important advantage of the membrane chromatography is convection of proteins through the binding sites. Pressure loss of membranes is significantly lower than that of packed beds. The binding is generally independent of feed flow rate resulting ability to work with high working flow rates. The other advantage is the ability to scale up. The interaction between the protein and the material is performed through the interconnected pores of the membranes as can be seen at Figure 2.10. The convection is dominant mass transfer process through pores of membranes since molecules are transferred via diffusion through dead-ended pores of beads. The diffusional resistance is avoided when used membranes and thus the only mass transfer resistance becomes the film diffusion on the surface of the membrane. Mass transfer limitations are significantly lowered since film diffusion is much more faster process than pore diffusion. Despite the membranes are thinner than beads, pressure losses are lowered with the help of interconnected pores of the membranes and thus working flow rates and efficiency will be increased.



A) Packed bed chromatography



B) Membrane chromatography

Figure 2.10. Mass transfer mechanisms through bead (A) and membrane (B)
 Reprinted from ref. [85].

The development of materials for purification and recognition of proteins with high capacity and selectivity becomes important issue for the economical and efficient purification of valuable products after the developments of production of biotherapeutics. In the lights of development of nanotechnology, preparation of molecularly imprinted polymers in nanoscale has been gaining more attention since these nanostructures show superior properties compared with conventional macrostructures [86], [87]. Recently the preparation of nanosized molecularly imprinted polymers and their application areas have been reviewed elsewhere [88], [89], [90]. Figure 2.11 demonstrates the distribution of effective recognition sites of nanosized MIPs comparing with conventional MIPs. Nanosized MIPs perform better site accessibility thus resulting fast binding kinetics and higher rebinding capacity than traditional MIPs since all the templates can be easily removed from the surface of the nanosized matrix leaving binding sites ready for target molecules [91].

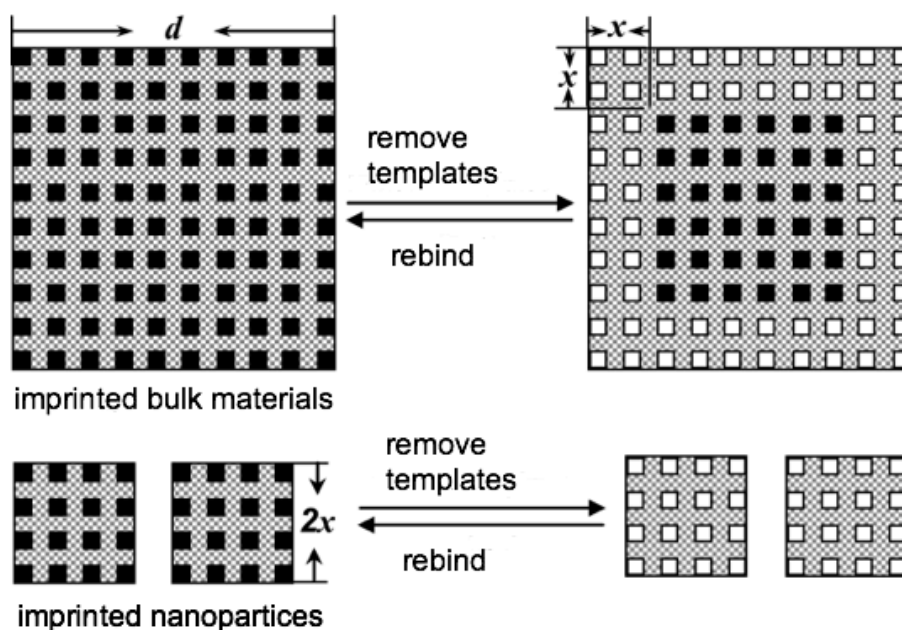


Figure 2.11. Schematic presentation of accessible binding sites of bulk and nanosized MIPs. Reprinted from ref. [78].

Affinity matrices are materials having specific recognition binding sites between ligand and target molecules. Despite membranes perform fast binding kinetics and low operation time; the adsorption capacity of membranes may be low. To overcome this issue affinity nanofibers draw attention as remarkable alternatives. Affinity nanofiber chromatography is a promising method for protein purification having both high efficiency of nanofibers and selectivity of chromatographic materials [92]. Nanofibers having high surface area/volume ratio show great potential to utilize in the various application areas requiring porosity. Electrospinning is one of the most widely used techniques for the preparation of fibers having diameter of nanometer/micrometer scale. Electrospinning has many advantages such as simplicity of handling, ability to scale up and easy-to-apply to various polymeric structures. Electrospun nanofibers having 10-100 nm diameters can be utilized in various application areas such as tissue engineering, drug delivery, enzyme immobilization, removal of heavy metals, biosensors and production of reinforced composite materials [93], [94], [95], [96], [97]. Also using this method nanofibers having different morphologies such as beaded, porous, non-porous and core-shell can be prepared (Figure 2.12).

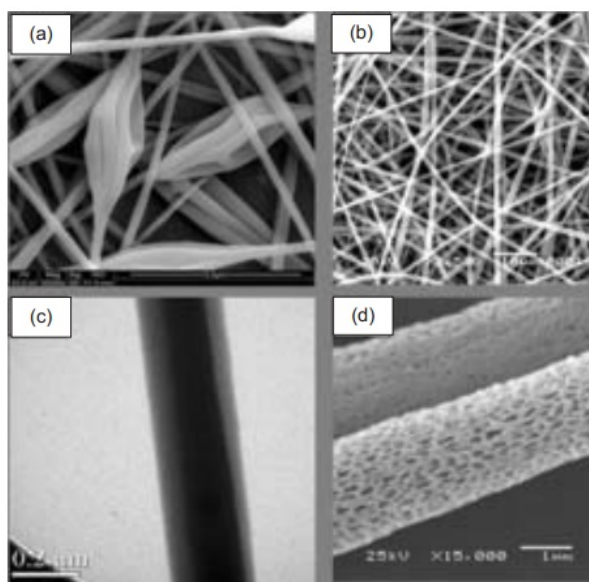


Figure 2.12. SEM images of nanofibers having different morphologies. Beaded (a), non-porous (b), core-shell (c), porous (d). Reprinted from ref. [98].

Nanofibers has been gaining much attention because of having higher surface area/volume ratio than microfibers. Surface area increases with decreasing of the fiber diameter. Novel electrospun carbon nanofibers modified with carboxylic acid

having high capacity was prepared for protein adsorption. Fiber diameter of the electrospun carbon nanofibers was 300 nm since fiber diameters of conventional carbon microfibers is typically 10 μm . Increment of the surface area of the nanofibers by 30 fold enhanced protein adsorption capacity significantly [99].

Specific purification of many molecules such as bisphenol A, glutamic acid, propranolol and herbicides is performed with porous and non-porous nanofibers [100-102], [102]. Non-porous matrices for protein purification providing fast binding kinetics and high adsorption capacity have been gaining much attention since porous materials having high diffusional mass transfer limitations. Thus diffusional resistances of small molecules like metal ions, amino acids and drug molecules and macromolecules like proteins can be reduced via the utilization of non-porous nanofibers [103]. The most important advantage of affinity adsorption with non-porous nanofibers is the convection of fluid through pores of the nanofibers and high recognition of proteins on the surface of nanofibers. Non-porous electrospun nanofibers having these superior properties exhibits great potential for protein purification.

Cellulose, polysulfone, polyacrylonitrile and nylon/chitosan electrospun nanofibers have been prepared recently [104], [105], [106]. Zhang and coworkers prepared ion-exchange support material modified with anion exchange ligand diethylaminoethyl (DEAE) using electrospun cellulose acetate nanofibers having diameters of 10 nm-1 μm for protein purification [107]. DEAE-nanofibers exhibit higher albumin adsorption capacity compared with DEAE-cellulose microfibers and commercial DEAE-cellulose fibers. Zhu and coworkers have synthesized polyvinylalcohol-polyethylene nanofibers. They immobilized dye ligand namely Cibacron Blue F3GA that is cheap and chemically stable instead of antibodies that are expensive, requiring special conditions for storage and immobilization (Figure 2.13). It was shown that Cibacron Blue F3GA-attached nanofibers exhibited higher albumin adsorption capacity compared with Cibacron blue F3GA-attached chitosan microbeads.

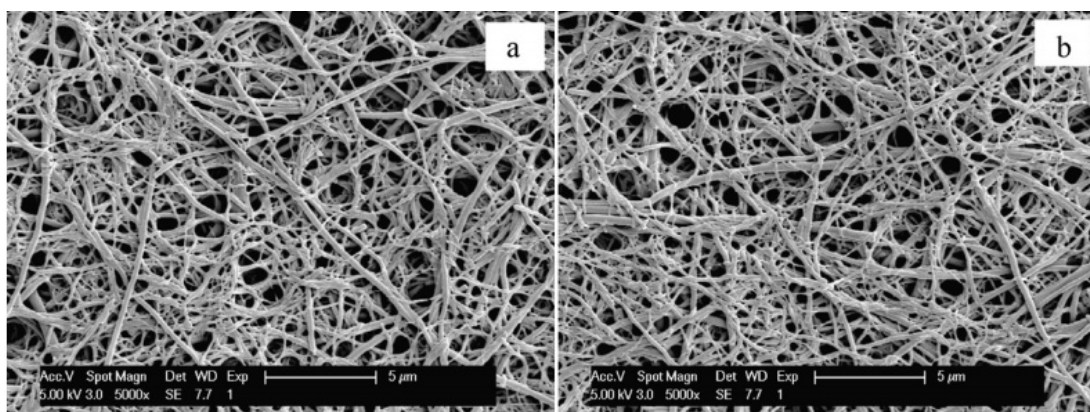


Figure 2.13. SEM images of PVA-PE nanofibers (A), Cibacron Blue F3GA-attached PVA-PE nanofibers. Reprinted from ref. [108].

Nanofibrous electrospun glycopolymers were also prepared with two glycopolymers containing cyclic poly (acrylonitrile-co-(α -allyl glucoside)) (PANCAG) and linear poly (acrylonitrile-co-(D-gluconamidoethyl methacrylate)) (PANCGAMA) performing high protein binding capacity with the help of the nanosized structure [109]. This type of materials having superior flow features and high permselectivity provide chiral separation from racemic mixtures.

The novel molecularly imprinting procedure for the fabrication of selective binding sites directly by electrospinning containing the polymerization medium with template molecule, 2,4-dichlorophenoxyacetic acid which is a herbicide, was developed [101]. The polymerization mixture was electrospun onto the aluminum foil placed 20 cm from the capillary tip using experimental system shown in the Figure 2.14. Poly(ethylene terephthalate) (PET) was utilized as a supporting matrix. The recognition sites were fabricated via interaction between polyallylamine and template molecule. Molecularly imprinted nanofibers with high surface area was also prepared via electro spray deposition [110].

To obtain selective glutamic acid recognition, alumina membranes were utilized as a nanomold to synthesize MIP nanowires via template synthesis method [112]. Template molecule in that case glutamic acid, was covalently immobilized onto the walls of alumina membrane having pores of 100 nm diameter (Figure 2.15). After the polymerization using pyrrole as a monomer, alumina membrane was removed via chemical dissolution method resulting polypyrrole nanowires with glutamic acid recognition sites. High imprinting factor was achieved however binding kinetics was not so satisfactory since it reached equilibrium after 20 min. The same

research group prepared magnetic MIP nanowires showing high specificity to template molecule and imprinting factor was approximately 6 using alumina membrane as a nanomold [113].

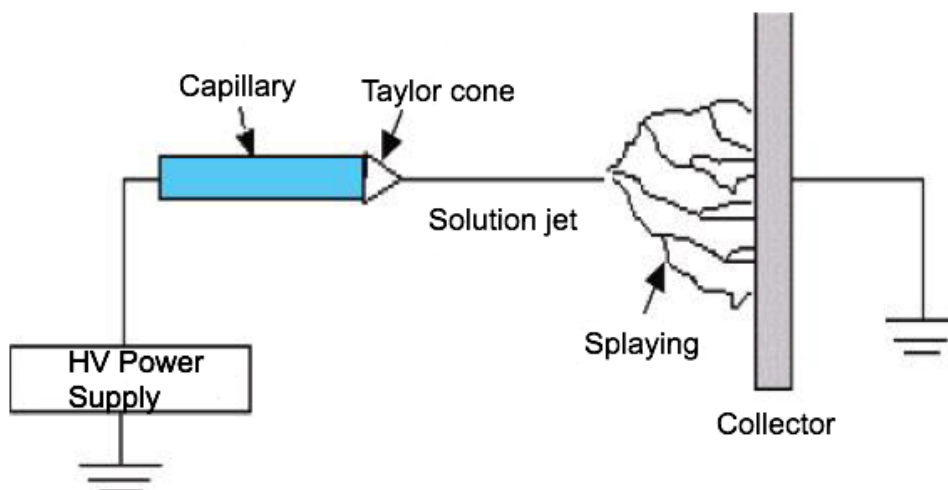


Figure 2.14. Schematic representation of preparation of electrospun MIP nanofibers using electrospinning equipments. Reprinted from ref. [111].

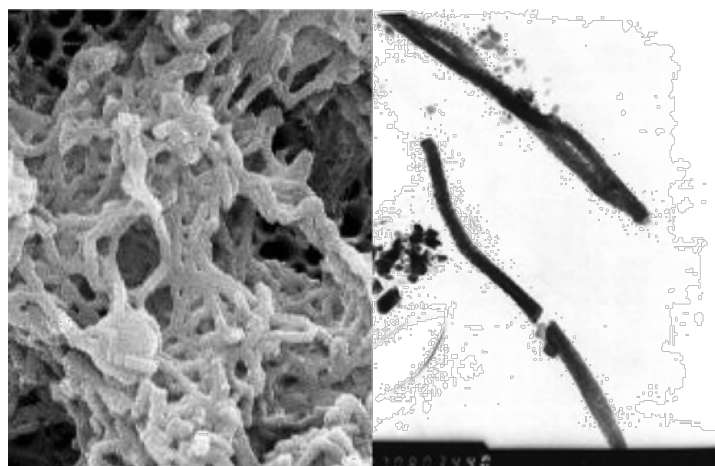
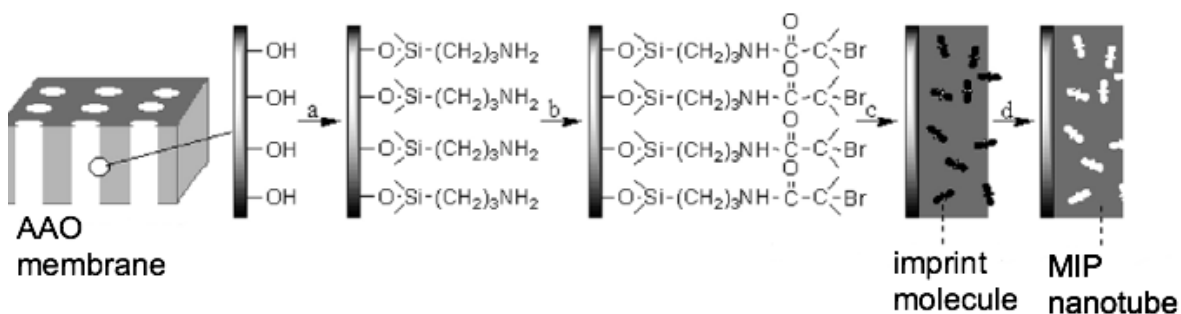


Figure 2.15. SEM images of polypyrrole nanowires. Reprinted from ref. [50].

MIP nanotubes using anodic alumina oxide membrane with 100 nm pore diameter were prepared via ATRP, which is a kind of controlled radical polymerization technique [114]. ATRP initiators were immobilized onto the walls of alumina membrane and then membrane was immersed into polymerization medium containing template molecule (Figure 2.16). After removal of alumina membrane, it

was achieved 11 fold higher rebinding capacity and 13 fold higher imprinting factor comparing with conventionally prepared bulk MIPs with MIP nanotubes with controlled size.



a: Silanization with 3-aminopropyltrimethoxysilane

b: Reaction with 2-Bromo-2-methylpropionyl bromide

c: Polymerization of estradiol:4-vinylpyridine complex and ethylene glycol dimethacrylate

d: Remove of estradiol

Figure 2.16. Schematic presentation of preparation strategy of MIP nanotube membrane. Reprinted from ref. [115].

Silicon nanowires (SiNW) with unique mechanical properties, large surface area, high hydrophilicity and biocompatibility were used as a supporting matrix to obtain MIP coated silicon nanowires for fast and selective bovine hemoglobin recognition [116]. Thin PDA layer attached onto SiNW with a thickness of 10 nm was created with DA as a functional monomer (Figure 2.17). Template extraction after polymerization was found very high as %96.3 w/w since template molecules placed on the surface or near the surface of the nanowires. The imprinted nanowires showed high binding kinetics, it took 5 min to reach the 75% of the equilibrium. Molecularly imprinted nanowires achieving high specificity and fast binding kinetics was created.

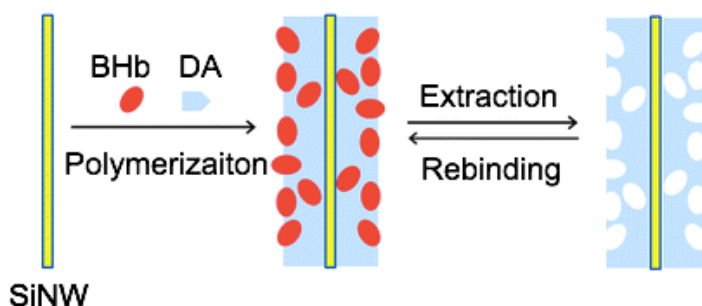


Figure 2.17. Schematic presentation of fabrication of MIP-PDA nanowires. Reprinted from ref. [78].

Also the development of electrospun nanofibers embedded with molecularly imprinted nanoparticles is an promising approach to enhance surface area of the material [117], [118]. The theophylline and 17 β -estradiol imprinted nanoparticles 200-300 nm in diameter were encapsulated onto PET nanofibers having 150 nm diameter (Figure 2.18).

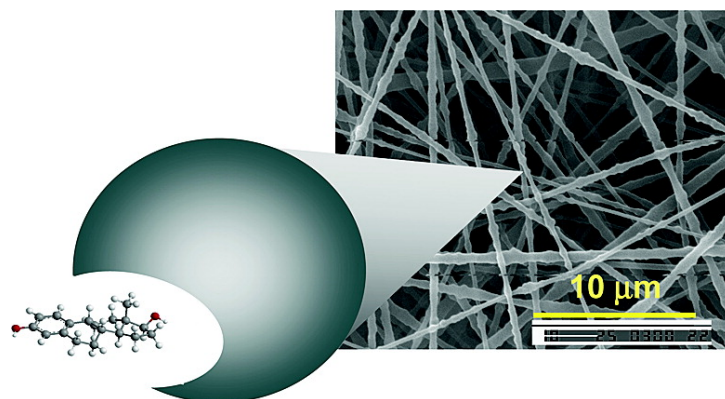


Figure 2.18. Schematic presentation of MIP-NPs on the SEM image of PET nanofibers. Reprinted from ref. [119].

2. 4. Bacterial Cellulose

Bacterial cellulose (BC) is produced by the genera *Acetobacter*, *Rhizobium*, *Agrobacterium*, and *Sarcina*. The most efficient producer is *Acetobacter xylinum*, which is a gram-negative acetic acid bacteria [120]. Bacterial cellulose is the primary metabolism product of the bacteria providing oxygen-rich surface and moisture for bacteria. Also it is considered that the pellicle protects the bacteria cell from the negative effects of UV light by surrounding it like a cage. The bacterial cellulose nanofiber ribbon with the producers bacteria cells is seen in Figure 2.19. The bacteria cell from its terminal complexes extrudes the linear glucan chains, which aggregate to form the nanofibers via twisting. These nanofibers then aggregate to form a ribbon possessing the diameter of 50-100 nm. Bacterial cellulose occurs at liquid-air interface with the inoculation of *A.xylinum* into the Hestrin-Schramm medium [121]. BC pellicles appear as a gelatinous material of variable thickness when floating on the surface of the medium. For its recovery, BC is firstly washed with distilled water to remove culture medium

remaining in the pores of the membrane. Then BC is boiled in 1-3 w% NaOH solution to eliminate the cells and the components of the medium [122].

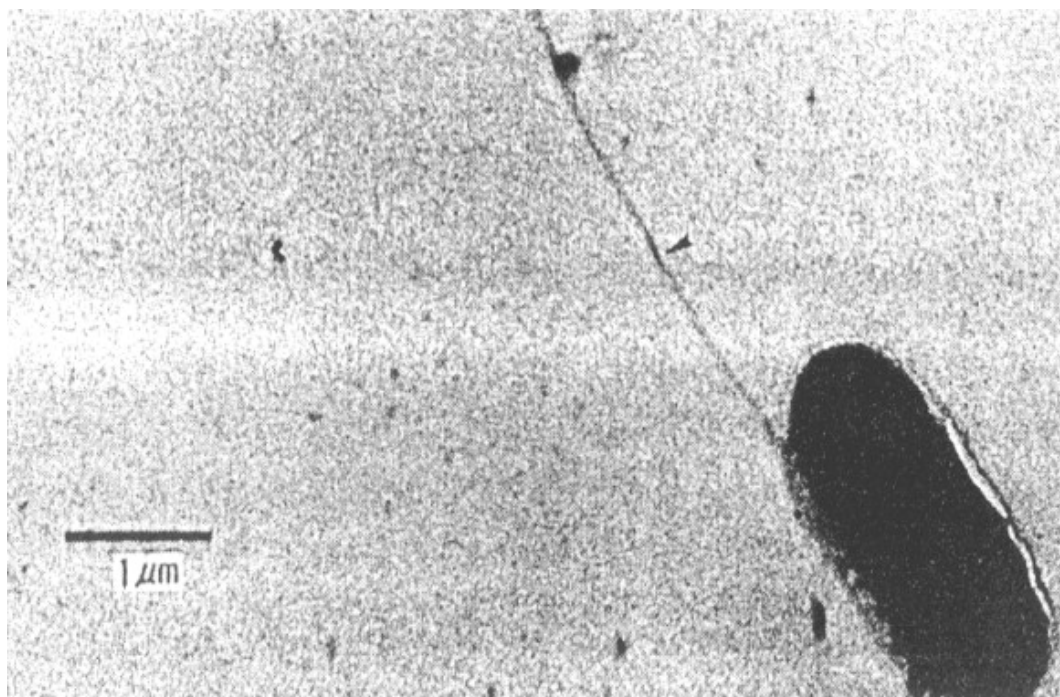


Figure 2.19. TEM image of bacterial cellulose ribbon produced by the bacteria. Reprinted from ref. [123].

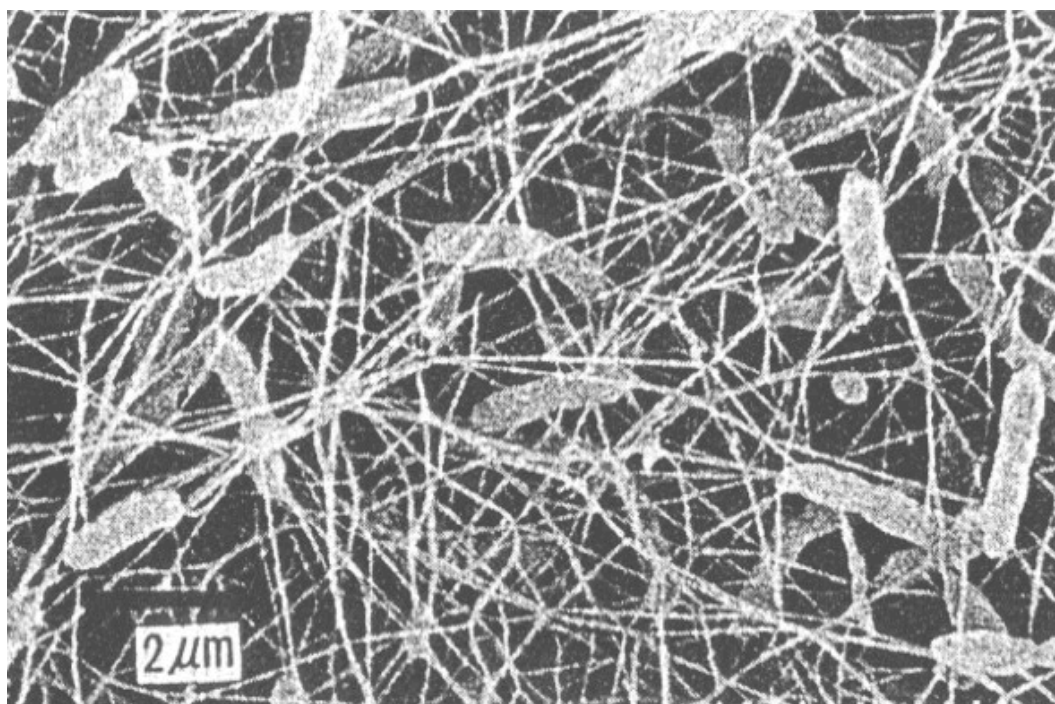


Figure 2.20. SEM image of bacterial cellulose network containing bacteria cells. Reprinted from ref. [124].

The chemical structure of bacterial cellulose is identical to plant cellulose and is shown in Figure 2.21. BC nanofibers are hundred times thinner than that of plant cellulose. Also bacterial cellulose has great purity avoiding lignin and hemicellulose. It has gained great attention since it possesses unique properties such as remarkable mechanical properties, high porosity, water uptake ratio, and biocompatibility. Also it can be molded in situ. Bacterial cellulose has many application areas including paper industry [125], food additive [126], metal removal from waste-water [127], antimicrobial filtration [128], enzyme immobilization [129], tissue engineering as a scaffold, vascular prosthetic device [130], [131], [132], skin tissue repair [133], and drug delivery [134].

Bacterial cellulose nanofibers are prepared with high purity, however electrospun nanofibers are not pure after the synthesis. Since electrospun nanofibers are synthesized via polymerization processes, it is necessary to wash them with several times. This drawback of synthetic nanofibers makes bacterial cellulose nanofibers important alternative. Since BC nanofibers are non-porous nanofibers, they also demonstrate high capacity and high binding kinetics avoiding mass-transfer limitations. Furthermore preparation of BC is simple since synthesis procedure does not require any special equipment. Thus the utilization of bacterial cellulose nanofibers for protein purification is advantageous providing unique properties of nanofibers without any necessity for any spinning device.

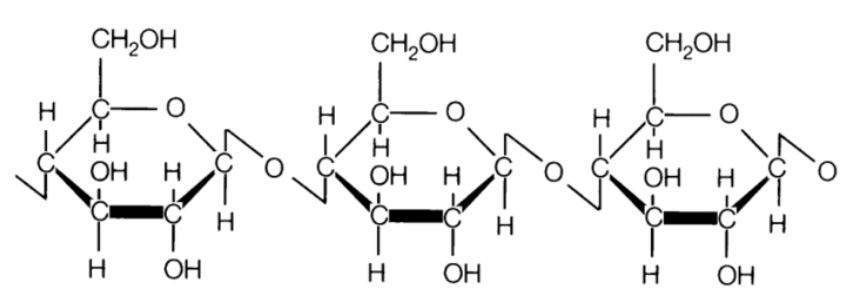


Figure 2.21. Chemical structure of cellulose.

2. 5. Cytochrome c

Cytochrome c (Cyt c) is an essential heme containing protein found in plants, animals, and many unicellular organisms [135], [136]. Molecular weight is about 12,000 daltons. It consists of a chain of about 100 amino acids as a primary

structure however some higher orders organisms possess a chain of 104 amino acids [137]. The porphyrin ring of active heme center coordinates central Fe atom due to pyrole nitrogens and forms a square planar complex. Cyt c is modulating electron transfer in the mitochondrial respiratory chain due to the iron center changing ferric (Fe^{3+}) and ferrous (Fe^{2+}) state and generally regarded as a universal catalyst of respiration which makes it an efficient biological electron-transporter [138]. It transfers electron between two large protein complexes called cytochrome bc₁ complex and cytochrome c oxidase complex. It is a small and sphere like in shape [139]. The amino acid sequence of cytochrome c is highly conserved among different organisms since the genetic similarity of mouse and rat cytochrome c is 91% with the human cytochrome c [140]. Due to its small size and sequence homology, it can be used as a model protein in studies of cladistics, which is an approach of classification of biological organisms [141].

There has been many research articles investigating the role of cytochrome c for apoptosis process and identifying it as a mediator in apoptotic mechanism [142], [115], [143]. It was shown that Cyt c release from the cell has occurred within 1 h only after apoptosis starts resulting a fast and apoptosis-specific process [144]. Thus the extracellular cytochrome c is suitable as a biomarker of apoptosis. There have been many articles reporting cytochrome c as a biochemical indicator for various diseases including cancer, liver damage and myocardial ischemia [145], [146], [147]. Thus screening of Cyt c may be useful as a clinical biomarker during cancer therapy [148]. Recently, there have been research articles investigating cytochrome c as a therapeutic protein. In this context, the approach for cancer therapy is to target cytochrome c as a therapeutic protein to cancer cells to initiate apoptotic process causing cell death [149], [150], [151]. These developments present cytochrome c as a valuable protein for medicine exhibiting great potential of being a biomarker of a disease and effective therapeutic choice.

Furthermore cytochrome c is widely used in adsorption studies as a model protein since Cyt c is nearly spherical (molecular dimensions $2.6 \times 3.2 \times 3.3 \text{ nm}^3$) in shape [152]. Also it was shown that cytochrome c as one of the hardest proteins due to adiabatic compressibility can be adsorbed onto solid support without any conformational change providing more reliable results than hemoglobin which is identified as a very soft protein [153], [154].

The MIP hydrogel was prepared for lysozyme recognition and obtained successful results with an imprinting factor of 1.72 [155]. In that study MIP hydrogel for cytochrome c recognition was also synthesized and the adsorption isotherms of lysozyme and cytochrome c were compared. Cyt c has It was concluded that cytochrome c is a better choice as a template since it enhanced the adsorption capacity and the selectivity of the MIP due to its higher charge density locating on the surface of the protein leading more specific pattern for binding site creation. However lysozyme has low amount of surface charge causing formed recognition sites less specific.

As mentioned before, the choice of template is one of the major steps that affect binding characteristics of MIPs. Thus it is an important parameter to determine for preparing selective adsorbents with high capacity. In conclusion the selection of cytochrome c as a model protein is suitable to utilize it as a template molecule to synthesize selective MIPs in this study.

2. 6. QCM Sensors

Over the past three decades, many developments have been taken place in the field of sensor technology. Since the biological sensing elements are not stable for long-term applications, synthetic receptors that mimic natural counterparts are desirable. In that field especially molecular imprinted biosensors present promising alternatives possessing extraordinary selectivity and sensitivity properties [156]. Molecular imprinting method provides preparation of highly stable and specific polymeric materials, which achieve selective recognition features with binding sites created complementary to template molecules in shape and size [157].

After Sauerbrey discovered the dependency of quartz oscillation frequency with mass change on the crystal surface in 1959, the use of term quartz crystal microbalance (QCM) arises. Thus the linear relation between the change of mass on the crystal surface and change in frequency of the oscillating crystal at a specific frequency is shown by the Sauerbrey equation:

$$\Delta m = -C \Delta f$$

This equation is valid for elastic surfaces such as thin adsorbed layers and it is not appropriate to use this equation for inelastic surface, which possess energy loss during oscillation. Therefore Sauerbrey equation becomes in valid when the mass

change is bigger than 2% of the crystal mass [158]. There has been many publications related to QCM biosensors for rapid and real-time detection of metal ion [159], small molecules [160], [161], [162], amino acid [163], protein [164] and even cell [165]. QCM sensor chip is shown schematically below.

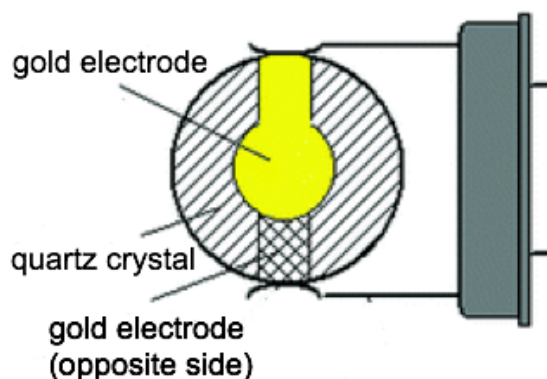


Figure 2.22. Schematic representation of QCM sensor chip Reprinted from ref. [166].

High surface area of sensing material is significant to improve the sensing properties of QCM sensors. Therefore nanomaterials such as nanoparticles, nanorods, nanowires and nanofibers have been received much attention since these nanostructures lead high sensitivity and fast response in sensor applications [167]. QCM sensors coated with bacterial cellulose were used for real-time detection of both humidity and formaldehyde [168], [169]. Highly stable, sensitive and cost-effective QCM sensors were fabricated via coating the crystal surface with bacterial cellulose nanofibers. The experimental setup was shown in the figure below. The results showed that bacterial cellulose with high surface area presented high sensitivity, good long-term stability and good linearity.

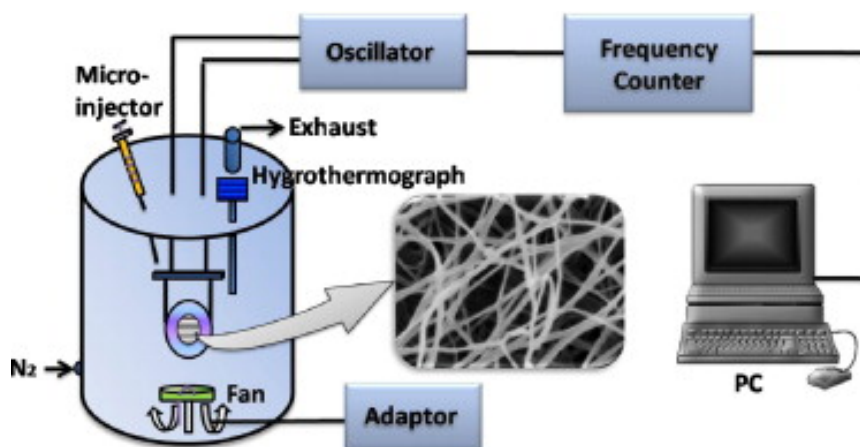


Figure 2.23. Schematic view of the experimental setup for humidity sensor of QCM with BC nanofibers. Reprinted from ref. [169].

Different types of sensor systems were used to detect cytochrome c such as Surface Plasmon Resonance (SPR). Alkyl thiols modified SPR sensors with different tail groups were evaluated for the detection of Cyt c [170]. The other one is Atomic Force Microscope (AFM) force spectroscopy to measure the force between protein and binding site [171].

In conclusion to prepare sensitive QCM sensor, bacterial cellulose nanofibers are great alternative to create selective recognition sites avoiding diffusional resistances especially for biomacromolecules.

3. EXPERIMENTAL METHOD

3. 1. Materials

Horse heart cytochrome c (Cyt c), chicken egg white lysozyme (Lys), bovine myoglobin (Myo), bovine serum albumin (BSA), bovine hemoglobin (Hb), N,N'-Methylenebisacrylamide (MBAAm), L-histidine methylester dihydrochloride and methacryloyl chloride were all purchased from Sigma (St. Louis, USA). Radical initiator azobisisobutyronitrile (AIBN) was supplied by Fluka (Switzerland). *Acetobacter xylinum* (ATCC10245) was supplied from Agricultural Research Service Culture Collection (ARS, USA) in lyophilized form. Growth medium components, D-glucose, peptone, yeast extract, K₂HPO₄ and KH₂PO₄ were obtained from Merck (Darmstadt, Germany) in analytical grade. All other chemicals used were purchased from Merck A.G. (Darmstadt, Germany) unless otherwise noted. The water used in the experiments was purified using a Barnstead (Dubuque, IA, USA) ROPure LP® reverse osmosis unit with a high-flow cellulose acetate membrane (Barnstead D2731) followed by a Barnstead D3804 NANOpure® organic/colloid removal and ion-exchange packed-bed system. The resulting purified water (deionized water) had a specific conductivity of 18 mS/cm. Buffer and sample solutions were filtered through 0.2-µm membrane (Sartorius, Göttingen, Germany).

3. 2. Preparation of Cyt c-MIP Nanofibers

3.2. 1. Production of Bacterial Cellulose Nanofibers

The production of BC was performed by growing *A. xylinum* (ATCC 10245) in Hestrin–Schramm medium. The medium containing 20 g/L glucose, 10 g/L bactopectone, 10 g/L yeast extract, 4 mM KH₂PO₄ and 6 mM K₂HPO₄ is used for the production of BC in static culture. The pH of the medium was adjusted to pH 5.1–5.2 using 1 M HCl. The inoculum was prepared by growing *A. xylinum* at 28 °C for 3 days using a rotary shaker. The BC nanofiber formation was led to occur over a period of 7 days after inoculating subculture in the proportion 1:10 in petri dishes statically. Then, the synthesized BC nanofibers were washed with 1 M NaOH solution at 70 °C for 90 min to remove all the microorganisms inside the

membrane. Finally, the BC nanofibers were redispersed in distilled water and stored at room temperature [172].

3.2. 2. Synthesis of N-methacryloyl L-histidine methylester (MAH)

The synthesis of MAH was described elsewhere [173] and the experimental procedure used was as follows: 5.0 g of L-histidine methylester and 0.2 g of hydroquinone were dissolved in 100 mL dichloromethane. This solution was cooled to 0 °C, 12.7 g of triethylamine was added to this solution, 5.0 mL of methacryloyl chloride was poured into this solution slowly and then it was stirred magnetically at room temperature for 2 h. At the end of the chemical reaction, extraction with 10% NaOH solution was performed to remove the unreacted methacryloyl chloride. The aqueous phase was evaporated and the residue was dissolved in ethanol.

3.2.2. 1. Characterization Studies of MAH

ATR-FTIR spectrum of MAH monomer was obtained by FTIR spectrometer (FTIR 8000 series, Shimadzu, Japan).

3.2. 3. Synthesis of MAH-Cu(II) Metal-chelate Monomer

In order to prepare MAH-Cu (II) complex, aqueous solutions of MAH (0.01 mmol) and copper ions (source: $\text{Cu}(\text{NO}_3)_2 \cdot 2.5 \text{H}_2\text{O}$) were mixed to prepare this complex with two different molar ratios, which was 1:1 and 2:1. Then the mixture was allowed to react at 25 °C for 1 h under stirring.

3.2.3. 1. Characterization Studies of MAH-Cu(II) Complex

The formation of MAH-Cu(II) complex was determined with UV-vis Spectrophotometer (Shimadzu UV-1601, Shimadzu Corp., Kyoto, Japan). The samples prepared with two different monomer/metal ion molar ratio (2:1 and 1:1) were recorded between 220-600 nm.

3.2. 4. Preorganization of MAH-Cu(II) Monomer with Cyt c

For the synthesis of MAH-Cu(II)-Cyt c complex, the buffer system to solubilize cytochrome c molecules was selected as pH 7 phosphate buffer since surface histidines are largely unprotonated and available to coordinate with the metal ion at this pH [174]. After mixing cytochrome c solution (1 mL) with metal chelate

monomer, MAH-Cu(II) (10 mL), the newly prepared complex, MAH-Cu(II)-Cyt c was left to react at 25 °C for 1 h under gentle stirring.

3.2. 5. Preparation of Cyt c-MIP Nanofibers

In order to achieve the creation of MIP layer onto the nanofibers, bacterial cellulose nanofiber membranes were reacted with 10% w/w of 3-MPS (3-methacryloxypropyltrimethoxysilane) in toluene medium at 80 °C for 5 h. Then the resultant membranes were washed with methanol [175]. The reacted membranes were placed in petri dish to contact with MAH-Cu(II)-Cyt c complex for 30 min. After the addition of MBAAm as a cross-linker, this polymerization syrup was bubbled with nitrogen gas for 5 min. The initiator, AIBN (0.5 mmol in 100 μ L DMF) was added under of UV light source (100 W, 365 nm) at room temperature. After the polymerization time of 30 min, the MIP layer coated nanofibers were taken out of the petri dish and washed with distilled water to remove the unreacted chemicals and stored at 4 °C to use at further experiments. The template molecules were removed with 1 M NaCl solution for 2 h. The non-imprinted nanofibers (NIP) were prepared with the same procedure but the absence of template molecules. The formation of recognition sites was presented schematically below.

3.2.5. 1. Characterization Studies of Cyt c-MIP Nanofibers

FTIR Studies

The characteristic functional groups of Cyt c imprinted nanofibers were characterized by FTIR-attenuated total reflectance (ATR) spectroscopy (FTIR 8000 Series, Shimadzu, Japan).

Surface Morphology

The surface morphology of the imprinted cellulose nanofibers was investigated with scanning electron microscope (SEM). The samples were lyophilized before being analysed. The samples were then sputtered with a thin layer of gold before SEM measurement.

Contact Angle Measurements

Contact angle of Cyt c-MIP nanofibers was evaluated with KRUSS DSA 100 (Hamburg, Germany). It was measured with Sessile Drop method by dropping 1

drop of water onto nanofibers. The measurements were the average of the 20 measurements.

3.3. Batch Adsorption Studies

3.3. 1. Rebinding Experiments

Adsorption of cytochrome c on the imprinted and non-imprinted nanofibers from aqueous solutions was investigated in batch-wise. The nanofibers (16 mg±2.5 mg) were incubated with 3 mL of cytochrome c solutions for 1 h at 20 rpm. To observe the optimum conditions of polymerization, the effect of monomer/template ratio, total monomer ratio and polymerization time with respect to adsorption capacity were investigated. The effects of cytochrome c concentration, pH, temperature, NaCl concentration on the adsorption capacity was also studied. Cytochrome c concentration was changed between 0.075-2.0 mg/mL. The effects of temperature were investigated for the temperatures 4, 15, 25 and 37 °C. The effect of ionic strength on adsorption capacity was carried out in salt-free solution and then in aqueous NaCl solutions with concentration of 0.001-0.1 M. Adsorbed amount of cytochrome c was determined by visible spectrophotometry at 409 nm. The calibration curve can be seen in Appendix. The protein adsorption capacity was calculated from mass balance according to the following equation:

$$Q = \frac{(C_0 - C)V}{m} \quad (1)$$

where Q is the adsorbed amount of Cyt c per unit mass (mg/g), C_0 and C are the amount of Cyt c before and after adsorption process respectively (mg/mL); V is the volume of cytochrome c solution (mL) and m is the dry mass of Cyt c-MIP nanofibers used (mg).

The desorption of the adsorbed Cyt c from the imprinted nanofibers was performed in a batch system. The nanofibers were incubated in 1 M NaCl solution for 1 h at room temperature under stirring at 20 rpm with rotator.

3.3. 2. Selectivity Studies

In order to demonstrate the selectivity of the Cyt c-MIP nanofibers in batch system toward template protein Cyt c (pI (isoelectric point)=10.6, MW=12.3 kDa), non-template proteins bearing surface histidine(s) such as bovine serum albumin (BSA, pI= 4.9, MW=67.0 kDa), hemoglobin (Hb, pI=6.7, MW=64.5 kDa), myoglobin

(Myo, $pI=6.8$, $MW=17.0$ kDa) and lysozyme (Lys, $pI=10.5$, $MW=14.6$ kDa) were used with initial concentration of 0.2 mg/mL. The concentration of proteins, i.e. unadsorbed, was measured by UV-vis spectroscopy at 280 nm for BSA and Lys, 409 nm for Myo and 406 nm for Hb. All the calibration curves belonging to each protein was shown in Appendix. In order to show the contribution of metal ions to selectivity properties of MIP nanofibers, the polymerization process without metal ion was also performed to obtain M(Cyt c). For the preparation of this MIP nanofiber, MAH monomers were complexed with Cyt c directly.

3. 4. Fabrication of QCM Nanosensors

The AT cut (5.0 MHz) QCM sensor chip was washed with piranha solution (7:3 $H_2SO_4 : H_2O_2$, v/v). This solution was treated with gold surface for 20 s and then washed with ethanol and water and dried with N_2 atmosphere. The prepared Cyt c-MIP nanofibers were pulped with the rotation speed of 12000 r/min by a homogenizer (T10, Ika Labortechnik, Germany) for 10 min at 25 °C [168]. Then 75 μL of the treated mixture was dispensed onto the cleaned surface of the electrode of the QCM chip with micropipette. The QCM sensor casted with Cyt c-MIP nanofiber was dried at 60 °C for 1 h in vacuum. The entire procedure of Cyt c-MIP QCM nanosensor was presented schematically below. NIP QCM nanosensor was prepared using the same procedure with NIP nanofibers.

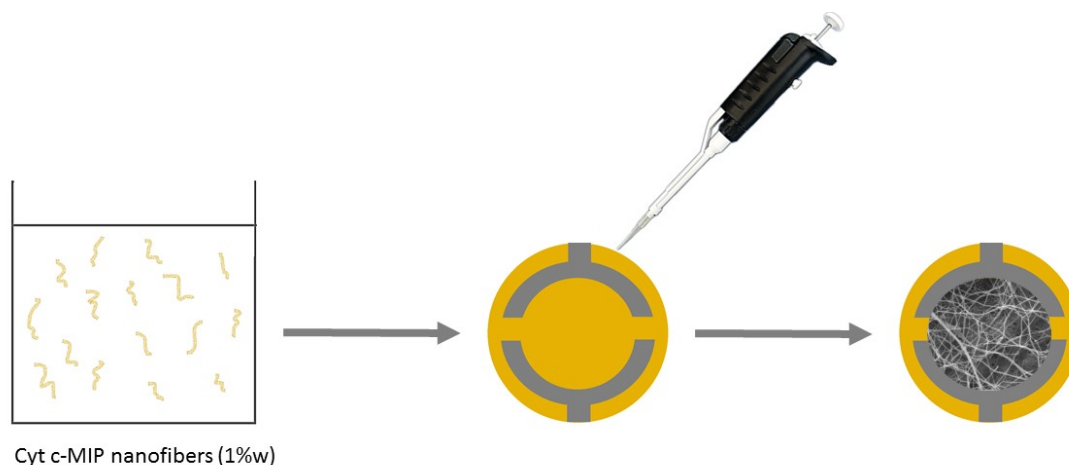


Figure 3. 1. Schematic presentation of preparation strategy of Cyt c-MIP QCM nanosensors.

3.4. 1. Surface Characterization of QCM Nanosensors

In order to characterize the surfaces of QCM nanosensors, atomic force microscope (AFM) was used. AFM observations were carried out with AFM (Nanomagnetics Instruments, Oxford, UK) in tapping mode. The AFM measurements were performed in high resolution such as 4096 x 4096 pixels with free cantilever interferometer. The Cyt c-MIP QCM nanosensors and NIP QCM nanosensors were placed onto sample holder with double-side carbon strip. All observations were taken using tapping mode in air atmosphere. The oscillation frequency, vibration amplitude and free vibration amplitude was applied as 341.30 kHz, 1 V_{RMS} and 2 V_{RMS} . Samples were scanned to obtain the view of the area of 2 μm x 2 μm using 2 $\mu\text{/s}$ scanning rate and 256 x 256 pixels resolution.

3.4. 2. Kinetic Studies with QCM Nanosensors

To perform the real-time monitoring of QCM nanosensors, different concentrations of Cyt c solutions (1-75 $\mu\text{g/mL}$) were used in the system, which constitute frequency counter, oscillator, peristaltic pump and computer. The experimental procedure is as follows: firstly, Cyt c-MIP QCM nanosensors were washed with distilled water (50 mL). Then the equilibration was performed using pH 7 phosphate buffer and the resonance frequency was determined (f_0). After equilibration process for 3 min, different concentrations of Cyt c solutions (5 mL) were given to the system with the flow rate of 1 mL/min. When the resonance frequency came to the equilibrium value (approximately 90 min), desorption was carried out with 1 M NaCl solution (5 mL, 1 mL/min). The nanosensors were washed with distilled water and then with phosphate buffer to equilibrate. The resonance frequencies were measured by the QCM digital controller. For each of the concentration of Cyt c solution, the adsorption-desorption cycle was utilized. The data was analyzed with Software of QCM (Maxtek).

3.4. 3. Selectivity Studies of QCM Nanosensors

The non-template proteins that were used in batch rebinding experiments were also utilized to show the selectivity of QCM nanosensors. These protein solutions were prepared in phosphate buffer (pH:7.0). The resonance frequencies were determined for these selectivity experiments. The data was analyzed with Software of QCM (Maxtek).

4. RESULTS AND DISCUSSION

The production of biological materials is becoming increasingly attractive and developing field. However the isolation and purification steps of the targeted molecule often requires expensive treatments which typically account up to 80% of the total cost for production [176]. Thus, in order to overcome the high purification costs of biological materials there is great demand for the development of adsorbents with high specificity and high recognition capacity. Surface imprinting is a promising method to create highly specific recognition sites of analyte on the surface of the polymer. Nanofibers have been gaining more attention since they avoid intraparticle diffusion resistances having high surface area. Surface imprinting which is a molecular imprinting process performing onto a solid support surface and adopting nanofibers having high surface area are two effective approaches to overcome mass transfer resistances especially for biomacromolecules like proteins. Fast separation of proteins is very useful for many biotechnological areas such as quality control and on-line monitoring [2]. The aim of this thesis is to find a cost effective and reusable affinity nanofibers having high recognition capacity and high selectivity for purification of Cyt c. Surface imprinting has been widely used molecular imprinting method since it improves the protein adsorption performance of MIPs by reducing mass transfer resistances and enables easy removal of template [5]. In this thesis, surface imprinted bacterial cellulose nanofibers for cytochrome c recognition, which was abbreviated as Cyt c-MIP, was prepared successfully for efficient purification of Cyt c from aqueous solutions.

4. 1. Preparation of Surface Imprinted MIP Nanofibers

4.1.1. Synthesis of MAH-Cu(II) Complex

Metal chelating monomer MAH having imidazole group of chelating property with transition metals was complexed with metal ion Cu(II) in molar ratios of 1:1 and 2:1 and characterized with UV-vis spectrum (Figure 4.1) [177]. It was determined that MAH monomer and copper ions were complexed because of the decrement of band absorbances [178]. The absorbance of MAH-Cu(II) complex prepared in the molar ratio of 1:1 was lower than that of the molar ratio of 2:1. Thus it was determined that MAH-Cu(II) complex prepared in the molar ratio of 1:1 namely

1MAH-1Cu was selected and it was used for the rest of the study.

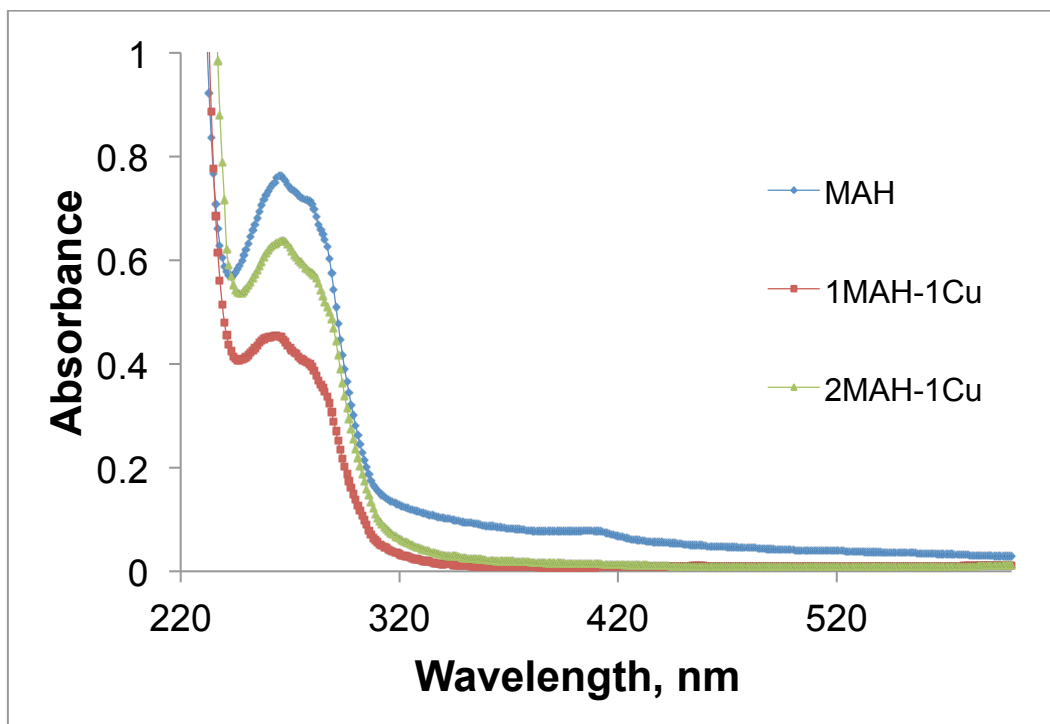


Figure 4. 1. UV-vis spectra of MAH and MAH-Cu(II) complexes.

4.1.2. Characterization of Cyt c-MIP nanofibers

The chemical structure of MAH monomer was characterized by ATR-FTIR. The specific bands of MAH monomer were determined as amide bands at 1740 cm^{-1} , and 1677 cm^{-1} (Figure 4.2) [179]. The broad band presenting in the region of $3600\text{-}3000\text{ cm}^{-1}$ correspond to the O-H stretching frequencies of cellulose and the band at around 1430 cm^{-1} is assigned to a symmetric CH_2 bending vibration and the C-O-C glycosidic ether band arises at $\sim 1105\text{ cm}^{-1}$ (Figure 4.3) [180]. ATR-FTIR spectrum of Cyt c-MIP nanofibers was given below representing characteristic amide bands of MAH that occur at 1539 and 1633 cm^{-1} (Figure 4.4).

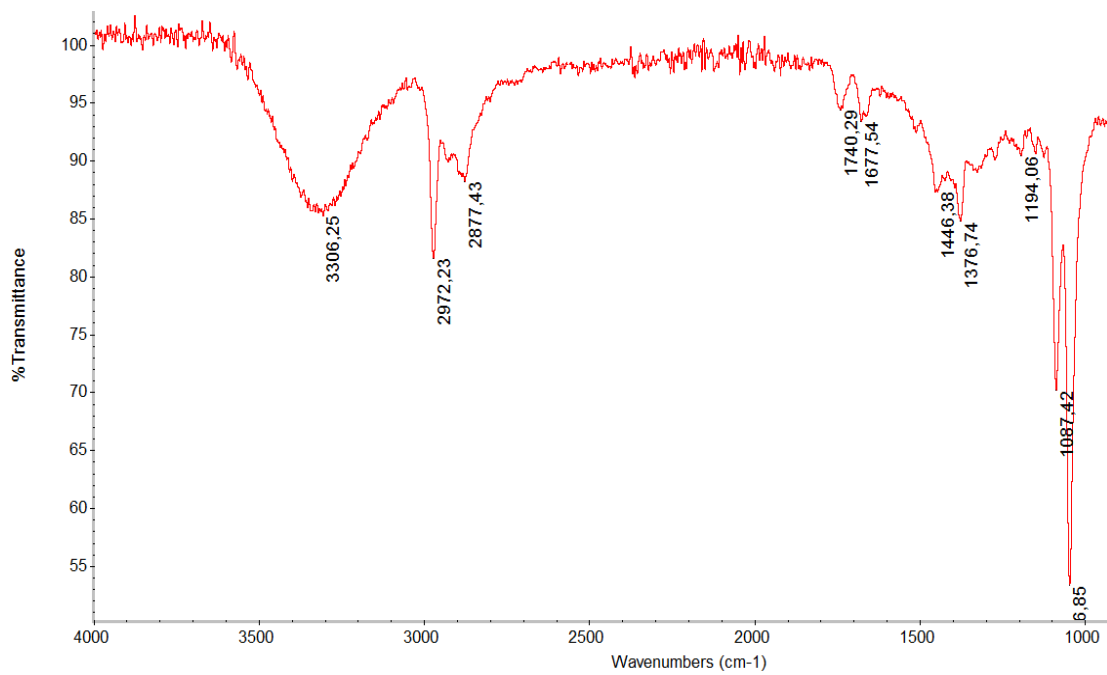


Figure 4. 2. ATR-FTIR spectrum of MAH monomer.

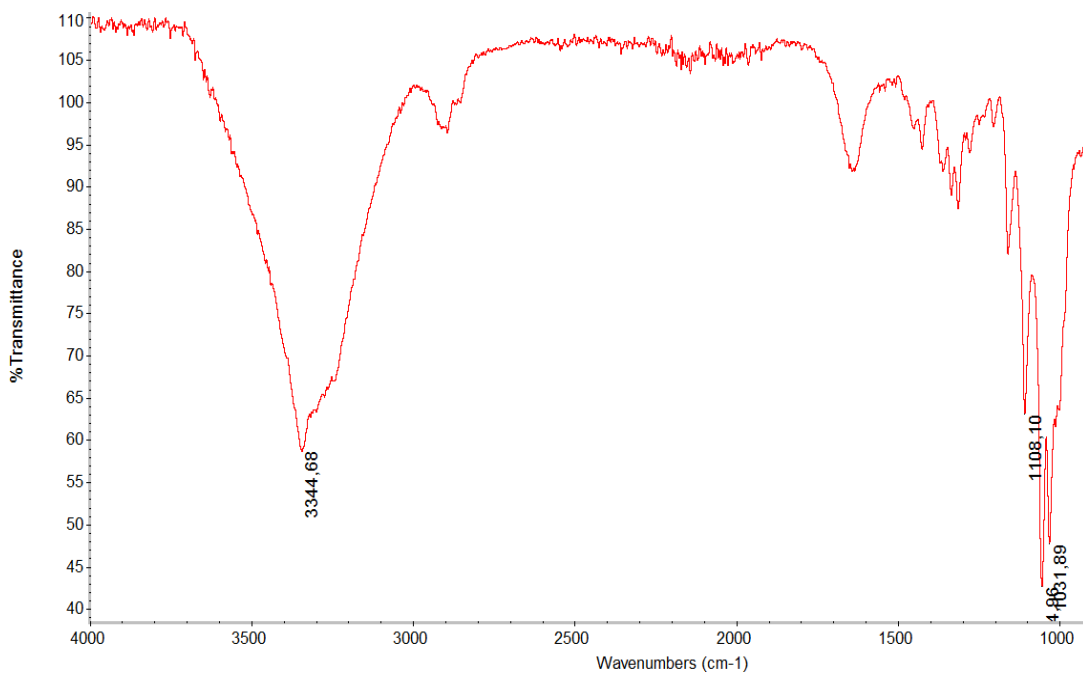


Figure 4. 3. ATR-FTIR spectrum of BC.

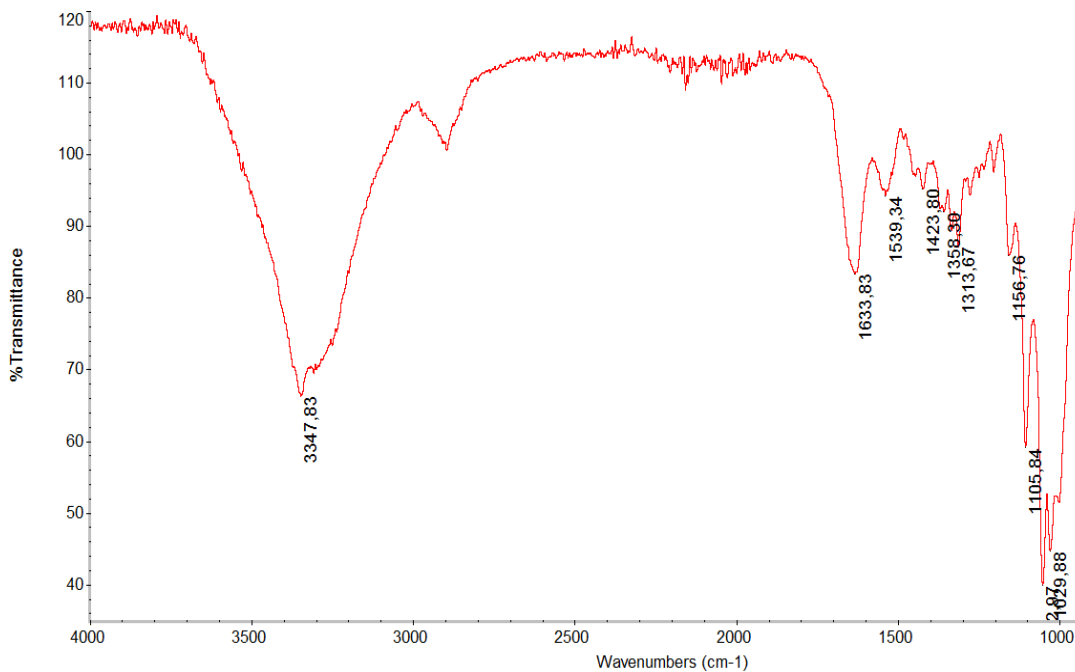


Figure 4. 4. ATR-FTIR spectrum of Cyt c-MIP nanofibers.

Surface morphology of Cyt c-MIP nanofibers that were used for batch rebinding studies was investigated with SEM (Figure 4.5) indicating that resultant Cyt c-MIP bacterial cellulose nanofibers were continuous and randomly oriented as porous structure of 3-D non-woven interconnected network nanofibrous mat. As seen from the SEM photograph, it was evidently considered that the bacterial cellulose nanofibers provide excellent surface area for easy diffusion of cytochrome c molecules into and out of the entire membrane facilitating mass transfer properties of adsorption process. This nanoweb structure composed of nanofibers contributes to the rapid diffusion of template molecules into the recognitive MIP layer enhancing rebinding kinetics [181]. Also it was clear that there was no bacteria and debris in the polymer structure which indicating that washing procedure used was successful to remove all the microorganisms.

The contact angle measurements were performed to demonstrate the hydrophilic character of MIP nanofibers (Figure 4.6). The average contact angle of Cyt c-MIP nanofiber was found as 49.72°.

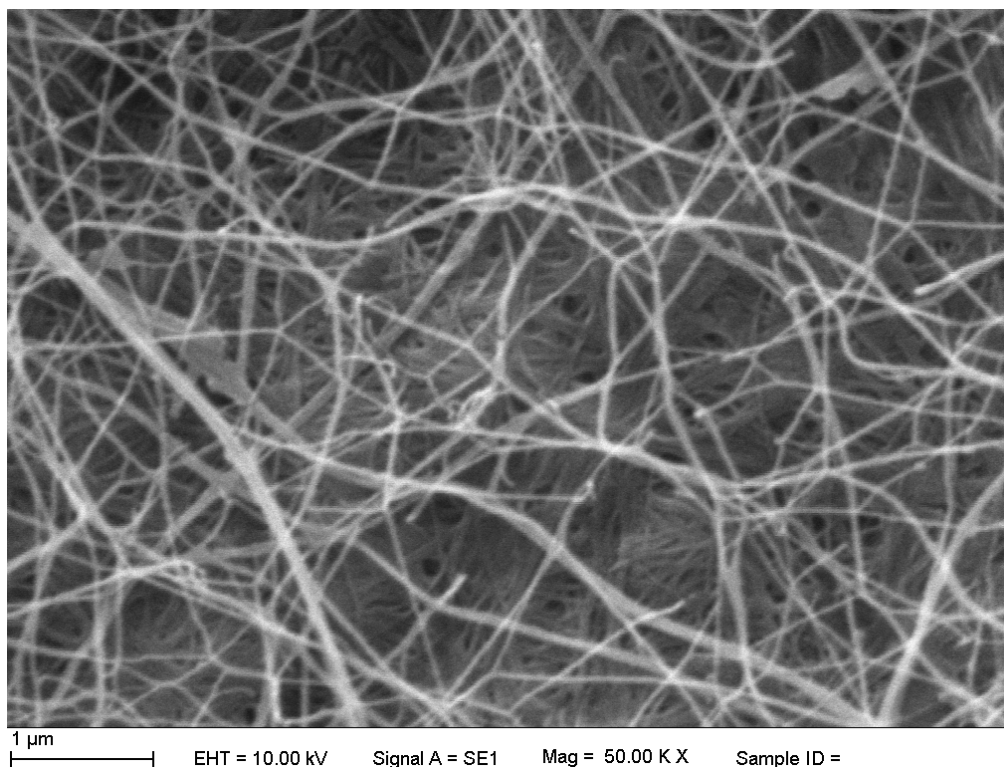


Figure 4. 5. SEM image of Cyt c-MIP nanofibers.

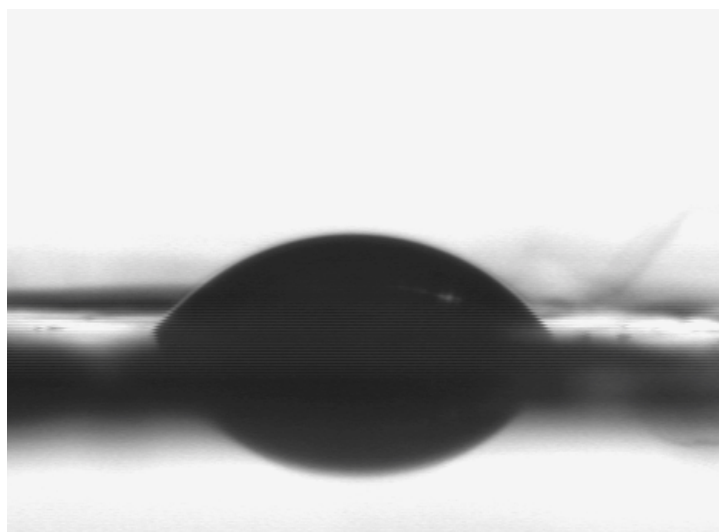


Figure 4. 6. Contact angle measurement of Cyt c-MIP nanofiber.

4. 2. Study of Conditions of Polymerization

In order to evaluate the Cyt c adsorption capacity of MIP nanofibers, batch binding experiments were performed in a well-mixed vessel. The importance of polymer composition for molecular imprinting was reviewed elsewhere [182]. The careful choice of functional monomer is very important to obtain highly specific recognition

binding sites. Actually the selection of functional monomer is determined by the structure of the template. The optimization of monomer/template ratio is crucial to create binding sites with high fidelity. For non covalent imprinting process it should be achieved empirically. For instance, if there is only one interaction point between template and monomer, the amount of template gets saturation after all the functional monomer is complexed with template molecules. However there is no saturation when there is two point interaction between template and monomer. Functional monomer/crosslinker ratio is also a critical parameter since high percentage of functional monomer will cause non specific adsorption and also low amount of cross linker will cause loose polymer structure resulting insufficient imprinting and low percentage of functional monomer will cause weak interactions with template giving low capacity of binding [29], [183], [20].

4.2. 1. Effect of Monomer/Template Ratio

It is significant to determine the amount of metal chelating monomer, for this project MAH-Cu(II), templating Cyt c to form a cavity both chemically and geometrically complementary to template molecule. In order to optimize the polymerization conditions firstly template/monomer ratio was investigated. It was changed in the range of 1 and 200 by keeping total monomer ratio constant at 1 w% and evaluated with respect to Cyt c adsorption capacity. The maximum adsorption capacity was found when monomer/template ratio was 20. Below this value the amount of metal chelating monomer, MAH-Cu(II) complex is not enough to form a well-defined cavity complementary to template molecule, Cyt c. Above this value it is hard to remove template from polymer network since MAH-Cu(II) complex interacts with Cyt c via stronger coordination bonds. Cooperation of amino acid groups able to coordinate with metal ions and local conformations may contribute to this phenomenon. The amount of created nanocavities well-fitted to template molecule is the major parameter to obtain adsorbent possessing high specificity and high adsorption capacity. For this purpose template molecule should interact functional groups of monomer molecules with high specificity creating a cavity which is complementary to only that template molecule and also after formation of these monomer-template assemblies via polymerization, the template molecules should be removed efficiently from the MIPs [184], [185],

[186]. Thus monomer/template ratio was selected as 20 and used for the rest of the study.

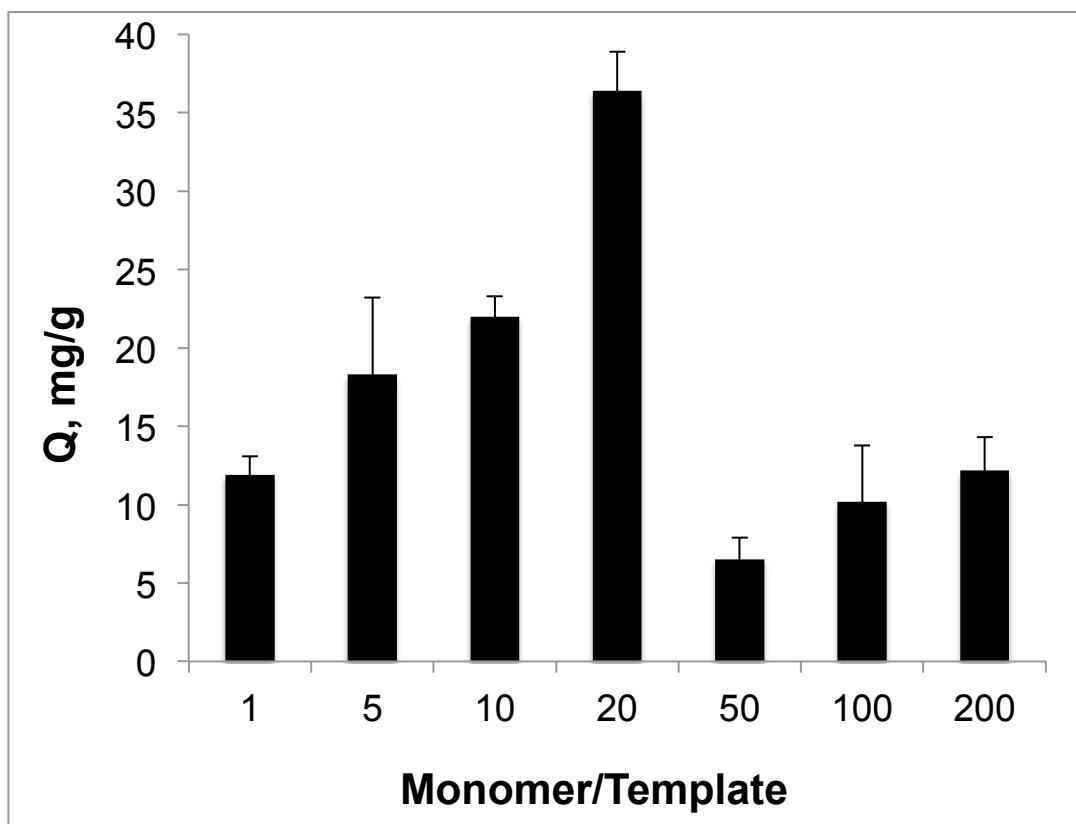


Figure 4. 7. Adsorption capacities of the MIP nanofibers with different monomer/template ratio. Experimental conditions; C_{cytc} : 0.2 mg/mL Cyt c, pH : 7, T: 25°C.

4.2. 2. Effect of Total Monomer Ratio

The investigation of the effect of total monomer ratio on adsorption capacity was required to obtain the maximum adsorption capacity and thus changed in the range of 0.5-1.5. After selection of monomer/template ratio as 20, it was seen that the maximum adsorption capacity was found when total monomer ratio was 1 w% (Figure 4.8). It is well known that cross linking is crucial for creation of well-defined molecularly imprinted polymers since monomers and cross linkers form a self assembly around the template during this process. MIP nanofibers having total monomer ratio of 0.5 w% obtain low adsorption capacity since sufficient amount of cross linker should be utilized to form a well-defined cavity for template molecule. MIP nanofibers prepared with total monomer ratio of 1.5 w% also have low

adsorption capacity since too much cross linker could not provide efficient removal of template molecules from MIP nanofibers after polymerization due to the possible buried protein molecules deep inside polymer network. Also high amount of cross linkers may cause conformational change of protein structure [27].

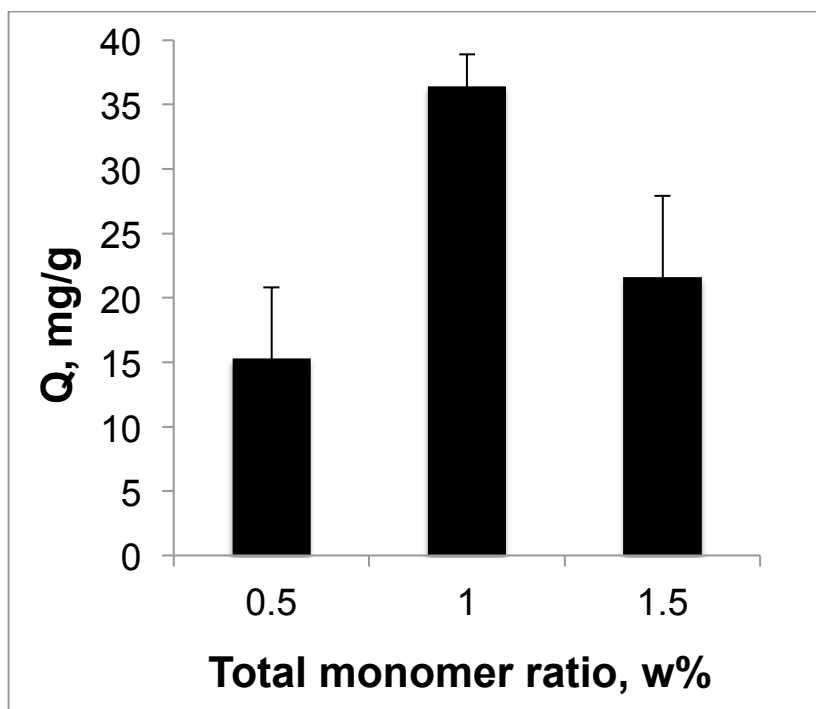


Figure 4. 8. Adsorption capacities of MIP nanofibers with different weight ratio of total monomer. Experimental conditions; $C_{\text{Cyt c}}$: 0.2 mg/mL Cyt c, pH : 7, T: 25°C.

4.2. 3. Effect of Polymerization Time

The polymerization time is one of the key factors to obtain well-defined binding sites [187]. Short polymerization time will cause the formation of binding sites which does not fit to the template molecule precisely since there will be not enough time for cross linkers to form a cavity available for template. Long polymerization time will cause low template removal since the polymer structure will be rigid and many template molecules will be buried deep inside the polymer network. As can be seen from the figure below, optimum polymerization time is 30 min for this study.

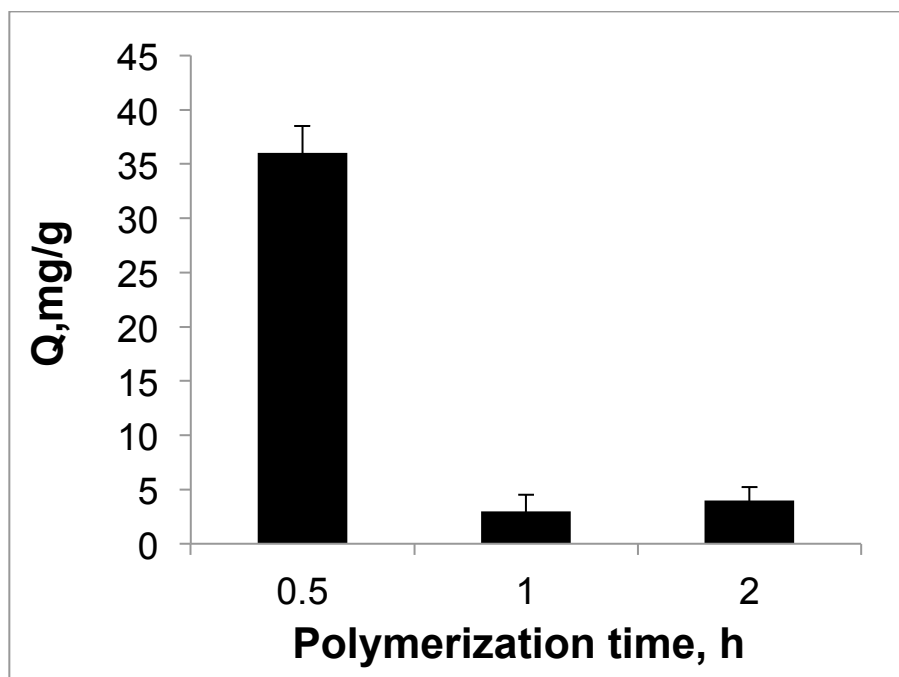


Figure 4. 9. Adsorption capacities of MIP nanofibers with different polymerization time. Experimental conditions; $C_{\text{cyt c}}$: 0.2 mg/mL Cyt c, pH : 7, T: 25°C.

4. 3. Rebinding studies

4.3. 1. Effect of pH

Cyt c adsorption studies were performed in phosphate buffer at different pH values. Proteins are affected by conditions of their environment and pH is one of the most important influence on protein folding. During the molecular imprinting process template molecule is imprinted forming a nanocavity corresponding to the structure how the template is in that polymerization medium. It is mentioned in many molecular imprinting studies that pH of solution used for adsorption tests is generally same with the pH of polymerization medium of molecular imprinting procedure utilized to obtain MIP [63], [188], [189]. In that project, MAH-Cu(II)-Cyt c ternary complex was prepared at pH 7 phosphate buffer. In the figure below it is seen that maximum adsorption capacity was obtained at pH 7 phosphate buffer via the conformational memory fitting to recognition nanocavity through distribution of the chelate groups and the shape of the template molecule.

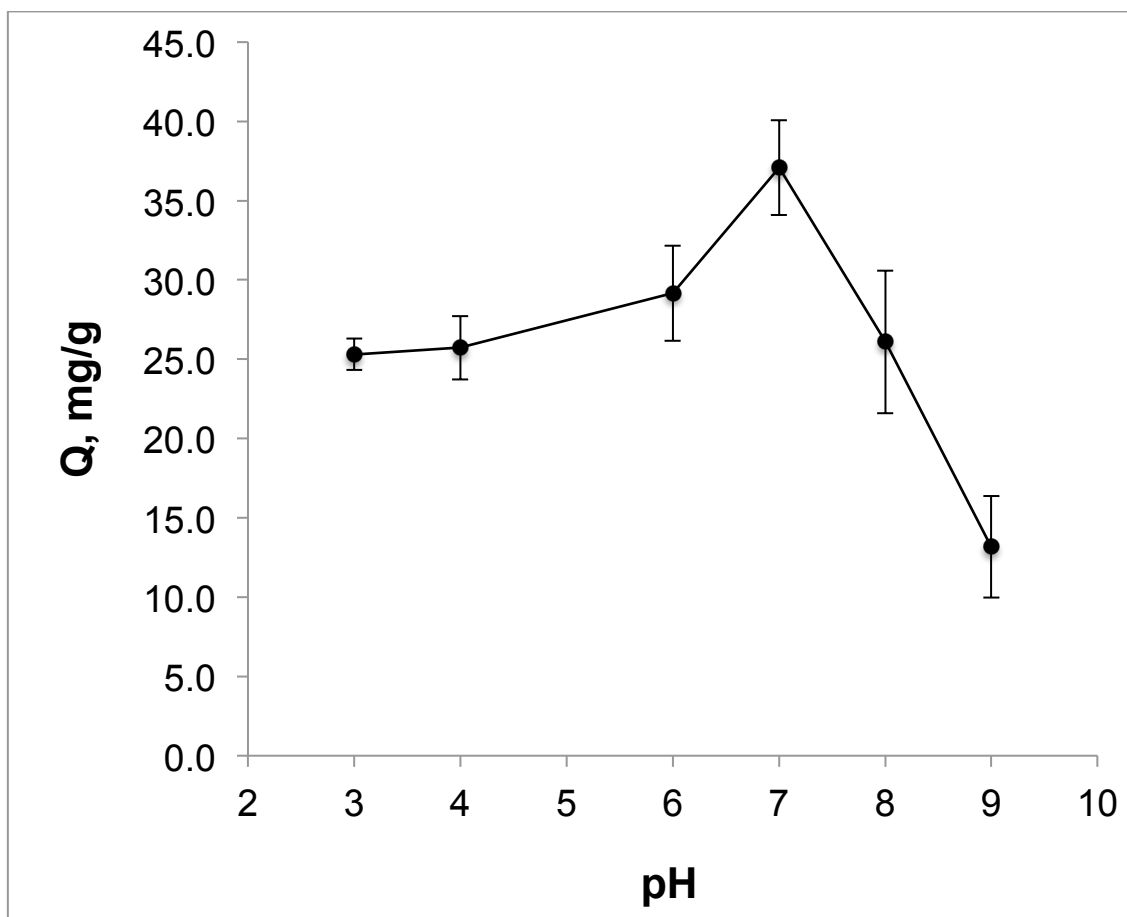


Figure 4. 10. Effect of pH of adsorption solution on adsorption capacity of MIP nanofibers. Experimental conditions; C_{cytc} : 0.2 mg/mL Cyt c, T: 25°C.

4.3. 2. Effect of Temperature

The conformational arrangement of proteins is strongly dependent on temperature. The temperature effect on adsorption process was also investigated and adsorption tests of Cyt c was carried out at 4, 14 and 25 °C (Figure 4.11). The maximum adsorption capacity was found at 25 °C which demonstrates memory effect of binding sites since the polymerization was performed at this temperature. The shape and chemical structure of the binding sites were complementary to template molecule at 25°C which was the temperature of polymerization process. Below that value the shape and structure of the binding sites was not suited well to target protein, Cyt c referring to conformational memory at that temperature [190], [191]. This result was in parallel with the result of pH effect explained above which shows MIP nanofibers was able to memorise pH and temperature used in polymerization procedure.

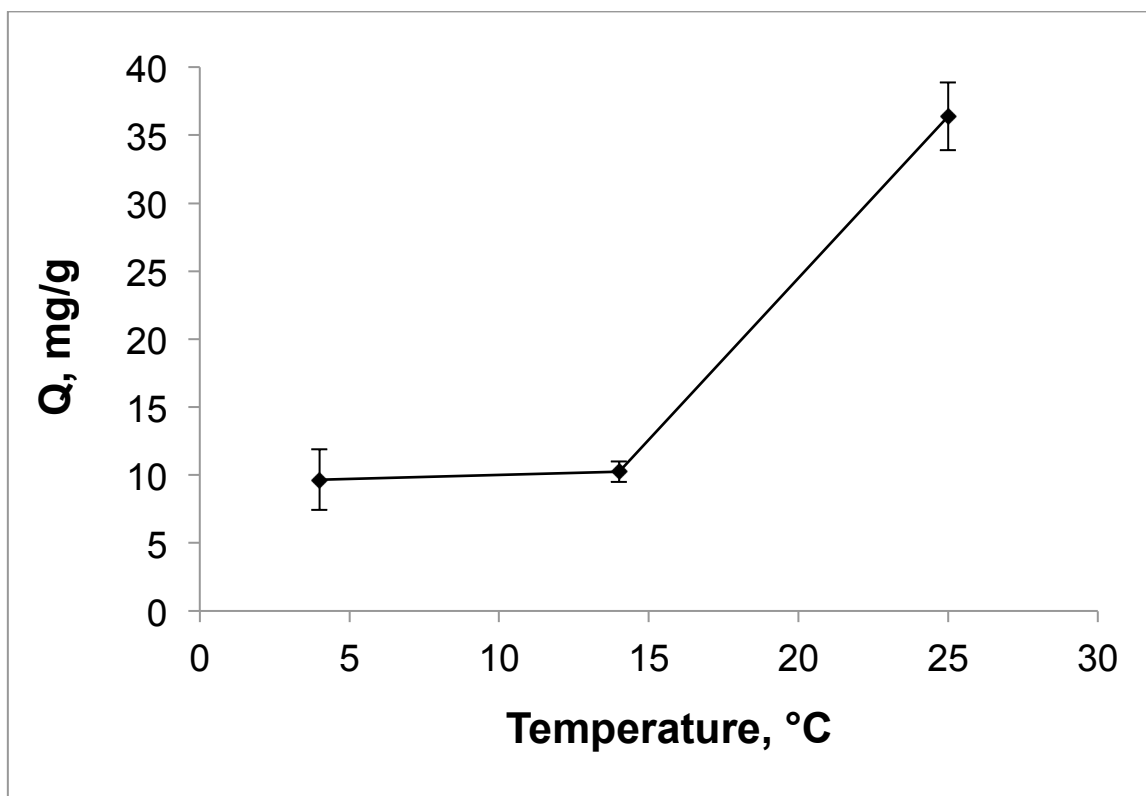


Figure 4. 11. Effect of temperature of adsorption solution on adsorption capacity of MIP nanofibers. Experimental conditions; C_{cytc} : 0.2 mg/mL Cyt c, pH: 7.0.

4.3. 3. Effect of NaCl Concentration

The effect of NaCl concentration on Cyt c adsorption was also evaluated. Increasing ionic strength resulted the decrement of adsorption capacity of MIP nanofibers. The salt molecules may interact with Cyt c molecules via electrostatic interactions and mask the binding sites [192]. The binding was occurred up to 0.05 M NaCl concentration and after that value all the binding sites are placed by salt molecules resulting a saturation value (Figure 4.12). This may tell that the electrostatic interactions may contribute to the binding of Cyt c to MIP nanofibers.

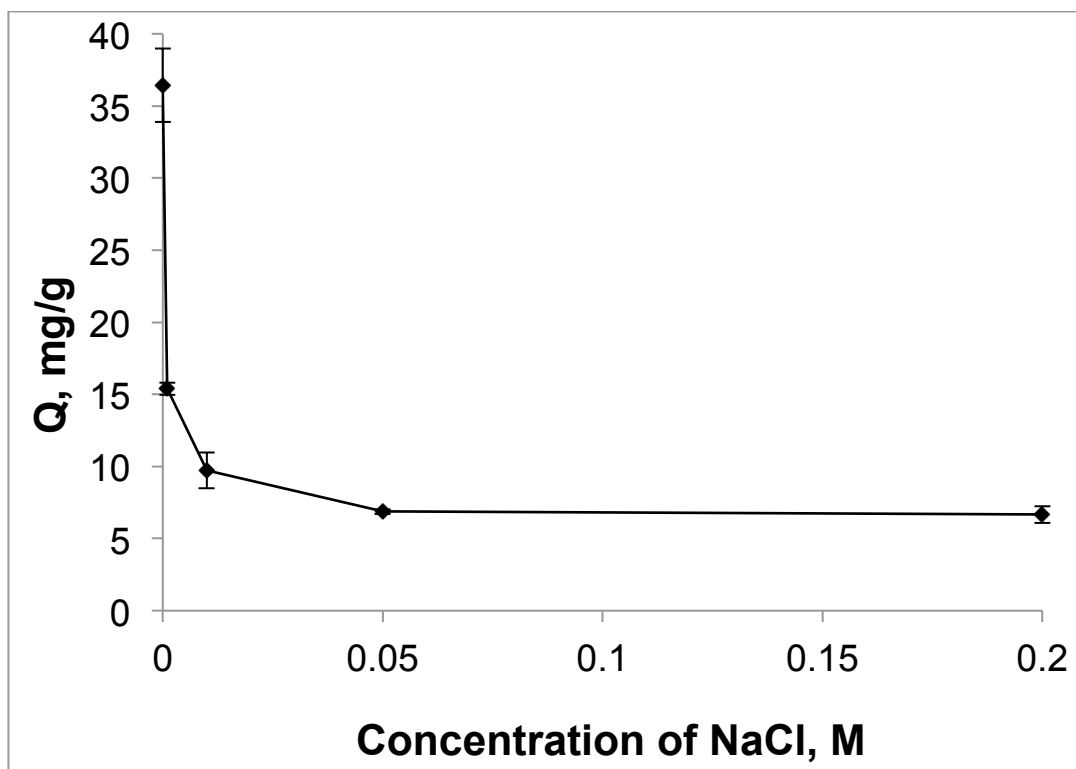


Figure 4. 12. Effect of NaCl concentration on adsorption capacity of MIP nanofibers. Experimental conditions; C_{cytc} : 0.2 mg/mL Cyt c, T: 25°C, pH:7.0.

4. 4. Binding Isotherms

Figure 4.13 shows the adsorption isotherm of MIP nanofibers and demonstrates that the adsorption capacity of MIP nanofibers increases with increasing Cyt c concentration. The saturation value is achieved at 0.5 mg/mL of Cyt c solution which means after that concentration value there is no recognition sites accessible to Cyt c molecules. As can be seen from the figure the maximum capacity is 36.4 mg/g.

An adsorption isotherm is a curve correlating amount of solute adsorbed onto the solid (q_e) and the concentration of the solute in the liquid phase (C_e) at a given temperature. Langmuir isotherm is one of the most widely used isotherms based on adsorption at homogeneous sites within the adsorbent concerning assumptions of monolayer adsorption and equivalent surface binding sites. Energy distribution is constant due to Langmuir since the model assumes a homogeneous surface and no interaction between adjacent adsorbed molecules.

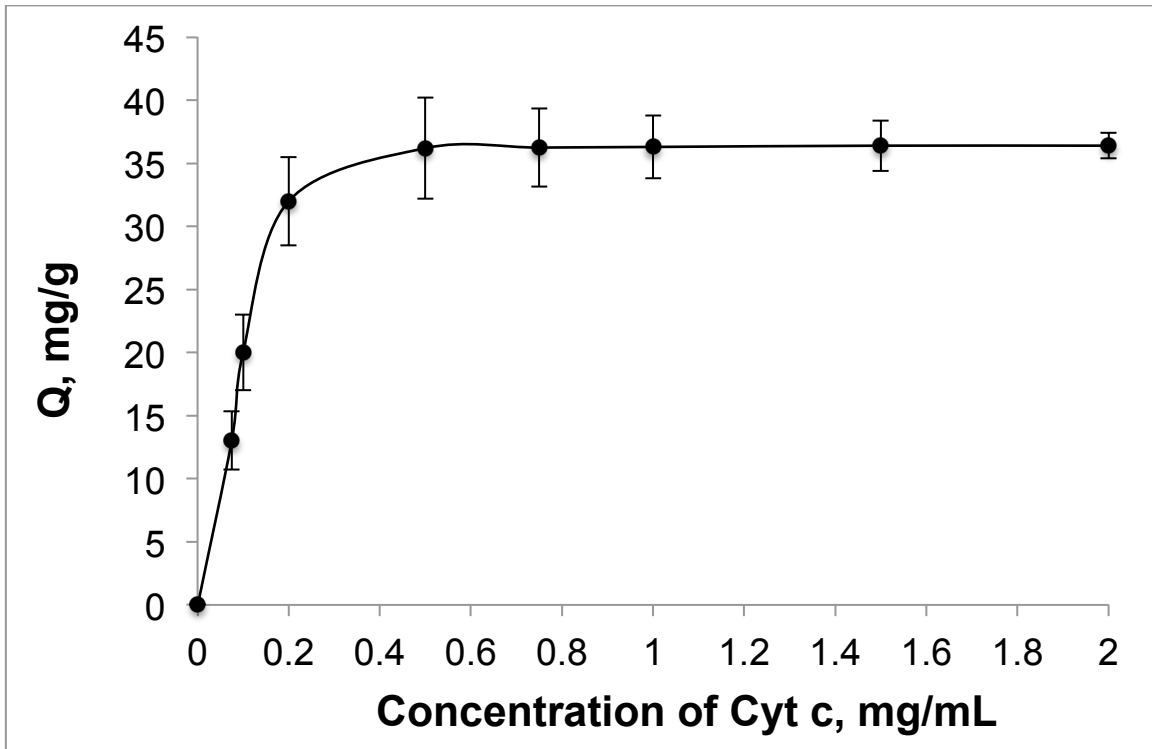


Figure 4. 13. Effect of equilibrium concentration Cyt c on adsorption capacity of MIP nanofibers. Experimental conditions; C_{cytc} : 0.2 mg/mL Cyt c, T: 25°C, pH: 7.0.

It is expressed as follows [193]:

$$q_e = q_{\max} K_L \frac{C_e}{(1 + K_L C_e)} \quad (2)$$

and linearized as $\frac{C_e}{q_e} = \frac{C_e}{q_{\max}} + 1/K_L q_{\max}$ where q_{\max} is the maximum adsorption capacity (mg/g) and K_L is the Langmuir adsorption equilibrium constant (mL/g). The values of q_{\max} and K_L can be derived from the plot of $1/q_e$ versus $1/C_e$ [124].

The Freundlich isotherm model is based on adsorption on heterogenous surface and predict can be expressed as follows [194]:

$$q_e = K_F C_e^{1/n} \quad (3)$$

It can be linearized as $\ln q_e = \frac{\ln C_e}{n} + \ln K_F$ where K_F is Freundlich parameter regarding binding affinity and n is heterogeneity index. The Freundlich parameters can be calculated from the plot of $\ln q_e$ versus $\ln C_e$.

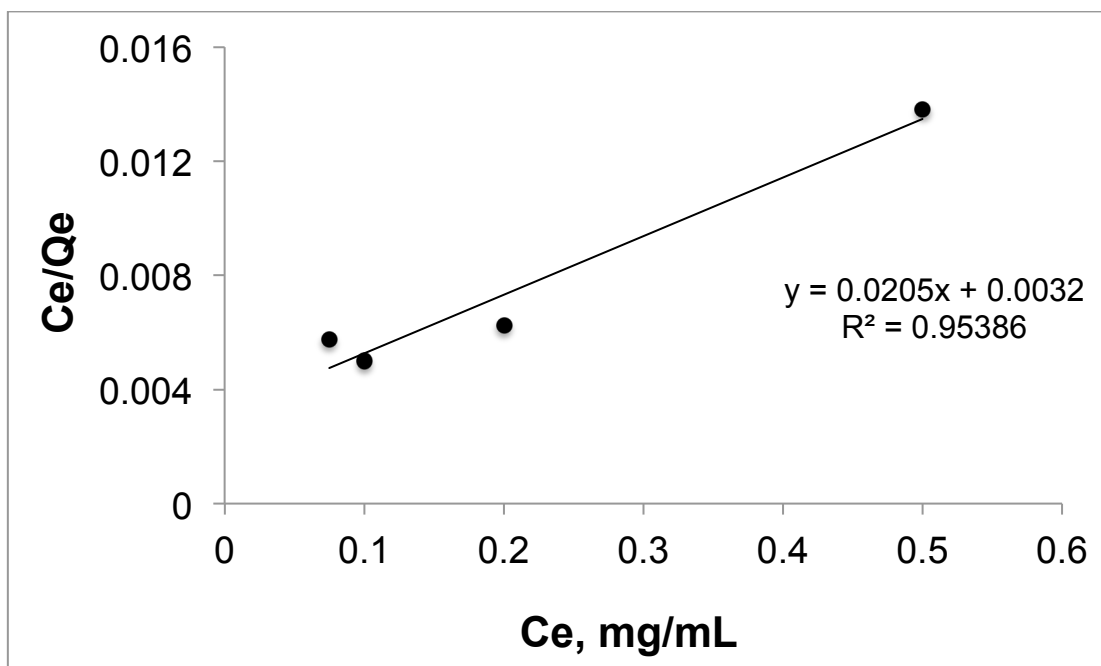


Figure 4. 14. Langmuir isotherm of MIP nanofibers.

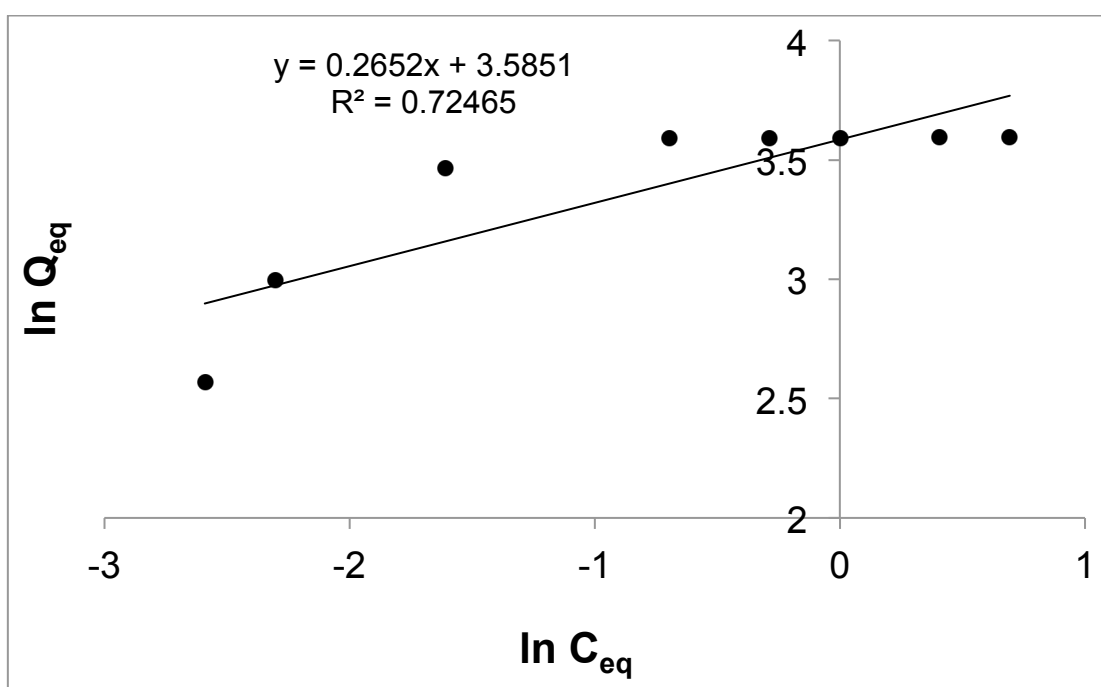


Figure 4. 15. Freundlich isotherm of MIP nanofibers.

The plots of Langmuir and Freundlich adsorption isotherms were shown in Figure 4.14 and 4.15 respectively. According to higher regression coefficients it was determined that adsorption of Cyt c onto MIP nanofibers was in more conformity with Langmuir isotherm than Freundlich isotherm.

Table 4. 1. Langmuir and Freundlich parameters of MIP nanofibers

Langmuir	Freundlich
Q_{max} : 48.78 mg/g	K_F : 35.50 mg/g
K_L : 6.40 mL/mg	n : 3.83
R^2 : 0.953	R^2 : 0.724

Table 4. 2. Comparison of Cyt c adsorption capacities of different adsorbents with MIP nanofibers prepared in this study

Reference number	Q_{max} , mg/g
187	31.7
144	30
188	42
189	40.1
190	20.8
191	222
70	19.7
146	75
183	100
192	126

The results were compared with the results of research studies based on Immobilized Metal Affinity Chromatography, IMAC [195], [153], [196], [197], [198], [50]. Poly(HEMA-MAH) beads were prepared for Cyt c adsorption with a Cu^{2+} loading of 658 $\mu\text{mol/g}$. The maximum Cyt c adsorption capacity was achieved 31.7 mg/g. The recovery of recombinant metal-binding protein was performed with IDA- Cu^{2+} adsorbents and the maximum adsorption capacity of Cyt c was obtained approximately 30 mg/g. IDA was coupled to the surface of magnetic agarose and then chelated with Cu^{2+} ions. It was determined that the maximum adsorption capacity of Cyt c with the IDA- Cu^{2+} magnetic agarose was 42 mg/g. Magnetic poly(2-hydroxyethylmethacrylate) (mPHEMA) beads were reacted with poly(ethyleneimine) (PEI) and then chelated with Cu^{2+} ions (20-793 $\mu\text{mol/g}$). The maximum Cyt c adsorption capacity was obtained 40.1 mg/g with mPHEMA/PEI beads. Poly(hydroxyethyl methacrylate-N-methacryloyl-(L)-histidine methyl ester) (PHEMAH) monolithic cryogel column was prepared with MAH monomer as a metal-chelating ligand and then chelated with Cu^{2+} ions. The maximum adsorption capacity of Cyt c was performed as 20.8 mg/g with the monolithic column containing 113.7 μmol MAH/g and 58.7 μmol Cu^{2+} /g. Magnetic beads (mag-

poly(EGDMA-MAH)) utilizing MAH as a metal-chelating monomer was synthesized via suspension polymerization of ethylene glycol dimethacrylate (EGDMA) and then chelated with Cu^{2+} ions. The maximum adsorption capacity of Cyt c with mag-poly(EGDMA-MAH) beads containing 70 μmol MAH/g and 68 μmol Cu^{2+} /g was obtained 222 mg/g. The maximum Cyt c adsorption capacity of this study is quite comparable with the literature explained above. The adsorption capacity of this study is higher than that of surface imprinted nanowires for Cyt c recognition (19.7 mg/g) [75]. Despite the other MIP studies from the literature performed higher adsorption capacity for Cyt c, there is not enough information about selectivity factors [155], [192]. The Cyt c-MIP cryogel demonstrated maximum adsorption capacity as 126 mg/g although the selectivity factor toward lysozyme was less than that of this study which will be discussed later (Section 4.7) [199]. MIP nanofibers prepared in that study exhibited high recognition characteristics to Cyt c molecules due to their unique properties bearing high surface area and high specificity.

4. 5. Binding Kinetics

As it is well known MIPs exhibit fast binding kinetics as well as high recognition capacity and high selectivity. The recognition time of MIP nanomaterials templating different molecules and prepared due to different approaches changes in the range of 5 min to 10 h [200], [201]. From the figure below it is clearly seen that the recognition time required to reach equilibrium for MIP nanofibers is only 5 min which is much shorter than that of molecularly imprinted nanomaterials templating proteins [202], [203]. This unique characteristics can be attributed to the very thin polymer layer formed over the nanofibers via the combination of surface imprinting approach and high surface area/volume ratio of nanofibers avoiding mass transfer limitations and thus leading target molecules easily accessible to imprinted sites [204]. Also metal ion coordination may contribute to the high affinity since metal ions mediates protein molecules possessing high selectivity.

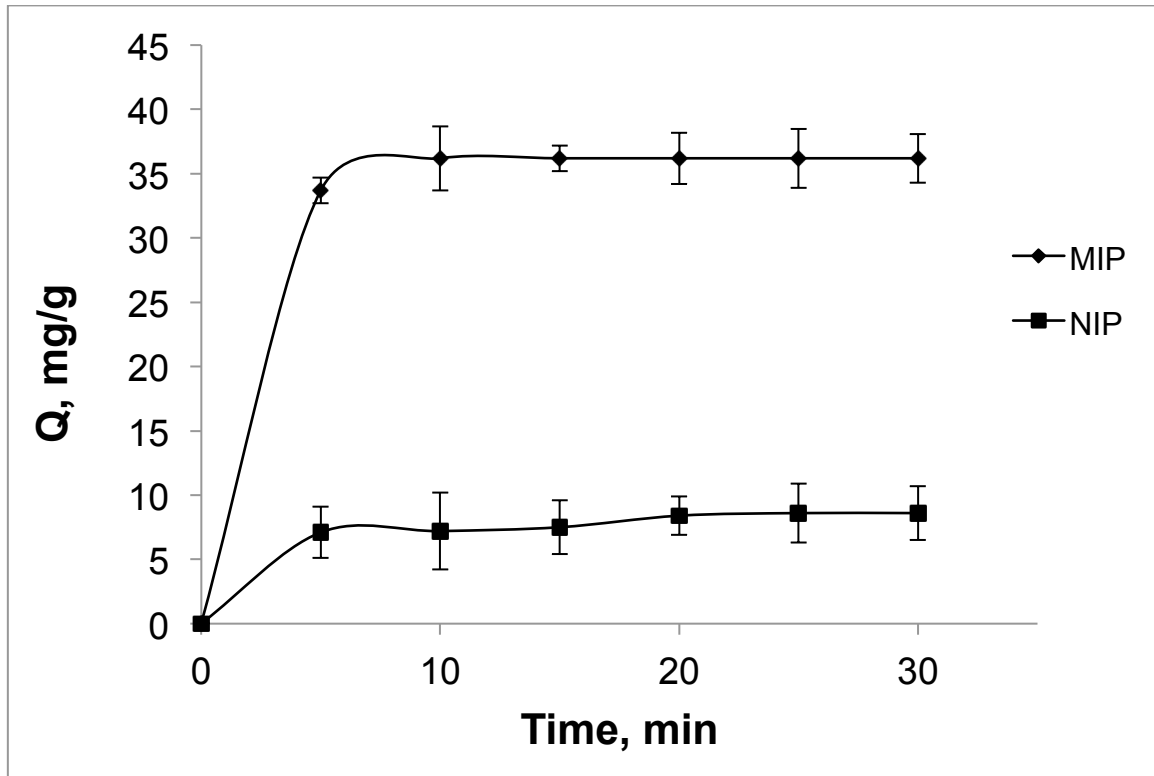


Figure 4. 16. Binding kinetics of MIP nanofibers. Experimental conditions; C_{cytc} : 0.2 mg/mL Cyt c, T: 25°C, pH: 7.0.

Adsorption is multi-step process regarding transport of analyte molecules in the solution phase via bulk diffusion, film diffusion, intraparticle diffusion and adsorption of molecules onto the surface of adsorbent material. In order to determine the underlying mechanism of Cyt c adsorption onto MIP and NIP nanofibers (whether it is based on physical or chemical mechanism), three kinetic models [205] used to test experimental data are as follows:

a.) Pseudo-first order kinetic model is generally expressed as

$$\frac{dq}{dt} = k_1 (q_{\text{eq}} - q) \quad (4)$$

where q_{eq} and q are the amounts of adsorption capacity of nanofibers at equilibrium and time t respectively; k_1 is the rate constant of first-order adsorption.

This equation can be linearized as follows:

$$\log (q_{\text{eq}} - q) = \log q_{\text{eq}} - k_1 \frac{t}{2.303} \quad (5)$$

b.) Pseudo-second order kinetic model is generally expressed as

$$\frac{dq}{dt} = k_2 (q_{\text{eq}} - q)^2 \quad (6)$$

where k_2 is the rate constant of second-order adsorption. It is linearized as

$$\frac{t}{q} = \frac{1}{k_2 q_{eq}^2} + \frac{t}{q_{eq}} \quad (7)$$

c.) Intraparticle diffusion model is defined as

$$q = k_p t^{0.5} + C \quad (8)$$

where k_p is intraparticle diffusion rate constant and C is the intercept which represents resistance to mass transfer in the external liquid film.

Pseudo-first order kinetic, pseudo-second order kinetic and intraparticle kinetic model were tested and shown by the linear analysis $\log(q_{eq}-q)$ vs. t , t/q vs. t and q vs. $t^{0.5}$ respectively. The kinetic parameters were calculated and listed. The applicability of appropriate kinetic model is evaluated by the magnitude of the correlation coefficients R^2 shown in Table 3.4 and determined as Cyt c adsorption onto MIP and NIP nanofibers fits to second-order kinetics since correlation coefficient of second-order kinetic model was far higher than that of first-order kinetic model. Furthermore calculated values of q_{eq} of second order kinetic model coincide with the experimental values of q_{eq} .

Kinetic results should be evaluated with intraparticle diffusion since second order kinetic model cannot explain diffusion mechanism. If the regression of plot of intraparticle diffusion model is linear and passes through origin, the rate limiting step is only due to intraparticle diffusion [206], [207]. In that case it is linear but it did not pass through origin (Figure 4.19). Furthermore the regression coefficient is lower than that of second order kinetics model, thus Cyt c adsorption may be controlled by intraparticle diffusion but dominant effect is caused by chemical adsorption.

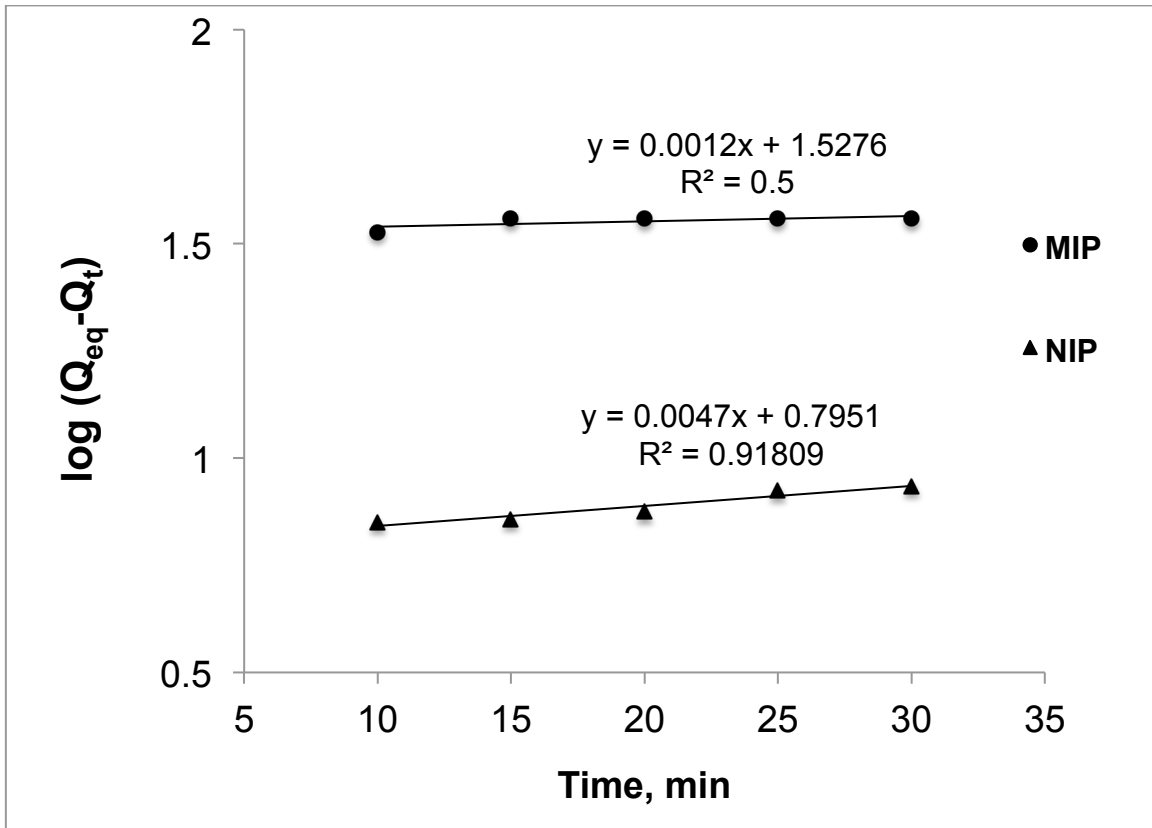


Figure 4. 17. First-order kinetics of adsorption of MIP and NIP nanofibers.

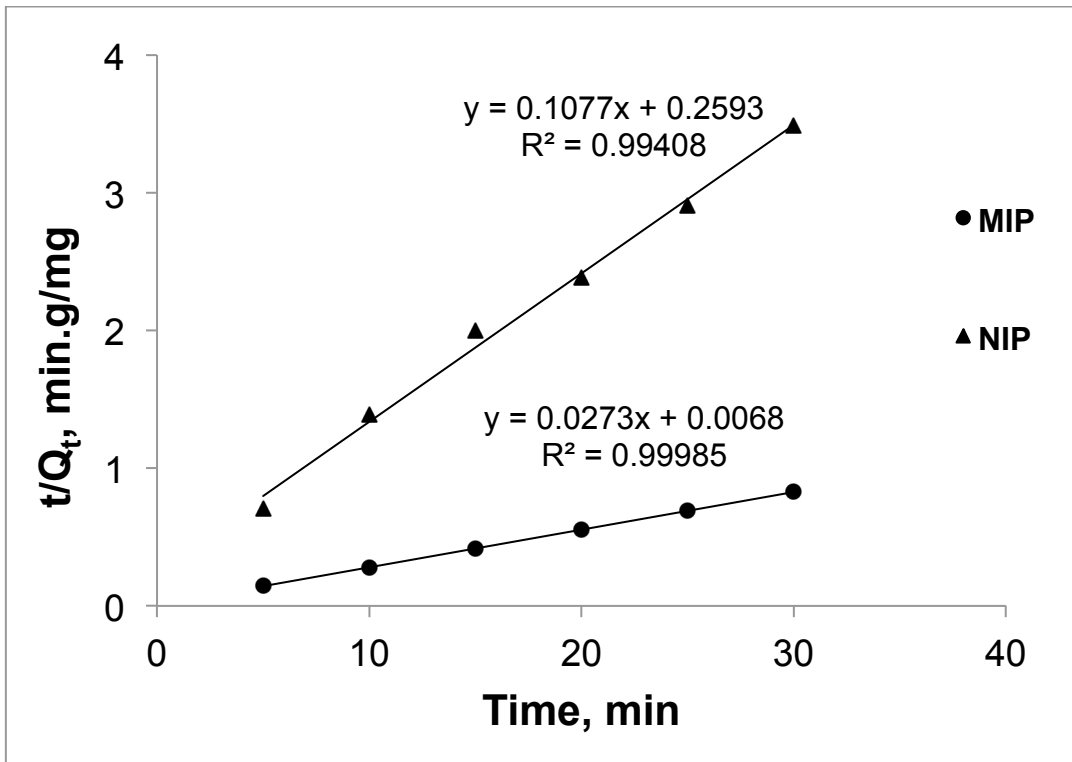


Figure 4. 18. Second-order kinetics of adsorption of MIP and NIP nanofibers.

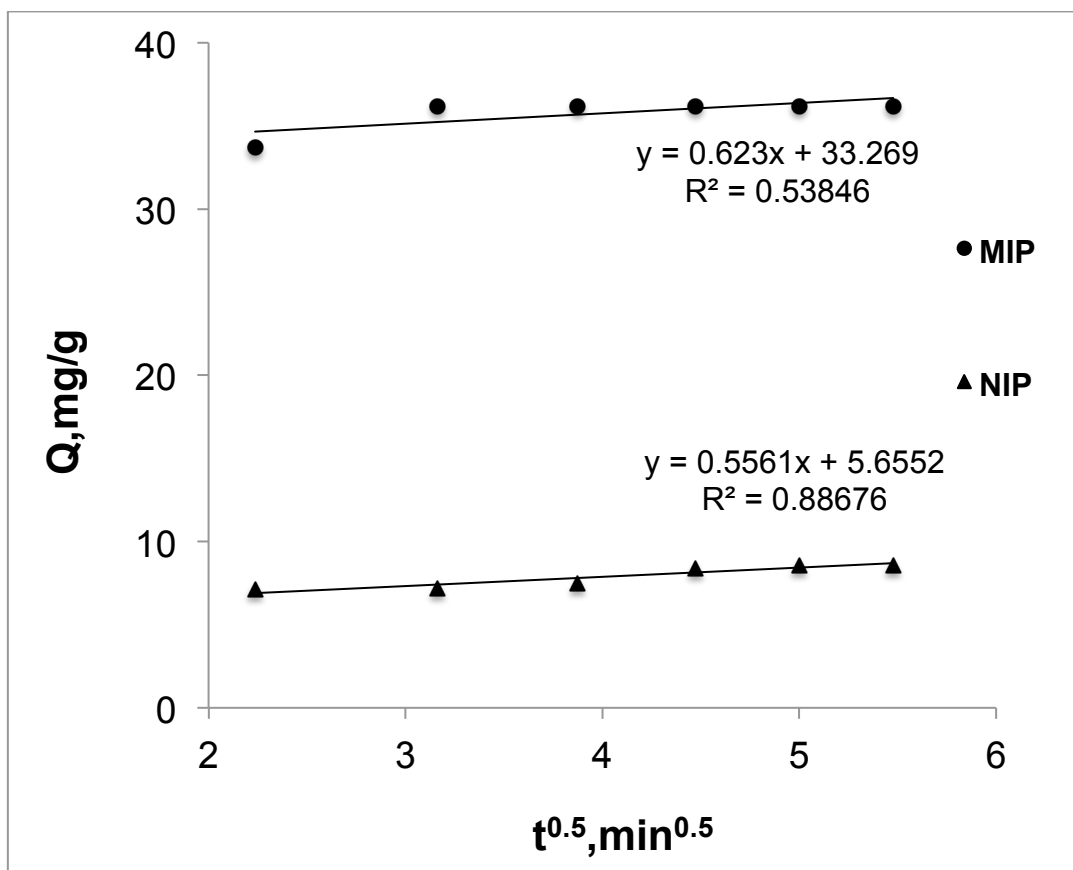


Figure 4. 19. Intraparticle diffusion kinetic model of MIP and NIP nanofibers.

Table 4. 3. Constants for first and second order kinetic and intraparticle diffusion kinetic model of adsorption of MIP and NIP nanofibers

	Kinetic parameters	MIP	NIP
First-order	$k_1 (x10^2 \text{ min}^{-1})$	0.0027	0.010
	$Q_{eq, \text{cal}} (\text{mg g}^{-1})$	33.69	6.23
	R^2	0.500	0.918
Second-order	$k_2 (x10^3 \text{ g mg}^{-1} \text{ min}^{-1})$	0.11	0.044
	$Q_{eq, \text{cal}} (\text{mg g}^{-1})$	36.63	9.28
	R^2	0.999	0.994
Intraparticle diffusion	$k_p (\text{mg g}^{-1} \text{ min}^{0.5})$	0.62	0.55
	$C (\text{mg g}^{-1})$	33.26	5.65
	R^2	0.538	0.886

4. 6. Thermodynamic Analyses

Binding process occurs through the attractive forces between binding site of the protein and complimentary groups of recognition cavity of the MIPs. Binding of the protein to binding site takes place when these forces lead protein-binding site complex which results in either entropy or enthalpy reduction in free energy of the system [208]. Since thermodynamic parameters give significant information about energy changes of adsorption, thus these parameters should be determined. Gibbs free energy change ΔG° that provides the level of spontaneity of adsorption, enthalpy change ΔH° and entropy change ΔS° were calculated in this study using the following equations:

$$\Delta G^\circ = -RT \ln K_L \quad (9)$$

$$\Delta G^\circ = \Delta H^\circ - T\Delta S^\circ \quad (10)$$

Thus rearranged as;

$$\ln K_L = -\frac{\Delta H^\circ}{RT} + \frac{\Delta S^\circ}{R} \quad (11)$$

where K_L is Langmuir adsorption constant, R is gas constant (8.314 J/mol K), T is temperature (K). From the plot of $\ln K_L$ versus $1/T$ namely van't Hoff plot, ΔH° and ΔS° was calculated and listed in table below. Negative values of ΔG° indicates the spontaneous and thermodynamically feasible adsorption of cytochrome c onto MIP nanofibers which is comparable with that of lysozyme [209]. Positive value of ΔS° shows an increased randomness at solid-liquid interface during adsorption of protein molecules on the recognition sites [210]. According to negative value of ΔH° , it infers that adsorption of cytochrome c was exothermic.

Table 4. 4. Thermodynamic parameters of MIP nanofibers

Temperature, °C	ΔG° (kJ/mol)	ΔH° (kJ/mol)	ΔS° (J/mol)
4	-69.40	-27.69	150.6
15	-71.06		
25	-72.56		

4. 7. Selectivity Studies

The selectivity of MIP nanofibers based on the level of correspondence of protein surface and imprinted binding cavity. During imprinting process functional groups are spatially distributed and directed complementary to protein surface chemistry and geometry. In that study MAH-Cu(II) functional monomers via metal ion coordination orientate Cyt c molecules via self assembly and after fixing protein molecules into the polymer network during polymerization and removal of them via extraction, there exist highly specific recognition sites based on both shape and conformational memory [211], [212]. The combination of IMAC principles and molecular imprinting provides promising method to achieve highly selective protein recognition using metal ions as pivot. The best affinity for Cyt c was found when MIP nanofibers were used for adsorption experiments (Figure 4.20). The amount of adsorption of Cyt c-MIP was higher than the amount of adsorption of Cyt c of both NIP and M(Cyt c). NIP is the polymer prepared via the polymerization of same polymerization medium without target protein Cyt c. Polymer layer created without recognition cavities thus performed low adsorption capacity since functional groups, MAH-Cu(II) in that case, distributed randomly throughout the polymer network. M(Cyt c) is the polymer without Cu(II) ions prepared via complexation of MAH and Cyt c prepared with lack of metal ion coordination between metal ions and protein molecules. Without metal ions assistance, polymer layer showed weak affinity to template. All results prove that both metal ion coordination and recognitive binding sites complementary to Cyt c was necessary to achieve highly selective recognition [213].

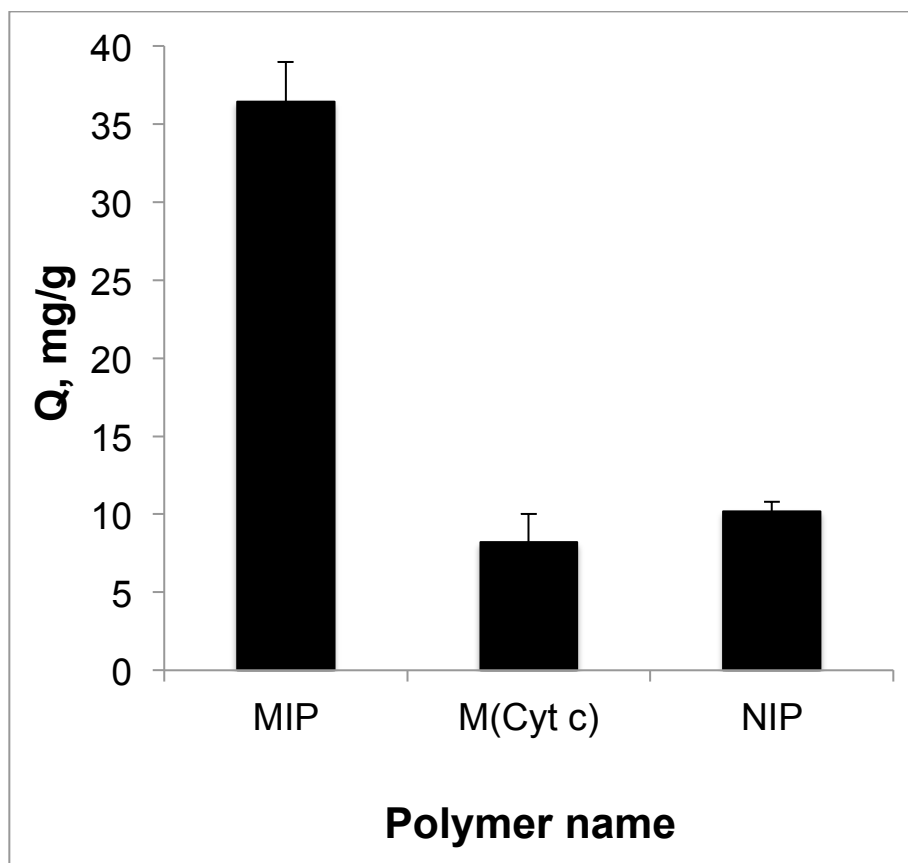


Figure 4. 20. Effect of metal ion coordination and molecular imprinting process on adsorption capacity of Cyt c. Experimental conditions; C_{cytc} : 0.2 mg/mL Cyt c, T: 25°C, pH: 7.0.

Imprinting factor (IF) was evaluated with respect to the ratio of cytochrome c adsorption capacity of MIP and NIP nanofibers and found as 3.6 which was significantly higher than that of Cyt c-MIP cryogels reported by Tamahkar et al. which was achieved as 1.74 by using MAH-Cu(II) as metal chelating monomer, 2-hydroxyethyl metacrylate (HEMA) as assistant monomer and N-N'methylenebisacrylamide (MBAAm) as crosslinker. Selectivity factor (α) of MIP nanofibers which was calculated as the ratio of IF of template molecule to the IF of non-template molecule was determined as 2.7 which was basically consistent with that of other materials for protein recognition [82], [214]. These results show that MIP nanofibers recognize cytochrome c molecules preferentially due to the matching of template protein to the well-defined imprinted binding sites.

Selective recognition of MIP nanofibers were determined using template protein and competing proteins which differ in molecular weight, isoelectric point and number of surface histidine(s) [215], [153]. As can be seen from the figure below,

MIP nanofibers show highest affinity to cytochrome c since other non-template proteins did not fit to Cyt c imprinted nanocavities. Eventhough lysozyme has isoelectric point very similar to template protein cytochrome c, MIP nanofibers present higher affinity to cytochrome c than lysozyme. All the non template proteins did not match to the imprinted nanocavities since recognition mechanism might be attributed to shape memory as a dominating factor [216], [217].

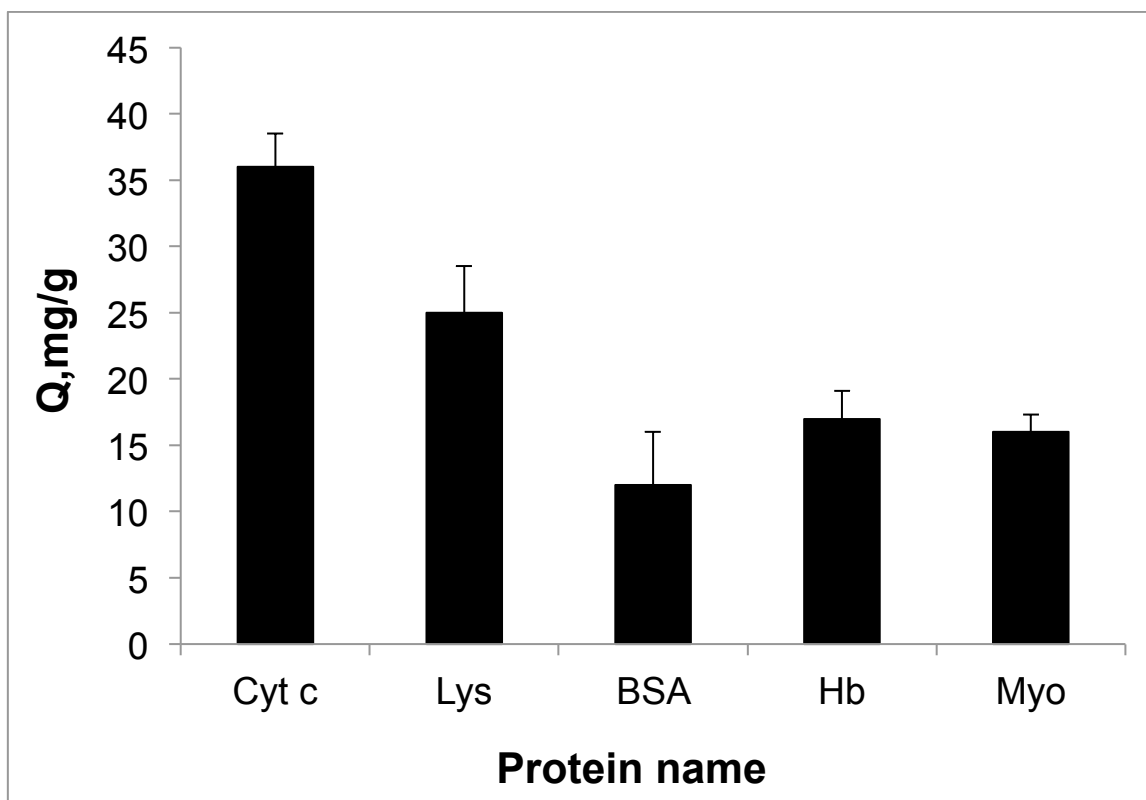


Figure 4. 21. The adsorption capacity of cyt c and competing proteins on Cyt c-MIP nanofibers. Experimental conditions; C_{protein} : 0.2 mg/mL, T: 25°C, pH: 7.0.

4. 8. QCM Studies

In order to demonstrate the recognition capability of Cyt c-MIP nanofibers, also QCM studies were performed with Cyt c-MIP nanofibers casted onto QCM sensor chip surface. Obtained data were analysed with RQCM (Maxtek) software and the curves were plotted for the determination of real-time monitoring, selectivity and reproducibility.

4.8. 1. Surface Morphology of QCM nanosensor

Surface morphology of Cyt c-MIP nanofibers cast onto QCM sensor chip was characterized with AFM (Figure 4.23). It was obviously seen that bacterial cellulose nanofibers were achieved to establish well onto QCM sensor chip showing the efficiency of the procedure used for the preparation of sensor chip surface. It was observed that there was no significant difference in diameter of the nanofibers since thin MIP layer was established onto the bacterial cellulose nanofibers. The diameter of nanofibers was 50-100 nm which is consistent with literature [218]. MIP bacterial cellulose nanofibers with large specific surface area present great potential for preparation of sensing materials. As a conclusion, coherency was seen between AFM and SEM (Figure 4.5) measurements.

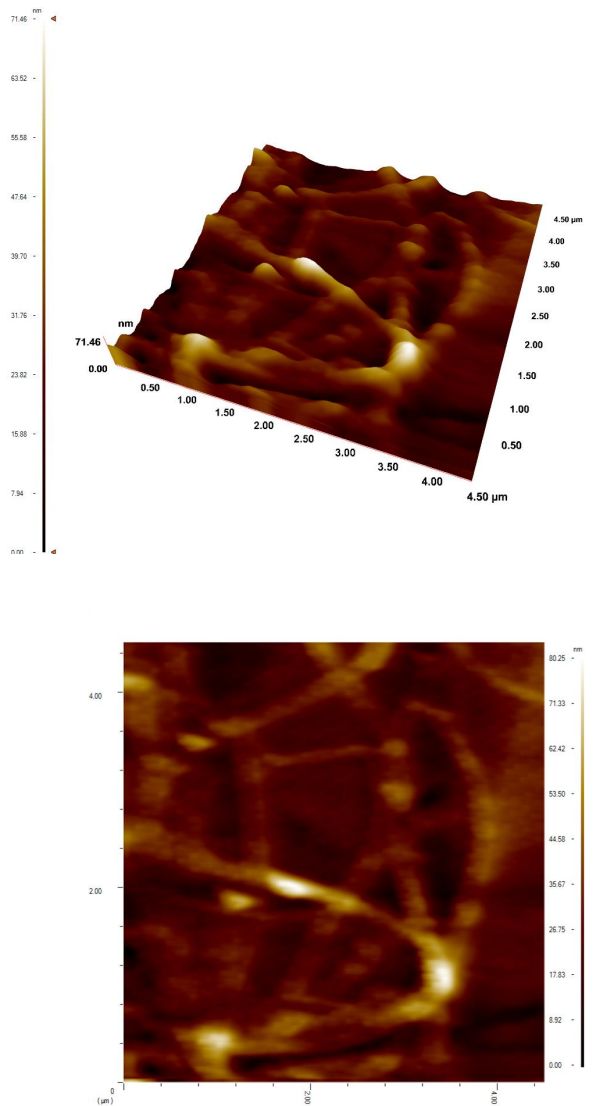


Figure 4. 22. AFM images of MIP nanofiber QCM chip.

4.8. 2. Kinetic Studies with Cyt c-MIP QCM nanosensor

To evaluate the relation between QCM signal and Cyt c concentration, the Cyt c aqueous solutions having concentration in the range of 1-75 $\mu\text{g/mL}$ were prepared. The solutions were injected to the system and contacted with QCM chip surface with the help of peristaltic pump. Figure 4.24 displays the sensorgrams obtained from different concentrations of Cyt c solutions. The frequency shift increases with the increase in cytochrome c concentration which yields the increase in driving force between protein and binding sites. The binding process arises as a result of interaction forces that exhibit between complementary sites on the protein and the recognition site fabricated onto the QCM chip surface. After desorption solution was applied, frequency value returns to the initial state. The response bears a dramatical drop just after the injection of cytochrome c molecules to the chamber and achieves a steady value after several minutes. That fast response was enabled because of highly specific recognition of cytochrome c molecules through easily accessible binding sites [219]. Figure 4.25 is the sensorgrams that show relation between mass shift (Δm) and cyt c concentration.

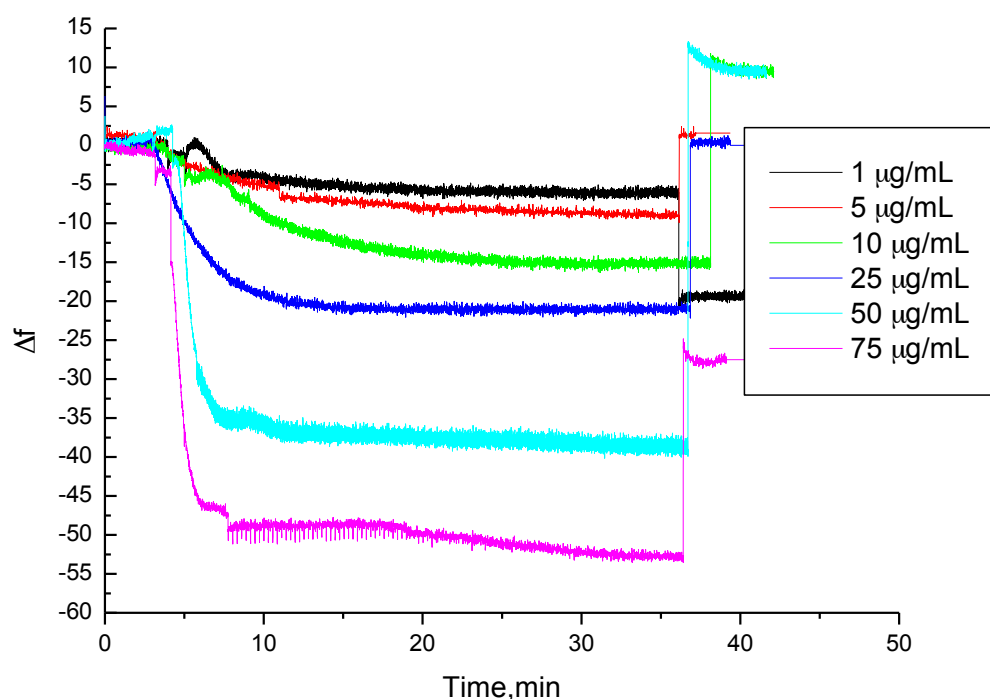


Figure 4. 23. Dynamic response of Cyt c-MIP nanofibers QCM sensors with respect to frequency change.

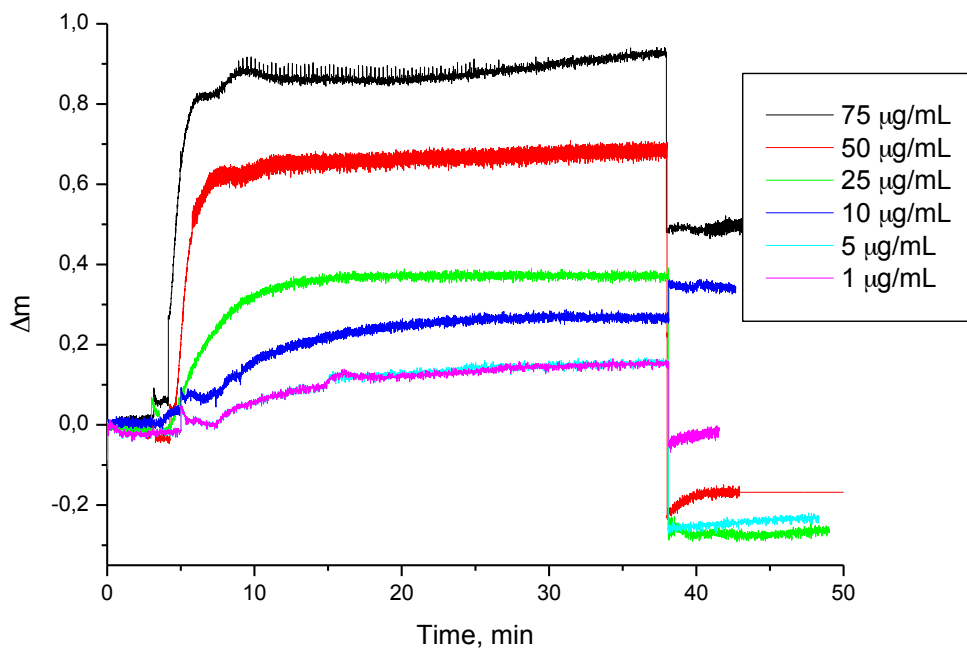


Figure 4. 24. Dynamic response of Cyt c-MIP nanofibers QCM sensors with respect to mass change.

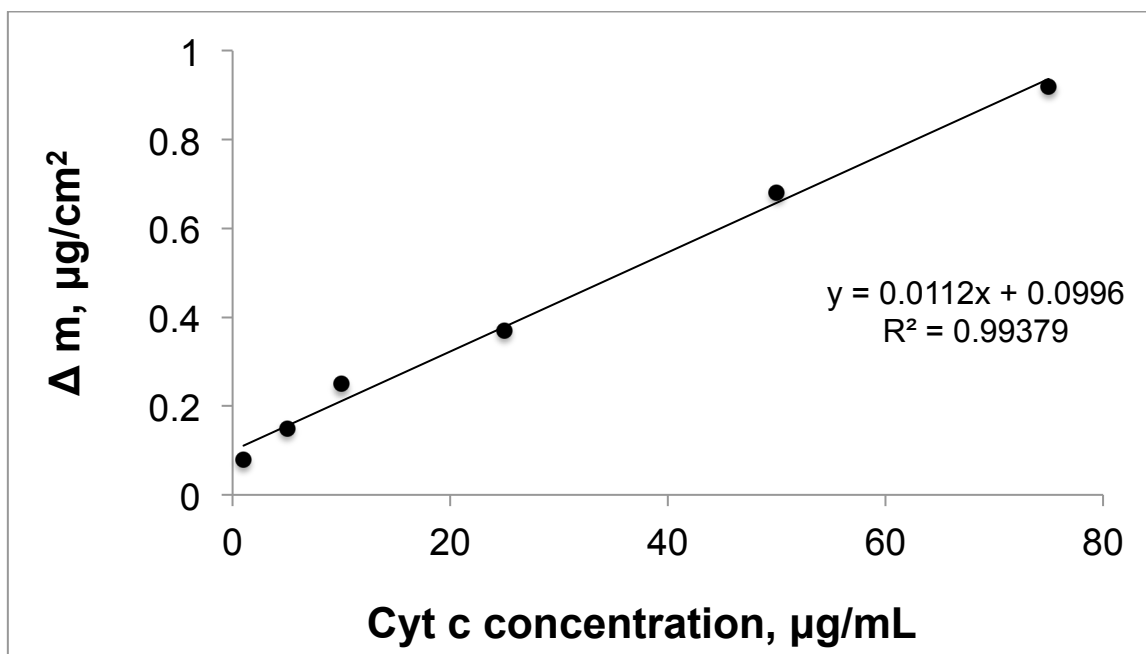


Figure 4. 25. The relation between mass shift and cytochrome c concentration.

Figure 4.26 displays the cytochrome c concentration effect on frequency change of QCM sensor. According to the data evaluation between 1-75 $\mu\text{g/mL}$ the equation of the curve and the linearity (R^2) was calculated as ($y=0.6327x+5.6939$) and 0.99454 respectively. The prepared QCM sensor can be used in the cytochrome c concentration range of 10-75 $\mu\text{g/mL}$ with %99 linearity.

4.8. 3. Mathematical analysis of Cyt c-MIP QCM sensor data

QCM data were analysed for the determination of kinetic and equilibrium isotherm parameters. For this purpose pseudo first order kinetic analysis and four equilibrium adsorption models Scatchard, Langmuir, Freundlich and Langmuir-Freundlich isotherms were applied to Cyt c-MIP QCM sensor data [220]. The binding according to pseudo-first order kinetic model can be expressed as :

$$\frac{d\Delta m}{dt} = k_a C \Delta m_{\max} - (k_a C + k_d) \Delta m \quad (12)$$

where, $d\Delta m/dt$ is the QCM frequency change rate, Δm is mass change on unit area of QCM sensor ($\mu\text{g/cm}^2$) and Δm_{\max} is the maximum mass change on unit area of QCM sensor ($\mu\text{g/cm}^2$), C is the cytochrome c concentration ($\mu\text{g/mL}$), k_a ($\mu\text{g/mL}$) and k_d (1/s) are forward and reverse kinetic rate constant respectively.

Since $d\Delta m/dt = 0$ at equilibrium, the equation above becomes as:

$$\frac{\Delta m_{\text{eq}}}{C} = K_A \Delta m_{\max} - K_A \Delta m_{\text{eq}} \quad (13)$$

where m_{eq} is the frequency shift at equilibrium, K_A ($\mu\text{g/mL}$) is equilibrium constant as the ratio of k_a and k_d and is calculated from the plot of $\frac{\Delta m_{\text{eq}}}{C}$ versus Δm_{eq} . The dissociation constant, K_D can be calculated as $1/ K_A$.

$$d\Delta m/dt = k_a C \Delta m_{\max} - (k_a C + k_d) \Delta m \quad (14)$$

Table 4. 5. Kinetic parameters.

Equilibrium analysis (Scatchard)		Association kinetics analysis	
Δm_{\max} ($\mu\text{g/cm}^2$)	125.01	k_a ($\mu\text{g/mLs}$)	1.10×10^{-4}
K_A ($\mu\text{g/mL}$)	0.0092	k_d (1/s)	0.0067
K_D (mL/ μg)	108.69	K_a ($\mu\text{g/mL}$)	0.0314
R^2	0.958	K_D	31.84
		R^2	0.931

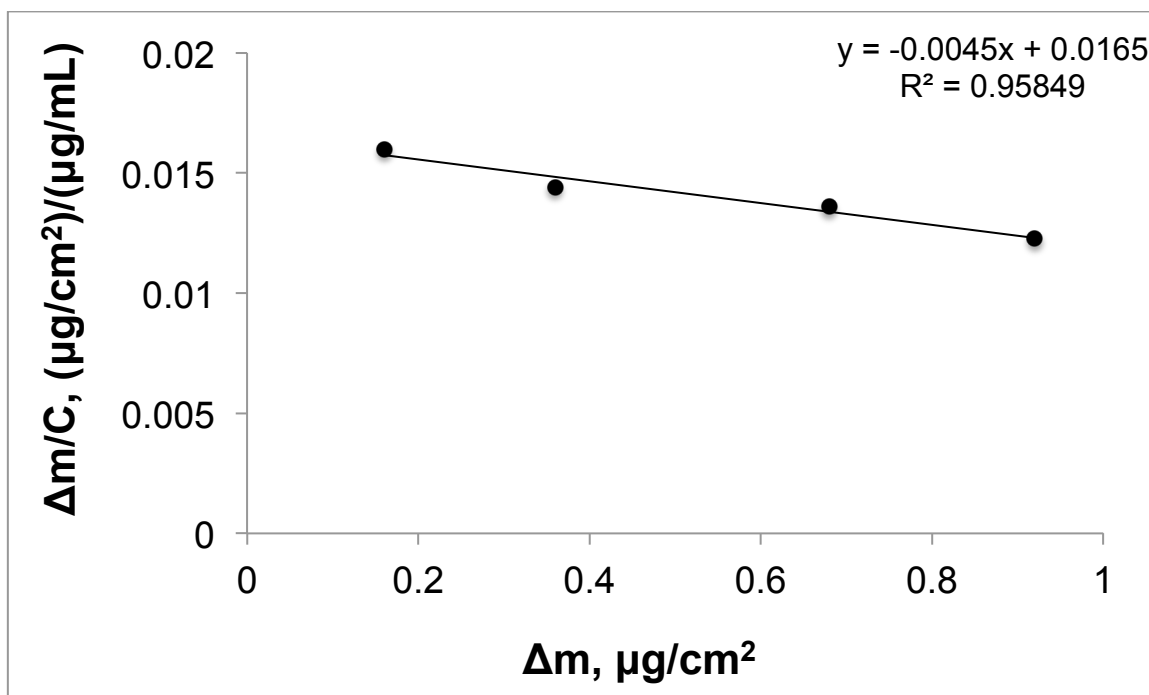


Figure 4. 26. Determination of equilibrium analysis (Scathard).

4.8. 4. Equilibrium isotherm models

Langmuir and Freundlich models were used to define the interaction model between cytochrome c molecules and QCM sensor.

Table 4. 6. The equilibrium isotherms

Model	Equation
Langmuir	$\Delta m = \Delta m_{\max} C / (K_D + C)$
Freundlich	$\Delta m = \Delta m_{\max} C^{1/n}$
Langmuir-Freundlich	$\Delta m = (\Delta m_{\max} C^{1/n}) / (K_D + C^{1/n})$

Here K_D ($\text{mL}/\mu\text{g}$) is equilibrium association constant and $1/n$ is Freundlich exponent. Langmuir isotherm is based on homogeneous distribution of recognition sites with equivalent energy and no lateral interactions and Freundlich isotherm is based on heterogeneous adsorption. According to the regression coefficients, it was determined that Langmuir model was suitable (Table 4.8). The calculated Δm_{\max} was very close to the experimental value. K_D and K_A values were found

0.0119 mL/μg and 83.63 μg/mL respectively. The detection limit that was defined as the concentration of analyte giving frequency shift equivalent to 3 standard deviation of the equilibration solution was found as 1.4 ng/mL.

Table 4. 7. The parameters of equilibrium isotherms.

Langmuir	Freundlich	Langmuir-Freundlich
Δm_{\max} (μg/cm ²) : 102.04 K_D (mL/μg) : 0.0119 K_A (μg/mL) : 83.63 R^2 : 0.996	Δm_{\max} (μg/cm ²) : 14.35 $1/n$: 0.56 R^2 : 0.979	Δm_{\max} (μg/cm ²): $1/n$: 0.423 K_A (μg/mL) : 0.612 K_D (mL/μg) : 1.913 R^2 : 0.979

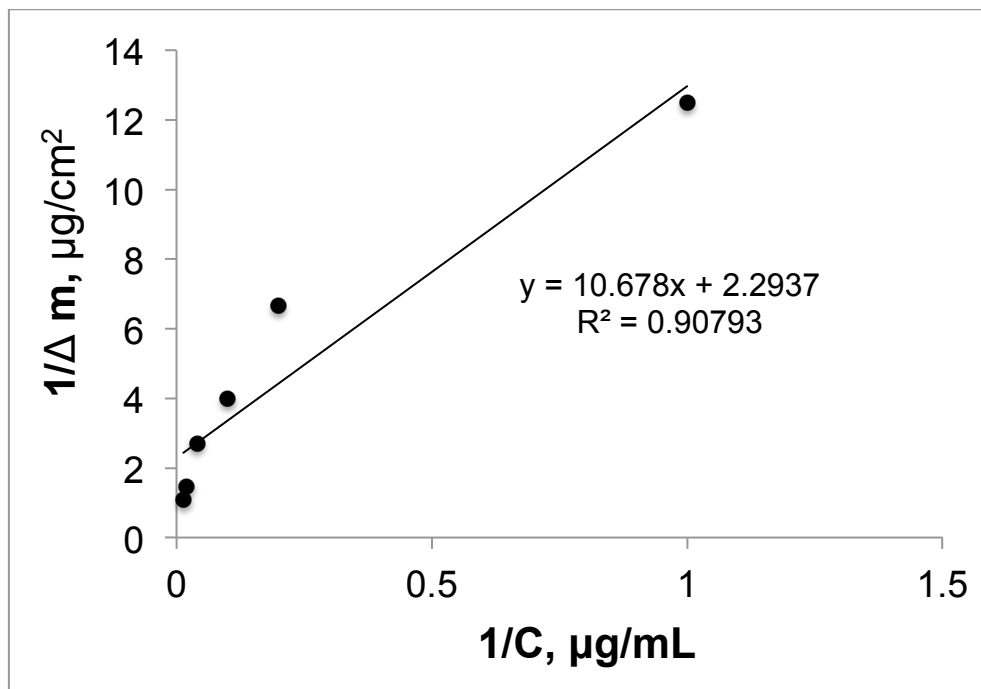


Figure 4. 27. Langmuir adsorption model.

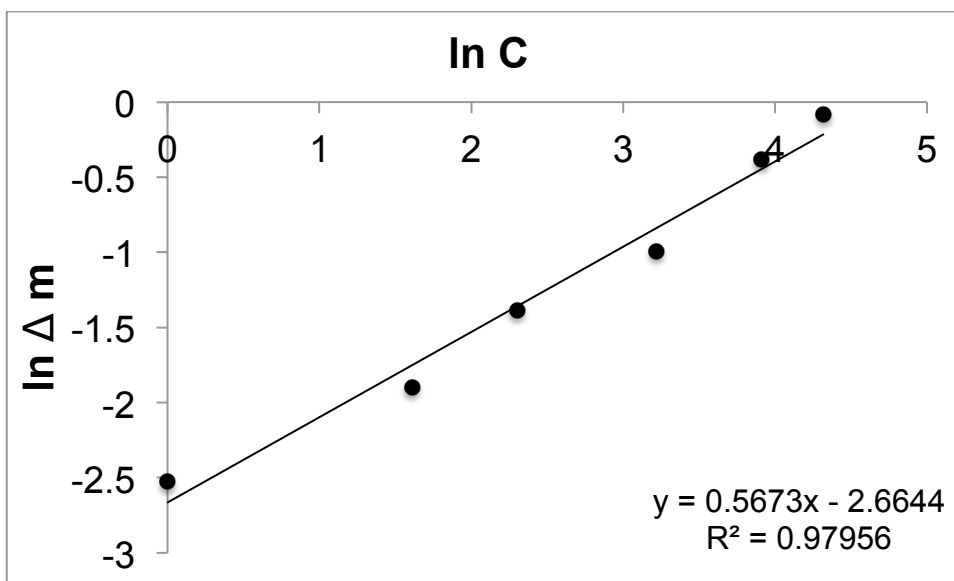


Figure 4. 28. Freundlich adsorption isotherm.

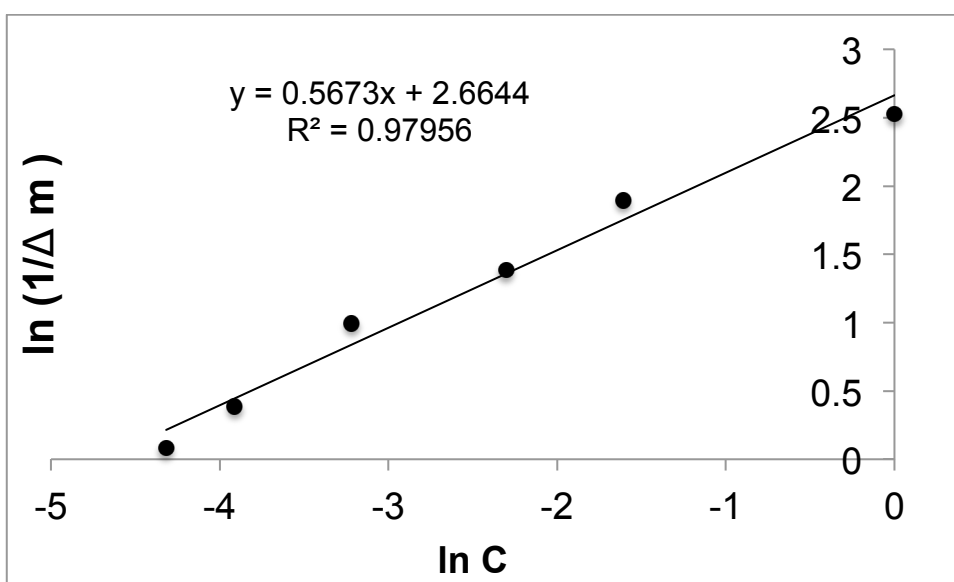


Figure 4. 29. Langmuir-Freundlich adsorption isotherm.

4.8. 5. Selectivity studies

To show the selectivity of Cyt c-MIP and NIP QCM sensors, real-time detection of non-template proteins was performed at concentration of 25 $\mu\text{g/mL}$ for each protein. The frequency shift of Cyt c-MIP QCM sensor was higher than that of the other proteins bearing the highly specific recognition sites well fitted to cytochrome c. For all the non-template proteins the frequency shifts of MIP and NIP QCM sensors are nearly same indicating no imprinting sites complementary to non-

template proteins. Since Hb, BSA and Myo have bigger molecular weights, the binding of these proteins was low. The binding of lysozyme was higher than that of other non-template proteins due to its similar properties such as number of surface histidine, molecular weight and isoelectric point. The results present that Cyt c-MIP QCM sensors were able to detect Cyt c molecules selectively which are in consistency with the results of rebinding studies.

Based on the amount of protein adsorption capacity, imprinting factor (IF) was found as 2.5 for Cyt c, which was consistent with the results of batch-wise experiments (Section 4.7). Table 4.9 shows the selectivity factors to non-template proteins. BSA, Hb and Myo, which are larger than Cyt c did not access to the recognition sites easily due to the steric hindrance of large proteins by polymer chains. Despite Lys has similar pI and molecular weight, the spatial orientation of the functional monomers in the cavity was not proper to it resulting low recognition of Lys.

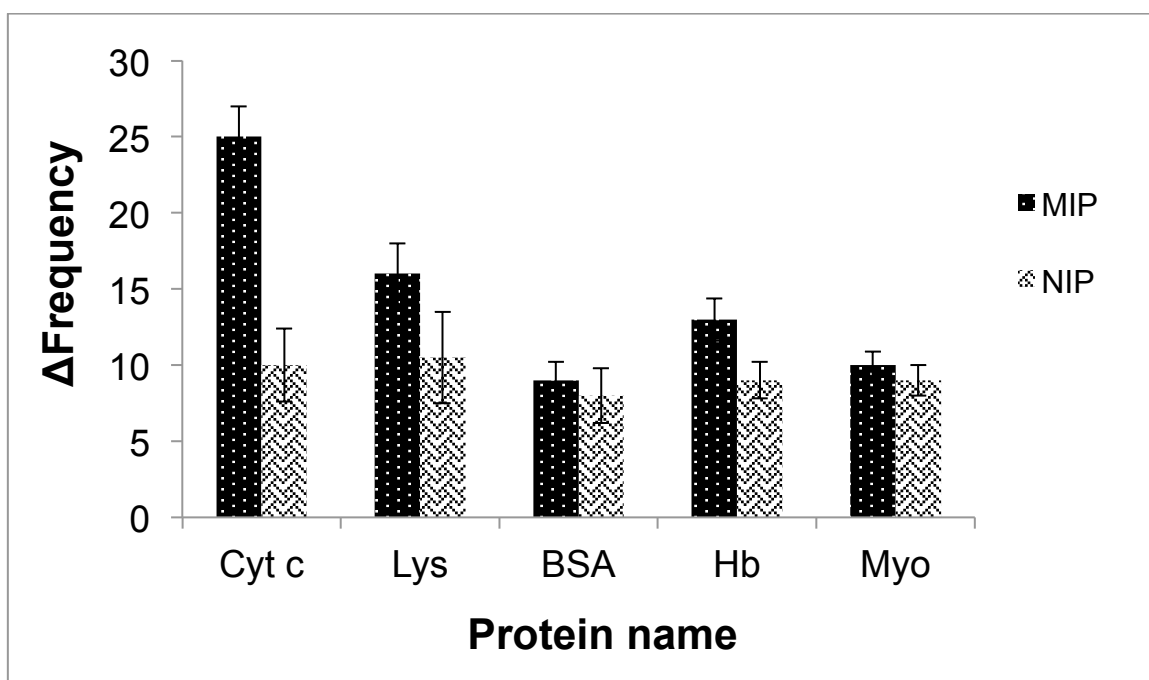


Figure 4. 30. Selectivity of Cyt c-MIP QCM sensors.

Table 4. 8. Selectivity of Cyt c-MIP QCM nanosensors to Cyt c and non-template proteins.

Parameter	Cyt c	Lys	BSA	Hb	Myo
IF	2.5	0.9	1.1	1.4	1.1
α	-	2.8	2.2	1.7	2.3

4.8. 6. Reproducibility

The reproducibility of QCM sensor is one of the major parameters for the practical use of a sensor. To examine the reproducibility of Cyt c-MIP QCM sensors, four adsorption-desorption-regeneration cycles were performed with 25 $\mu\text{g/mL}$ of Cyt c solution. As shown in Figure 4.29, the frequency of the sensor was backshifted to its initial value after desorption showing nearly the same frequency shift when injected the same Cyt c concentration at different times after Cyt c desorption. The results present that Cyt c-MIP QCM sensors can be used for several times with good reproducibility and reversibility.

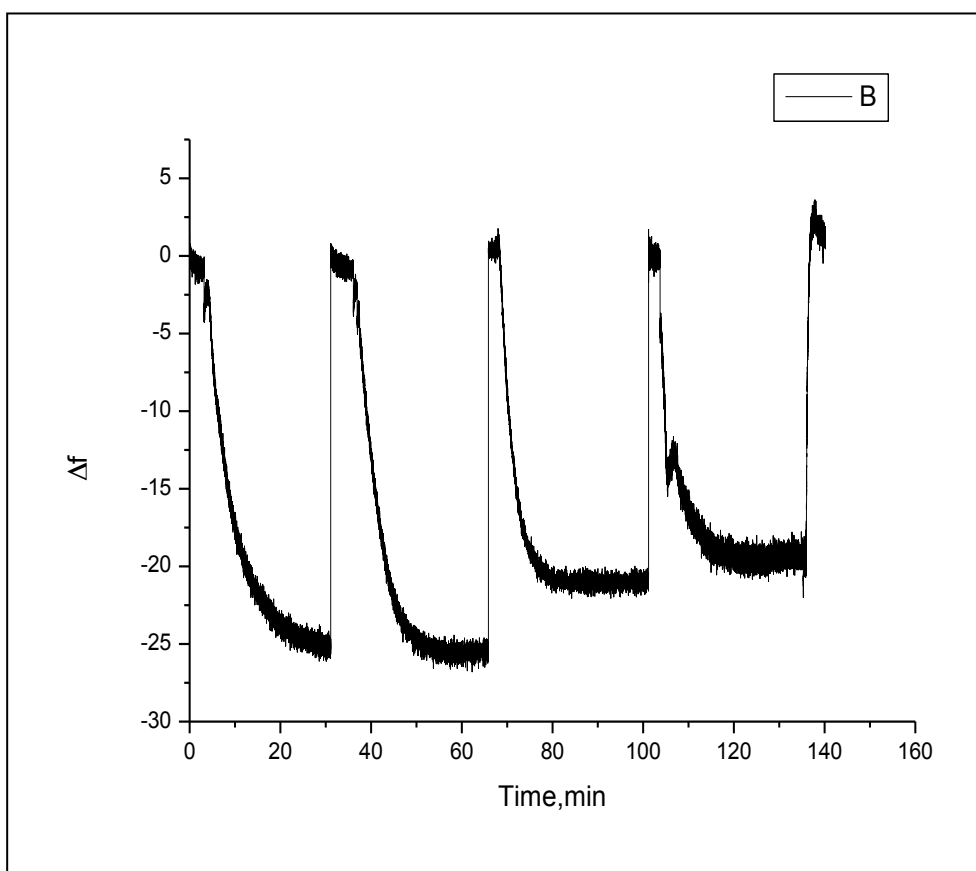


Figure 4.29. Reproducibility of Cyt c-MIP QCM sensors.

5. CONCLUSION

- N-methacryoyl-L-histidine methyl ester (MAH) was synthesized from the reaction of metachryloyl chloride and L-histidine. It was characterized by FTIR. The characteristic peaks of the structure of MAH monomer was amide bands, which appear at 1539 and 1633 cm^{-1} .
- MAH and copper ions were complexed via metal chelation with different molar ratios of 2:1 and 1:1. This complex was then characterized with UV-vis spectroscopy with the decrement of absorbance of this complex. The suitable complexation ratio was found as 1:1 as MAH/Cu(II) molar ratio.
- The metal chelate monomer MAH-Cu(II) was then pre-organized with Cyt c molecules via self assembling to create well-oriented recognition sites.
- After polymerization with MBAAm as cross-linker, template molecules were removed with 1 M NaCl solution to obtain specific cavities complementary to Cyt c molecules.
- The polymerization conditions such as monomer/template ratio, total monomer ratio and polymerization time were investigated to determine the most suitable conditions for the improvement of the binding properties of MIP nanofibers.
- The optimum monomer/template ratio was found as 20, optimum total monomer ratio was 1%w and optimum polymerization time was 0.5 h.
- The prepared Cyt c-MIP nanofibers were characterized by ATR-FTIR, SEM and contact angle measurements.
- The effect of pH on the rebinding properties was investigated for different pH values in the range of 3-9. The highest adsorption capacity was observed when used pH 7.0 in the rebinding experiments.
- The effect of temperature was also examined and adsorption tests were carried out at 4, 14, 25 and 37 °C. The optimum temperature was 25 °C since the highest adsorption capacity was obtained at that temperature.
- Furthermore, the effect of ionic strength was evaluated with respect to adsorption capacity. The experiments were taken place in salt-free solution and in aqueous NaCl solutions with concentration of 0.001-0.1 M. The

adsorption capacity was highest when the experiments were carried out in salt-free Cyt c solution.

- The MIPs prepared using defined polymerization conditions memorize the conditions since template molecules are oriented with respect to the properties of environment such as pH, temperature, solvent type, ionic strength etc. The results were in good conformity with each other pointing out memory effect of prepared MIP nanofibers.
- The adsorption capacity of Cyt c-MIP nanofibers increased with increasing Cyt c concentration and reached a plateau at 0.5 mg/mL Cyt c concentration. There was no accessible binding sites available for Cyt c molecules until that concentration value. The maximum adsorption capacity was 36.4 mg/g, which is quite comparable with literature.
- Langmuir and Freundlich equilibrium isotherms were used to evaluate binding characteristics of Cyt c-MIP nanofibers. Langmuir isotherm was more suitable with higher regression coefficient than that of Freundlich isotherm.
- Fast binding kinetics is a significant issue for MIPs. The recognition of Cyt c with Cyt c-MIP nanofibers was achieved in 10 min. Since MIP nanomaterials targeting different template molecules have recognition time of 10 min to 10 h, the prepared MIP nanofibers achieved fast binding kinetics which can be attributed to thin polymeric film fabricated onto the bacterial cellulose nanofibers.
- In order to determine the appropriate kinetic model, pseudo-first order, pseudo-second order kinetics and intraparticle diffusion kinetics were used to explain the adsorption mechanism of Cyt c molecules through resultant MIP nanofibers. Pseudo-second order kinetic model was fitted well with higher correlation coefficient than that of other kinetic models.
- Since thermodynamic parameters give significant information about adsorption process, the parameters were calculated using van't Hoff plot and listed. Negative values of ΔG° show spontaneous and thermodynamically feasible adsorption of cytochrome c onto MIP nanofibers.
- To demonstrate the contribution of metal ion to the formation of specific cavities, MIP was prepared with the same procedure of Cyt c-MIP but without metal ion. The adsorption experiments show that both metal ion coordination

and recognition binding sites were necessary for specific recognition of template molecules.

- The selectivity properties of Cyt c-MIP nanofibers were tested with various non-template proteins that have accessible surface histidine(s). MIP nanofibers show highest affinity to Cyt c molecules because of the well-defined cavities created complementary to Cyt c molecules by both shape and functional groups.
- Lys-MIP nanofibers were also prepared with lysozyme as a template to show the generality of this method of preparation MIPs. Lys-MIP nanofibers have higher affinity for Lys molecules than Cyt c molecules that were used as non-template proteins.
- QCM nanosensors were prepared to show the recognition capability of Cyt c-MIP nanofibers. The nanofibers homogenized and casted onto the QCM sensor chip. NIP QCM nanosensors were prepared with the same procedure but with NIP nanofibers.
- Surface morphology of Cyt c-MIP QCM nanosensors was characterized with AFM measurements.
- Real-time monitoring of Cyt c-MIP QCM nanosensors was performed with the Cyt c solutions having concentrations in the range of 1-75 $\mu\text{g/mL}$. The frequency shift increased with increasing concentration of Cyt c. After desorption with 1 M NaCl solution, the frequency returned to the initial value.
- The prepared QCM nanosensors demonstrate 99 % of linearity.
- Langmuir, Freundlich and Langmuir-Freundlich equilibrium isotherms were also investigated and Langmuir isotherm was suited well to the system.
- The selectivity studies were also carried out with non-template proteins to show specificity of QCM nanosensors. The results showed that Cyt c-MIP nanosensors achieved to detect Cyt c molecules with high specificity.
- Four adsorption-desorption cycles were performed to evaluate the reproducibility of QCM nanosensors. The results showed that Cyt c-MIP nanosensors can be used for several times without any significant loss of frequency shift. Also it was demonstrated that the method of preparation of QCM nanosensors was able to perform successfully.

- The prepared Cyt c-MIP nanofibers show unique recognition characteristics. Also since bacterial cellulose is cost-effective material with unique properties, the surface molecularly imprinted nanofibers prepared in this thesis present promising alternative for protein purification.

REFERENCES

- [1]Nfor, BK, Verhaert, PDEM, van der Wielen, LAM, Hubbuch, J and Ottens, M. Rational and systematic protein purification process development: the next generation. *Trends in Biotechnology*. 27, 673-679, **2009**.
- [2]Hansen, DE. Recent developments in the molecular imprinting of proteins. *Biomaterials*. 28, 4178-4191, **2007**.
- [3]Ramström, O and Ansell, RJ. Molecular imprinting technology: challenges and prospects for the future. *Chirality*. 10, 195-209, **1998**.
- [4]Kryscio, DR and Peppas, NA. Critical review and perspective of macromolecularly imprinted polymers. *Acta Biomaterialia*. 8, 461-473, **2012**.
- [5]Tan, C and Tong, Y. Molecularly imprinted beads by surface imprinting. *Anal Bioanal Chem*. 389, 369-376, **2007**.
- [6]Shen, X, Zhu, L, Liu, G, Yu, H and Tang, H. Enhanced Photocatalytic Degradation and Selective Removal of Nitrophenols by Using Surface Molecular Imprinted Titania. *Environmental Science & Technology*. 42, 1687-1692, **2008**.
- [7]Poovarodom, S, Bass, JD, Hwang, S-J and Katz, A. Investigation of the Core-Shell Interface in Gold@Silica Nanoparticles: A Silica Imprinting Approach. *Langmuir : the ACS journal of surfaces and colloids*. 21, 12348-12356, **2005**.
- [8]Say, R, Erdem, M, Ersöz, A, Türk, H and Denizli, A. Biomimetic catalysis of an organophosphate by molecularly surface imprinted polymers. *Applied Catalysis A: General*. 286, 221-225, **2005**.
- [9]Yoshida, M, Uezu, K, Goto, M and Furusaki, S. Surface imprinted polymers recognizing amino acid chirality. *Journal of Applied Polymer Science*. 78, 695-703, **2000**.
- [10]Papaioannou, EH, Liakopoulou-Kyriakides, M, Papi, RM and Kyriakidis, DA. Artificial receptor for peptide recognition in protic media: The role of metal ion coordination. *Materials Science and Engineering: B*. 152, 28-32, **2008**.
- [11]Lynd, LR, Weimer, PJ, van Zyl, WH and Pretorius, IS. Microbial Cellulose Utilization: Fundamentals and Biotechnology. *Microbiology and Molecular Biology Reviews*. 66, 506-577, **2002**.
- [12]Kim, D-Y, Nishiyama, Y and Kuga, S. Surface acetylation of bacterial cellulose. *Cellulose*. 9, 361-367, **2002**.
- [13]Ward, WW and Swiatek, G. Protein purification. *Current Analytical Chemistry*. 5, 1-21, **2009**.
- [14]Chen, L, Xu, S and Li, J. Recent advances in molecular imprinting technology: current status, challenges and highlighted applications. *Chemical Society Reviews*. 40, 2922-2942, **2011**.
- [15]Mosbach, K. Molecular imprinting. *Trends in Biochemical Sciences*. 19, 9-14, **1994**.
- [16]Wulff, G, Molecular imprinting – a way to prepare effective mimics of natural antibodies and enzymes. *Studies in Surface Science and Catalysis*, (Sayari, A. and Jaroniec, M.), Elsevier, 35-44, **2002**.
- [17]Vasapollo, G, Sole, RD, Mergola, L, Lazzoi, MR, Scardino, A, Scorrano, S and Mele, G. Molecularly Imprinted Polymers: Present and Future Prospective. *International Journal of Molecular Sciences*. 12, 5908-5945, **2011**.
- [18]Ge, Y and Turner, APF. Too large to fit? Recent developments in macromolecular imprinting. *Trends in Biotechnology*. 26, 218-224, **2008**.

- [19]Al-Kindy, S, Badía, R, Suárez-Rodríguez, JL and Díaz-García, ME. Molecularly Imprinted Polymers and Optical Sensing Applications. *Critical Reviews in Analytical Chemistry*. 30, 291-309, **2000**.
- [20]Tom, LA, Schneck, NA and Walter, C. Improving the imprinting effect by optimizing template:monomer:cross-linker ratios in a molecularly imprinted polymer for sulfadimethoxine. *Journal of Chromatography B*. 909, 61-64, **2012**.
- [21]Selligren, B. Direct Drug Determination by Selective Sample Enrichment on an Imprinted Polymer. *Analytical Chemistry*. 66, 1578-1582, **1994**.
- [22]Toorisaka, E, Uezu, K, Goto, M and Furusaki, S. A molecularly imprinted polymer that shows enzymatic activity. *Biochemical Engineering Journal*. 14, 85-91, **2003**.
- [23]Hawkins, DM, Stevenson, D and Reddy, SM. Investigation of protein imprinting in hydrogel-based molecularly imprinted polymers (HydroMIPs). *Analytica Chimica Acta*. 542, 61-65, **2005**.
- [24]Doué, M, Bichon, E, Dervilly-Pinel, G, Pichon, V, Chapuis-Hugon, F, Lesellier, E, West, C, Monteau, F and Le Bizec, B. Molecularly imprinted polymer applied to the selective isolation of urinary steroid hormones: An efficient tool in the control of natural steroid hormones abuse in cattle. *Journal of Chromatography A*. 1270, 51-61, **2012**.
- [25]Halim, NFA, Ahmad, MN, Shakaff, AYM and Deraman, N. Grafting Amino-acid Molecular Imprinted Polymer on Carbon Nanotube for Sensing. *Procedia Engineering*. 53, 64-70, **2013**.
- [26]Peng, ZG, Hidajat, K and Uddin, MS. Adsorption and desorption of lysozyme on nano-sized magnetic particles and its conformational changes. *Colloids and Surfaces B: Biointerfaces*. 35, 169-174, **2004**.
- [27]Yano, K, Nakagiri, T, Takeuchi, T, Matsui, J, Ikebukuro, K and Karube, I. Stereoselective recognition of dipeptide derivatives in molecularly imprinted polymers which incorporate an L-valine derivative as a novel functional monomer. *Analytica Chimica Acta*. 357, 91-98, **1997**.
- [28]Wei, S, Jakusch, M and Mizaikoff, B. Capturing molecules with templated materials—Analysis and rational design of molecularly imprinted polymers. *Analytica Chimica Acta*. 578, 50-58, **2006**.
- [29]Yilmaz, E, Mosbach, K and Haupt, K. Influence of functional and cross-linking monomers and the amount of template on the performance of molecularly imprinted polymers in binding assays. *Analytical Communications*. 36, 167-170, **1999**.
- [30]Lin, H-Y, Rick, J and Chou, T-C. Optimizing the formulation of a myoglobin molecularly imprinted thin-film polymer—formed using a micro-contact imprinting method. *Biosensors and Bioelectronics*. 22, 3293-3301, **2007**.
- [31]O'Shannessy, DJ, Ekberg, B and Mosbach, K. Molecular imprinting of amino acid derivatives at low temperature (0°C) using photolytic homolysis of azobisnitriles. *Analytical Biochemistry*. 177, 144-149, **1989**.
- [32]Lin, J-M, Nakagama, T, Uchiyama, K and Hobo, T. Temperature effect on chiral recognition of some amino acids with molecularly imprinted polymer filled capillary electrochromatography. *Biomedical Chromatography*. 11, 298-302, **1997**.
- [33]Piletsky, SA, Mijangos, I, Guerreiro, A, Piletska, EV, Chianella, I, Karim, K and Turner, APF. Polymer Cookery: Influence of Polymerization Time and Different Initiation Conditions on Performance of Molecularly Imprinted Polymers. *Macromolecules*. 38, 1410-1414, **2005**.

- [34]Piletska, EV, Guerreiro, AR, Whitcombe, MJ and Piletsky, SA. Influence of the Polymerization Conditions on the Performance of Molecularly Imprinted Polymers. *Macromolecules*. 42, 4921-4928, **2009**.
- [35]Cormack, PAG and Elorza, AZ. Molecularly imprinted polymers: synthesis and characterisation. *Journal of Chromatography B*. 804, 173-182, **2004**.
- [36]Conrad, PG and Shea, KJ, The use of metal coordination for controlling the microenvironment of imprinted polymers. *Molecular imprinted polymers, Science and technology*, (eds.: Yan, M. and Ramström, O.), CRC Press, 123-180, **2004**.
- [37]Shiomi, T, Matsui, M, Mizukami, F and Sakaguchi, K. A method for the molecular imprinting of hemoglobin on silica surfaces using silanes. *Biomaterials*. 26, 5564-5571, **2005**.
- [38]Hwang, C-C and Lee, W-C. Chromatographic characteristics of cholesterol-imprinted polymers prepared by covalent and non-covalent imprinting methods. *Journal of Chromatography A*. 962, 69-78, **2002**.
- [39]Liu, J-q and Wulff, G. Functional Mimicry of Carboxypeptidase A by a Combination of Transition State Stabilization and a Defined Orientation of Catalytic Moieties in Molecularly Imprinted Polymers. *Journal of the American Chemical Society*. 130, 8044-8054, **2008**.
- [40]Dhal, PK and Arnold, FH. Metal-coordination interactions in the template-mediated synthesis of substrate-selective polymers: recognition of bis(imidazole) substrates by copper(II) iminodiacetate containing polymers. *Macromolecules*. 25, 7051-7059, **1992**.
- [41]Hart, BR and Shea, KJ. Synthetic Peptide Receptors: Molecularly Imprinted Polymers for the Recognition of Peptides Using Peptide-Metal Interactions. *Journal of the American Chemical Society*. 123, 2072-2073, **2001**.
- [42]Huang, J, Hu, Y, Hu, Y and Li, G. Development of metal complex imprinted solid-phase microextraction fiber for 2,2'-dipyridine recognition in aqueous medium. *Talanta*. 83, 1721-1729, **2011**.
- [43]Huang, J, Hu, Y, Hu, Y and Li, G. Disposable terbium (III) salicylate complex imprinted membrane using solid phase surface fluorescence method for fast separation and detection of salicylic acid in pharmaceuticals and human urine. *Talanta*. 107, 49-54, **2013**.
- [44]Lian, H, Hu, Y and Li, G. Novel metal-ion-mediated, complex-imprinted solid-phase microextraction fiber for the selective recognition of thiabendazole in citrus and soil samples. *Journal of Separation Science*. 37, 106-113, **2014**.
- [45]Mallik, S, Johnson, RD and Arnold, FH. Synthetic Bis-Metal Ion Receptors for Bis-Imidazole "Protein Analogs". *Journal of the American Chemical Society*. 116, 8902-8911, **1994**.
- [46]Wu, L and Li, Y. Metal ion-mediated molecular-imprinting polymer for indirect recognition of formate, acetate and propionate. *Analytica Chimica Acta*. 517, 145-151, **2004**.
- [47]Qu, G, Zheng, S, Liu, Y, Xie, W, Wu, A and Zhang, D. Metal ion mediated synthesis of molecularly imprinted polymers targeting tetracyclines in aqueous samples. *Journal of Chromatography B*. 877, 3187-3193, **2009**.
- [48]Hart, BR and Shea, KJ. Molecular Imprinting for the Recognition of N-Terminal Histidine Peptides in Aqueous Solution. *Macromolecules*. 35, 6192-6201, **2002**.
- [49]Krebs, JF and Borovik, AS. Metallo-Network Polymers: Reversible CO Binding to an Immobilized Copper(I) Complex. *Journal of the American Chemical Society*. 117, 10593-10594, **1995**.

- [50] Akkaya, B, Uzun, L, Candan, F and Denizli, A. N-methacryloyl-(l)-histidine methyl ester carrying porous magnetic beads for metal chelate adsorption of cytochrome c. *Materials Science and Engineering: C*. 27, 180-187, **2007**.
- [51] Li, S, Liao, C, Li, W, Chen, Y and Hao, X. Rationally Designing Molecularly Imprinted Polymer towards Predetermined High Selectivity by Using Metal as Assembled Pivot. *Macromolecular Bioscience*. 7, 1112-1120, **2007**.
- [52] Hierarchically Structured Electrospun Fibers. *Polymers*. 5, 19, **2013**.
- [53] Chaitidou, S, Kotrotsiou, O and Kiparissides, C. On the synthesis and rebinding properties of [Co(C₂H₃O₂)₂(z-Histidine)] imprinted polymers prepared by precipitation polymerization. *Materials Science and Engineering: C*. 29, 1415-1421, **2009**.
- [54] Dhal, PK and Arnold, FH. Template-mediated synthesis of metal-complexing polymers for molecular recognition. *Journal of the American Chemical Society*. 113, 7417-7418, **1991**.
- [55] Mallik, S, Johnson, RD and Arnold, FH. Selective recognition of bis-imidazoles by complementary bis-metal ion complexes. *Journal of the American Chemical Society*. 115, 2518-2520, **1993**.
- [56] Highly sensitive humidity sensor based on amorphous Al₂O₃ nanotubes. *Journal of Materials Chemistry*. 21, 1907, **2011**.
- [57] Sulkowski, E. Purification of proteins by IMAC. *Trends in Biotechnology*. 3, 1-7, **1985**.
- [58] Study on the Morphologies and Formational Mechanism of Poly(hydroxybutyrate-co-hydroxyvalerate) Ultrafine Fibers by Dry-Jet-Wet-Electrospinning. *Journal of Nanomaterials*. 2012, 1, **2012**.
- [59] Hochuli, E, Döbeli, H and Schacher, A. New metal chelate adsorbent selective for proteins and peptides containing neighbouring histidine residues. *Journal of Chromatography A*. 411, 177-184, **1987**.
- [60] Vidyasankar, S, Ru, M and Arnold, FH. Molecularly imprinted ligand-exchange adsorbents for the chiral separation of underivatized amino acids. *Journal of Chromatography A*. 775, 51-63, **1997**.
- [61] Kempe, M, Glad, M and Mosbach, K. An approach towards surface imprinting using the enzyme ribonuclease A. *Journal of Molecular Recognition*. 8, 35-39, **1995**.
- [62] Qin, L, He, X-W, Zhang, W, Li, W-Y and Zhang, Y-K. Macroporous Thermosensitive Imprinted Hydrogel for Recognition of Protein by Metal Coordinate Interaction. *Analytical Chemistry*. 81, 7206-7216, **2009**.
- [63] Bereli, N, Andaç, M, Baydemir, G, Say, R, Galaev, IY and Denizli, A. Protein recognition via ion-coordinated molecularly imprinted supermacroporous cryogels. *Journal of Chromatography A*. 1190, 18-26, **2008**.
- [64] Odabaşı, M, Say, R and Denizli, A. Molecular imprinted particles for lysozyme purification. *Materials Science and Engineering: C*. 27, 90-99, **2007**.
- [65] Özcan, AA, Say, R, Denizli, A and Ersöz, A. l-Histidine Imprinted Synthetic Receptor for Biochromatography Applications. *Analytical Chemistry*. 78, 7253-7258, **2006**.
- [66] The Effect of Anodization Time on the Properties of TiO₂ Nanotube Humidity Sensors. *MRS Proceedings*. 1479, 83, **2013**.
- [67] Adrus, N and Ulbricht, M. Molecularly imprinted stimuli-responsive hydrogels for protein recognition. *Polymer*. 53, 4359-4366, **2012**.

- [68]Mosbach, K and Ramstrom, O. The Emerging Technique of Molecular Imprinting and Its Future Impact on Biotechnology. *Nat Biotech.* 14, 163-170, **1996**.
- [69]Wulff, G. Molecular Imprinting in Cross-Linked Materials with the Aid of Molecular Templates— A Way towards Artificial Antibodies. *Angewandte Chemie International Edition in English.* 34, 1812-1832, **1995**.
- [70]Lundqvist, M, Sethson, I and Jonsson, B-H. Protein Adsorption onto Silica Nanoparticles: Conformational Changes Depend on the Particles' Curvature and the Protein Stability. *Langmuir : the ACS journal of surfaces and colloids.* 20, 10639-10647, **2004**.
- [71]Díaz-García, ME and Laíño, RB. Molecular Imprinting in Sol-Gel Materials: Recent Developments and Applications. *Microchim Acta.* 149, 19-36, **2005**.
- [72]Yilmaz, F, Bereli, N, Yavuz, H and Denizli, A. Supermacroporous hydrophobic affinity cryogels for protein chromatography. *Biochemical Engineering Journal.* 43, 272-279, **2009**.
- [73]Liu, J, Deng, Q, Yang, K, Zhang, L, Liang, Z and Zhang, Y. Macroporous molecularly imprinted monolithic polymer columns for protein recognition by liquid chromatography. *Journal of Separation Science.* 33, 2757-2761, **2010**.
- [74]Bossi, A, Bonini, F, Turner, APF and Piletsky, SA. Molecularly imprinted polymers for the recognition of proteins: The state of the art. *Biosensors and Bioelectronics.* 22, 1131-1137, **2007**.
- [75]Li, Y, Yang, H-H, You, Q-H, Zhuang, Z-X and Wang, X-R. Protein Recognition via Surface Molecularly Imprinted Polymer Nanowires. *Analytical Chemistry.* 78, 317-320, **2005**.
- [76]Titirici, M and Sellergren, B. Peptide recognition via hierarchical imprinting. *Anal Bioanal Chem.* 378, 1913-1921, **2004**.
- [77]Titirici, MM, Hall, AJ and Sellergren, B. Hierarchically Imprinted Stationary Phases: Mesoporous Polymer Beads Containing Surface-Confined Binding Sites for Adenine. *Chemistry of Materials.* 14, 21-23, **2001**.
- [78]Biomimicry via Electrospinning. *Critical Reviews in Solid State and Materials Sciences.* 37, 94, **2012**.
- [79]Rick, J and Chou, T-C. Using protein templates to direct the formation of thin-film polymer surfaces. *Biosensors and Bioelectronics.* 22, 544-549, **2006**.
- [80]Bossi, A, Piletsky, SA, Piletska, EV, Righetti, PG and Turner, APF. Surface-Grafted Molecularly Imprinted Polymers for Protein Recognition. *Analytical Chemistry.* 73, 5281-5286, **2001**.
- [81]Kan, X, Zhao, Q, Shao, D, Geng, Z, Wang, Z and Zhu, J-J. Preparation and Recognition Properties of Bovine Hemoglobin Magnetic Molecularly Imprinted Polymers. *The Journal of Physical Chemistry B.* 114, 3999-4004, **2010**.
- [82]He, H, Fu, G, Wang, Y, Chai, Z, Jiang, Y and Chen, Z. Imprinting of protein over silica nanoparticles via surface graft copolymerization using low monomer concentration. *Biosensors and Bioelectronics.* 26, 760-765, **2010**.
- [83]Electrospun nanofiber mats for evanescent optical fiber sensors. *Sensors and Actuators B: Chemical.* 176, 569, **2013**.
- [84]Thoemmes, J and Kula, MR. Membrane chromatography - an integrative concept in the downstream processing of proteins. *Biotechnology Progress.* 11, 357-367, **1995**.
- [85]Ghosh, R. Protein separation using membrane chromatography: opportunities and challenges. *Journal of Chromatography A.* 952, 13-27, **2002**.

- [86]Jia, H, Zhu, G, Vugrinovich, B, Kataphinan, W, Reneker, DH and Wang, P. Enzyme-Carrying Polymeric Nanofibers Prepared via Electrospinning for Use as Unique Biocatalysts. *Biotechnology Progress*. 18, 1027-1032, **2002**.
- [87]Vandeveld, F, Belmont, AS, Pantigny, J and Haupt, K. Hierarchically Nanostructured Polymer Films Based on Molecularly Imprinted Surface-Bound Nanofilaments. *Advanced Materials*. 19, 3717-3720, **2007**.
- [88]Tokonami, S, Shiigi, H and Nagaoka, T. Review: Micro- and nanosized molecularly imprinted polymers for high-throughput analytical applications. *Analytica Chimica Acta*. 641, 7-13, **2009**.
- [89]Poma, A, Turner, APF and Piletsky, SA. Advances in the manufacture of MIP nanoparticles. *Trends in Biotechnology*. 28, 629-637, **2010**.
- [90]Guijian Guan , BL, Zhenyang Wang , Zhongping Zhang. Imprinting of molecularly recognition sites on nanostructures and its applications in chemosensors. *sensors*. 8, 8291-8320, **2008**.
- [91]Gao, D, Zhang, Z, Wu, M, Xie, C, Guan, G and Wang, D. A Surface Functional Monomer-Directing Strategy for Highly Dense Imprinting of TNT at Surface of Silica Nanoparticles. *Journal of the American Chemical Society*. 129, 7859-7866, **2007**.
- [92]Denizli, A, *Protein kromatografisi ve yeni nesil polimerik sistemler*, Detay Copy Matbaa Yayıncılık, **2014**.
- [93]Moreira, S, Silva, NB, Almeida-Lima, J, Rocha, HAO, Medeiros, SRB, Alves Jr, C and Gama, FM. BC nanofibres: In vitro study of genotoxicity and cell proliferation. *Toxicology Letters*. 189, 235-241, **2009**.
- [94]Kontogiannopoulos, KN, Assimopoulou, AN, Tsivintzelis, I, Panayiotou, C and Papageorgiou, VP. Electrospun fiber mats containing shikonin and derivatives with potential biomedical applications. *International Journal of Pharmaceutics*. 409, 216-228, **2011**.
- [95]Wan, L-S, Ke, B-B, Wu, J and Xu, Z-K. Catalase Immobilization on Electrospun Nanofibers: Effects of Porphyrin Pendants and Carbon Nanotubes. *The Journal of Physical Chemistry C*. 111, 14091-14097, **2007**.
- [96]Vamvakaki, V, Tsagaraki, K and Chaniotakis, N. Carbon Nanofiber-Based Glucose Biosensor. *Analytical Chemistry*. 78, 5538-5542, **2006**.
- [97]Wan, YZ, Luo, H, He, F, Liang, H, Huang, Y and Li, XL. Mechanical, moisture absorption, and biodegradation behaviours of bacterial cellulose fibre-reinforced starch biocomposites. *Composites Science and Technology*. 69, 1212-1217, **2009**.
- [98]Ramakrishna, S, Fujihara, K, Teo, W-E, Yong, T, Ma, Z and Ramaseshan, R. Electrospun nanofibers: solving global issues. *Materials Today*. 9, 40-50, **2006**.
- [99]Schneiderman, S, Zhang, L, Fong, H and Menkhous, TJ. Surface-functionalized electrospun carbon nanofiber mats as an innovative type of protein adsorption/purification medium with high capacity and high throughput. *Journal of Chromatography A*. 1218, 8989-8995, **2011**.
- [100]Sueyoshi, Y, Fukushima, C and Yoshikawa, M. Molecularly imprinted nanofiber membranes from cellulose acetate aimed for chiral separation. *Journal of Membrane Science*. 357, 90-97, **2010**.
- [101]Chronakis, IS, Milosevic, B, Frenot, A and Ye, L. Generation of Molecular Recognition Sites in Electrospun Polymer Nanofibers via Molecular Imprinting. *Macromolecules*. 39, 357-361, **2005**.
- [102]Sueyoshi, Y, Utsunomiya, A, Yoshikawa, M, Robertson, GP and Guiver, MD. Chiral separation with molecularly imprinted polysulfone-aldehyde derivatized nanofiber membranes☆. *Journal of Membrane Science*. 401-402, 89-96, **2012**.

- [103]Che, A-F, Liu, Z-M, Huang, X-J, Wang, Z-G and Xu, Z-K. Chitosan-Modified Poly(acrylonitrile-co-acrylic acid) Nanofibrous Membranes for the Immobilization of Concanavalin A. *Biomacromolecules*. 9, 3397-3403, **2008**.
- [104]Zhang, H, Wu, C, Zhang, Y, White, CB, Xue, Y, Nie, H and Zhu, L. Elaboration, characterization and study of a novel affinity membrane made from electrospun hybrid chitosan/nylon-6 nanofibers for papain purification. *J Mater Sci*. 45, 2296-2304, **2010**.
- [105]Ma, Z, Kotaki, M and Ramakrishna, S. Electrospun cellulose nanofiber as affinity membrane. *Journal of Membrane Science*. 265, 115-123, **2005**.
- [106]Ma, Z and Ramakrishna, S. Electrospun regenerated cellulose nanofiber affinity membrane functionalized with protein A/G for IgG purification. *Journal of Membrane Science*. 319, 23-28, **2008**.
- [107]Zhang, L, Menkhaus, TJ and Fong, H. Fabrication and bioseparation studies of adsorptive membranes/felts made from electrospun cellulose acetate nanofibers. *Journal of Membrane Science*. 319, 176-184, **2008**.
- [108]Zhu, J, Yang, J and Sun, G. Cibacron Blue F3GA functionalized poly(vinyl alcohol-co-ethylene) (PVA-co-PE) nanofibrous membranes as high efficient affinity adsorption materials. *Journal of Membrane Science*. 385-386, 269-276, **2011**.
- [109]Yang, Q, Wu, J, Li, J-J, Hu, M-X and Xu, Z-K. Nanofibrous Sugar Sticks Electrospun from Glycopolymers for Protein Separation via Molecular Recognition. *Macromolecular Rapid Communications*. 27, 1942-1948, **2006**.
- [110]Yoshikawa, M, Tanioka, A and Matsumoto, H. Molecularly imprinted nanofiber membranes. *Current Opinion in Chemical Engineering*. 1, 18-26, **2011**.
- [111]Yoshikawa, M, Nakai, K, Matsumoto, H, Tanioka, A, Guiver, MD and Robertson, GP. Molecularly Imprinted Nanofiber Membranes from Carboxylated Polysulfone by Electro Spray Deposition. *Macromolecular Rapid Communications*. 28, 2100-2105, **2007**.
- [112]Yang, H-H, Zhang, S-Q, Tan, F, Zhuang, Z-X and Wang, X-R. Surface Molecularly Imprinted Nanowires for Biorecognition. *Journal of the American Chemical Society*. 127, 1378-1379, **2005**.
- [113]Li, Y, Yin, X-F, Chen, F-R, Yang, H-H, Zhuang, Z-X and Wang, X-R. Synthesis of Magnetic Molecularly Imprinted Polymer Nanowires Using a Nanoporous Alumina Template. *Macromolecules*. 39, 4497-4499, **2006**.
- [114]Wang, H-J, Zhou, W-H, Yin, X-F, Zhuang, Z-X, Yang, H-H and Wang, X-R. Template Synthesized Molecularly Imprinted Polymer Nanotube Membranes for Chemical Separations. *Journal of the American Chemical Society*. 128, 15954-15955, **2006**.
- [115]Ahlemeyer, B, Klumpp, S and Krieglstein, J. Release of cytochrome c into the extracellular space contributes to neuronal apoptosis induced by staurosporine. *Brain Research*. 934, 107-116, **2002**.
- [116]Chen, T, Shao, M, Xu, H, Zhuo, S, Liu, S and Lee, S-T. Molecularly imprinted polymer-coated silicon nanowires for protein specific recognition and fast separation. *Journal of Materials Chemistry*. 22, 3990-3996, **2012**.
- [117]Piperno, S, Tse Sum Bui, B, Haupt, K and Gheber, LA. Immobilization of molecularly imprinted polymer nanoparticles in electrospun poly(vinyl alcohol) nanofibers. *Langmuir : the ACS journal of surfaces and colloids*. 27, 1547-1550, **2011**.
- [118]Chronakis, IS, Jakob, A, Hagström, B and Ye, L. Encapsulation and Selective Recognition of Molecularly Imprinted Theophylline and 17 β -Estradiol

Nanoparticles within Electrospun Polymer Nanofibers. *Langmuir : the ACS journal of surfaces and colloids*. 22, 8960-8965, **2006**.

[119]One-step Electro-spinning/netting Technique for Controllably Preparing Polyurethane Nano-fiber/net. *Macromolecular Rapid Communications*. n/a, **2011**.

[120]Iguchi, M, Yamanaka, S and Budhiono, A. Bacterial cellulose—a masterpiece of nature's arts. *J Mater Sci*. 35, 261-270, **2000**.

[121]Hestrin, S and Schramm, M. Synthesis of cellulose by *Acetobacter xylinum*. 2. Preparation of freeze-dried cells capable of polymerizing glucose to cellulose. *Biochemical Journal*. 58, 345-352, **1954**.

[122]Park, W-I, Kang, M, Kim, H-S and Jin, H-J. Electrospinning of Poly(ethylene oxide) with Bacterial Cellulose Whiskers. *Macromolecular Symposia*. 249-250, 289-294, **2007**.

[123]Klemm, D, Schumann, D, Udhardt, U and Marsch, S. Bacterial synthesized cellulose — artificial blood vessels for microsurgery. *Progress in Polymer Science*. 26, 1561-1603, **2001**.

[124]Ayad, MM and El-Nasr, AA. Adsorption of Cationic Dye (Methylene Blue) from Water Using Polyaniline Nanotubes Base. *The Journal of Physical Chemistry C*. 114, 14377-14383, **2010**.

[125]Yamanaka, S, Watanabe, K, Kitamura, N, Iguchi, M, Mitsuhashi, S, Nishi, Y and Uryu, M. The structure and mechanical properties of sheets prepared from bacterial cellulose. *J Mater Sci*. 24, 3141-3145, **1989**.

[126]Okiyama, A, Motoki, M and Yamanaka, S. Bacterial cellulose IV. Application to processed foods. *Food Hydrocolloids*. 6, 503-511, **1993**.

[127]Chen, S, Zou, Y, Yan, Z, Shen, W, Shi, S, Zhang, X and Wang, H. Carboxymethylated-bacterial cellulose for copper and lead ion removal. *Journal of Hazardous Materials*. 161, 1355-1359, **2009**.

[128]Son, WK, Youk, JH and Park, WH. Antimicrobial cellulose acetate nanofibers containing silver nanoparticles. *Carbohydrate Polymers*. 65, 430-434, **2006**.

[129]Wu, S-C and Lia, Y-K. Application of bacterial cellulose pellets in enzyme immobilization. *Journal of Molecular Catalysis B: Enzymatic*. 54, 103-108, **2008**.

[130]Zaborowska, M, Bodin, A, Bäckdahl, H, Popp, J, Goldstein, A and Gatenholm, P. Microporous bacterial cellulose as a potential scaffold for bone regeneration. *Acta Biomaterialia*. 6, 2540-2547, **2010**.

[131]Bäckdahl, H, Helenius, G, Bodin, A, Nannmark, U, Johansson, BR, Risberg, B and Gatenholm, P. Mechanical properties of bacterial cellulose and interactions with smooth muscle cells. *Biomaterials*. 27, 2141-2149, **2006**.

[132]Charpentier, PA, Maguire, A and Wan, W-k. Surface modification of polyester to produce a bacterial cellulose-based vascular prosthetic device. *Applied Surface Science*. 252, 6360-6367, **2006**.

[133]Fu, L, Zhang, J and Yang, G. Present status and applications of bacterial cellulose-based materials for skin tissue repair. *Carbohydrate Polymers*. 92, 1432-1442, **2013**.

[134]Jantarat, C, Tangthong, N, Songkro, S, Martin, GP and Suedee, R. S-Propriolol imprinted polymer nanoparticle-on-microsphere composite porous cellulose membrane for the enantioselectively controlled delivery of racemic propranolol. *International Journal of Pharmaceutics*. 349, 212-225, **2008**.

[135]Harbury, HA and Loach, PA. Oxidation-linked Proton Functions in Heme Octa- and Undecapeptides from Mammalian Cytochrome c. *Journal of Biological Chemistry*. 235, 3640-3645, **1960**.

- [136]Dickerson, RE. The cytochrome fold and the evolution of bacterial energy metabolism. *Scientific American* 242, 136-153, **1980**.
- [137]Fuku, X, Iftikar, F, Hess, E, Iwuoha, E and Baker, P. Cytochrome c biosensor for determination of trace levels of cyanide and arsenic compounds. *Analytica Chimica Acta*. 730, 49-59, **2012**.
- [138]Fisher, WR, Taniuchi, H and Anfinsen, CB. On the Role of Heme in the Formation of the Structure of Cytochrome c. *Journal of Biological Chemistry*. 248, 3188-3195, **1973**.
- [139]Vinu, A, Murugesan, V, Tangermann, O and Hartmann, M. Adsorption of Cytochrome c on Mesoporous Molecular Sieves: Influence of pH, Pore Diameter, and Aluminum Incorporation. *Chemistry of Materials*. 16, 3056-3065, **2004**.
- [140]Pullerits, R, Bokarewa, M, Jonsson, IM, Verdrengh, M and Tarkowski, A. Extracellular cytochrome c, a mitochondrial apoptosis-related protein, induces arthritis. *Rheumatology*. 44, 32-39, **2005**.
- [141]Margoliash, E. Primary structure and evolution of cytochrome c *Proceedings of the National Academy of Sciences*. 50, 672-679, **1963**.
- [142]Jiang, X and Wang, X. Cytochrome c -mediated apoptosis. *Annual Review of Biochemistry*. 73, 87-106, **2004**.
- [143]Satchell, MA, Lai, Y, Kochanek, PM, Wisniewski, SR, Fink, EL, Siedberg, NA, Berger, RP, DeKosky, ST, P David, A and Clark, RSB. Cytochrome c, a biomarker of apoptosis, is increased in cerebrospinal fluid from infants with inflicted brain injury from child abuse. *J Cereb Blood Flow Metab*. 25, 919-927, **2005**.
- [144]Renz, A, Berdel, WE, Kreuter, M, Belka, C, Schulze-Osthoff, K and Los, M. Rapid extracellular release of cytochrome c is specific for apoptosis and marks cell death in vivo. *Blood*. 98, 1542-1548, **2001**.
- [145]Anderson, JE, Hansen, LL, Mooren, FC, Post, M, Hug, H, Zuse, A and Los, M. Methods and biomarkers for the diagnosis and prognosis of cancer and other diseases: Towards personalized medicine. *Drug Resistance Updates*. 9, 198-210, **2006**.
- [146]Radhakrishnan, J, Wang, S, Ayoub, IM, Kolarova, JD, Levine, RF and Gazmuri, RJ. Circulating levels of cytochrome c after resuscitation from cardiac arrest: a marker of mitochondrial injury and predictor of survival. *American Journal of Physiology - Heart and Circulatory Physiology*. 292, H767-H775, **2007**.
- [147]Adachi, N, Hirota, M, Hamaguchi, M, Okamoto, K, Watanabe, K and Endo, F. Serum cytochrome c level as a prognostic indicator in patients with systemic inflammatory response syndrome. *Clinica Chimica Acta*. 342, 127-136, **2004**.
- [148]Barczyk, K, Kreuter, M, Pryjma, J, Booy, EP, Maddika, S, Ghavami, S, Berdel, WE, Roth, J and Los, M. Serum cytochrome c indicates in vivo apoptosis and can serve as a prognostic marker during cancer therapy. *International Journal of Cancer*. 116, 167-173, **2005**.
- [149]Santra, S, Kaittanis, C and Perez, JM. Cytochrome c Encapsulating Theranostic Nanoparticles: A Novel Bifunctional System for Targeted Delivery of Therapeutic Membrane-Impermeable Proteins to Tumors and Imaging of Cancer Therapy. *Molecular Pharmaceutics*. 7, 1209-1222, **2010**.
- [150]Kim, SK, Foote, MB and Huang, L. The targeted intracellular delivery of cytochrome C protein to tumors using lipid-apolipoprotein nanoparticles. *Biomaterials*. 33, 3959-3966, **2012**.
- [151]Pilkington, GJ, Parker, K and Murray, SA. Approaches to mitochondrially mediated cancer therapy. *Seminars in Cancer Biology*. 18, 226-235, **2008**.

- [152]Hartmann, M. Ordered Mesoporous Materials for Bioadsorption and Biocatalysis. *Chemistry of Materials*. 17, 4577-4593, **2005**.
- [153]O'Brien, SM, Sloane, RP, Thomas, ORT and Dunnill, P. Characterisation of non-porous magnetic chelator supports and their use to recover polyhistidine-tailed T4 lysozyme from a crude E. coli extract. *Journal of Biotechnology*. 54, 53-67, **1997**.
- [154]Gekko, K and Hasegawa, Y. Compressibility-structure relationship of globular proteins. *Biochemistry*. 25, 6563-6571, **1986**.
- [155]Kimhi, O and Bianco-Peled, H. Study of the Interactions between Protein-Imprinted Hydrogels and Their Templates. *Langmuir : the ACS journal of surfaces and colloids*. 23, 6329-6335, **2007**.
- [156]Kriz, D, Ramström, O and Mosbach, K. Peer Reviewed: Molecular Imprinting: New Possibilities for Sensor Technology. *Analytical Chemistry*. 69, 345A-349A, **1997**.
- [157]Haupt, K and Mosbach, K. Molecularly Imprinted Polymers and Their Use in Biomimetic Sensors. *Chemical Reviews*. 100, 2495-2504, **2000**.
- [158]Vashist, SKV, Priya. Recent advances in quartz crystal microbalance-based sensors. *Journal of Sensors*. 2011, 1-13, **2011**.
- [159]Ayad, MM, Prastomo, N, Matsuda, A and Stejskal, J. Sensing of silver ions by nanotubular polyaniline film deposited on quartz-crystal in a microbalance. *Synthetic Metals*. 160, 42-46, **2010**.
- [160]Van Quy, N, Minh, VA, Van Luan, N, Hung, VN and Van Hieu, N. Gas sensing properties at room temperature of a quartz crystal microbalance coated with ZnO nanorods. *Sensors and Actuators B: Chemical*. 153, 188-193, **2011**.
- [161]Diltemiz, SE, Hür, D, Ersöz, A, Denizli, A and Say, R. Designing of MIP based QCM sensor having thymine recognition sites based on biomimicking DNA approach. *Biosensors and Bioelectronics*. 25, 599-603, **2009**.
- [162]Say, R, Gültekin, A, Özcan, AA, Denizli, A and Ersöz, A. Preparation of new molecularly imprinted quartz crystal microbalance hybride sensor system for 8-hydroxy-2'-deoxyguanosine determination. *Analytica Chimica Acta*. 640, 82-86, **2009**.
- [163]Liu, F, Liu, X, Ng, S-C and Chan, HS-O. Enantioselective molecular imprinting polymer coated QCM for the recognition of l-tryptophan. *Sensors and Actuators B: Chemical*. 113, 234-240, **2006**.
- [164]Lin, T-Y, Hu, C-H and Chou, T-C. Determination of albumin concentration by MIP-QCM sensor. *Biosensors and Bioelectronics*. 20, 75-81, **2004**.
- [165]Buchatip, S, Ananthanawat, C, Sithigorngul, P, Sangvanich, P, Rengpipat, S and Hoven, VP. Detection of the shrimp pathogenic bacteria, *Vibrio harveyi*, by a quartz crystal microbalance-specific antibody based sensor. *Sensors and Actuators B: Chemical*. 145, 259-264, **2010**.
- [166]Pirondini, L and Dalcanale, E. Molecular recognition at the gas-solid interface: a powerful tool for chemical sensing. *Chemical Society Reviews*. 36, 695-706, **2007**.
- [167]Wang, XD, Bin ; Yu, Jianyong; Wang, Moran; Pan, Fukui. A highly sensitive humidity sensor based on a nanofibrous membrane coated quartz crystal microbalance. *Nanotechnology*. 21, 1-6, **2010**.
- [168]Hu, W, Chen, S, Liu, L, Ding, B and Wang, H. Formaldehyde sensors based on nanofibrous polyethyleneimine/bacterial cellulose membranes coated quartz crystal microbalance. *Sensors and Actuators B: Chemical*. 157, 554-559, **2011**.

- [169]Hu, W, Chen, S, Zhou, B, Liu, L, Ding, B and Wang, H. Highly stable and sensitive humidity sensors based on quartz crystal microbalance coated with bacterial cellulose membrane. *Sensors and Actuators B: Chemical*. 159, 301-306, **2011**.
- [170]Ishihara, T and Arakawa, T. Detection of cytochrome C by means of surface plasmon resonance sensor. *Sensors and Actuators B: Chemical*. 91, 262-265, **2003**.
- [171]El Kirat, K, Bartkowski, M and Haupt, K. Probing the recognition specificity of a protein molecularly imprinted polymer using force spectroscopy. *Biosensors and Bioelectronics*. 24, 2618-2624, **2009**.
- [172]Svensson, A, Nicklasson, E, Harrah, T, Panilaitis, B, Kaplan, DL, Brittberg, M and Gatenholm, P. Bacterial cellulose as a potential scaffold for tissue engineering of cartilage. *Biomaterials*. 26, 419-431, **2005**.
- [173]Garipcan, B and Denizli, A. A Novel Affinity Support Material for the Separation of Immunoglobulin G from Human Plasma. *Macromolecular Bioscience*. 2, 135-144, **2002**.
- [174]Hemdan, ES, Zhao, YJ, Sulkowski, E and Porath, J. Surface topography of histidine residues: a facile probe by immobilized metal ion affinity chromatography. *Proceedings of the National Academy of Sciences*. 86, 1811-1815, **1989**.
- [175]Bodhibukkana, C, Srichana, T, Kaewnopparat, S, Tangthong, N, Bouking, P, Martin, GP and Suedee, R. Composite membrane of bacterially-derived cellulose and molecularly imprinted polymer for use as a transdermal enantioselective controlled-release system of racemic propranolol. *Journal of Controlled Release*. 113, 43-56, **2006**.
- [176]Owen, RO and Chase, HA. Direct purification of lysozyme using continuous counter-current expanded bed adsorption. *Journal of Chromatography A*. 757, 41-49, **1997**.
- [177]Akgöl, S, Türkmen, D and Denizli, A. Cu(II)-incorporated, histidine-containing, magnetic-metal-complexing beads as specific sorbents for the metal chelate affinity of albumin. *Journal of Applied Polymer Science*. 93, 2669-2677, **2004**.
- [178]Luo, W, Zhu, L, Yu, C, Tang, H, Yu, H, Li, X and Zhang, X. Synthesis of surface molecularly imprinted silica micro-particles in aqueous solution and the usage for selective off-line solid-phase extraction of 2,4-dinitrophenol from water matrixes. *Analytica Chimica Acta*. 618, 147-156, **2008**.
- [179]Denizli, A, Alkan, M, Garipcan, B, Özkara, S and Pişkin, E. Novel metal-chelate affinity adsorbent for purification of immunoglobulin-G from human plasma. *Journal of Chromatography B*. 795, 93-103, **2003**.
- [180]Garside, P and Wyeth, P. Identification of Cellulosic Fibres by FTIR Spectroscopy: Thread and Single Fibre Analysis by Attenuated Total Reflectance. *Studies in Conservation*. 48, 269-275, **2003**.
- [181]Ding, B, Wang, X, Yu, J and Wang, M. Polyamide 6 composite nano-fiber/net functionalized by polyethyleneimine on quartz crystal microbalance for highly sensitive formaldehyde sensors. *Journal of Materials Chemistry*. 21, 12784-12792, **2011**.
- [182]Verheyen, E, Schillemans, JP, van Wijk, M, Demeniex, M-A, Hennink, WE and van Nostrum, CF. Challenges for the effective molecular imprinting of proteins. *Biomaterials*. 32, 3008-3020, **2011**.
- [183]Yu, C and Mosbach, K. Influence of mobile phase composition and cross-linking density on the enantiomeric recognition properties of molecularly imprinted polymers. *Journal of Chromatography A*. 888, 63-72, **2000**.

- [184]Andersson, HS, Karlsson, JG, Piletsky, SA, Koch-Schmidt, A-C, Mosbach, K and Nicholls, IA. Study of the nature of recognition in molecularly imprinted polymers, II : Influence of monomer–template ratio and sample load on retention and selectivity. *Journal of Chromatography A*. 848, 39-49, **1999**.
- [185]Jie, Z and Xiwen, H. Study of the nature of recognition in molecularly imprinted polymer selective for 2-aminopyridine. *Analytica Chimica Acta*. 381, 85-91, **1999**.
- [186]Yano, K, Tanabe, K, Takeuchi, T, Matsui, J, Ikebukuro, K and Karube, I. Molecularly imprinted polymers which mimic multiple hydrogen bonds between nucleotide bases. *Analytica Chimica Acta*. 363, 111-117, **1998**.
- [187]Mijangos, I, Navarro-Villoslada, F, Guerreiro, A, Piletska, E, Chianella, I, Karim, K, Turner, A and Piletsky, S. Influence of initiator and different polymerisation conditions on performance of molecularly imprinted polymers. *Biosensors and Bioelectronics*. 22, 381-387, **2006**.
- [188]Bereli, N, Saylan, Y, Uzun, L, Say, R and Denizli, A. I-Histidine imprinted supermacroporous cryogels for protein recognition. *Separation and Purification Technology*. 82, 28-35, **2011**.
- [189]Derazshamshir, A, Baydemir, G, Andac, M, Say, R, Galaev, IY and Denizli, A. Molecularly Imprinted PHEMA-Based Cryogel for Depletion of Hemoglobin from Human Blood. *Macromolecular Chemistry and Physics*. 211, 657-668, **2010**.
- [190]Pan, G, Guo, Q, Cao, C, Yang, H and Li, B. Thermo-responsive molecularly imprinted nanogels for specific recognition and controlled release of proteins. *Soft Matter*. 9, 3840-3850, **2013**.
- [191]Uzun, L, Say, R, Ünal, S and Denizli, A. Hepatitis B surface antibody purification with hepatitis B surface antibody imprinted poly(hydroxyethyl methacrylate-N-methacryloyl-L-tyrosine methyl ester) particles. *Journal of Chromatography B*. 877, 181-188, **2009**.
- [192]Chen, Z, Hua, Z, Xu, L, Huang, Y, Zhao, M and Li, Y. Protein-responsive imprinted polymers with specific shrinking and rebinding. *Journal of Molecular Recognition*. 21, 71-77, **2008**.
- [193]García-Calzón, JA and Díaz-García, ME. Characterization of binding sites in molecularly imprinted polymers. *Sensors and Actuators B: Chemical*. 123, 1180-1194, **2007**.
- [194]Umpleby li, RJ, Baxter, SC, Rampey, AM, Rushton, GT, Chen, Y and Shimizu, KD. Characterization of the heterogeneous binding site affinity distributions in molecularly imprinted polymers. *Journal of Chromatography B*. 804, 141-149, **2004**.
- [195]Emir, S, Say, R, Yavuz, H and Denizli, A. A New Metal Chelate Affinity Adsorbent for Cytochrome c. *Biotechnology Progress*. 20, 223-228, **2004**.
- [196]Abudiab, T and Beitle Jr, RR. Preparation of magnetic immobilized metal affinity separation media and its use in the isolation of proteins. *Journal of Chromatography A*. 795, 211-217, **1998**.
- [197]Türkmen, D, Yavuz, H and Denizli, A. Synthesis of tentacle type magnetic beads as immobilized metal chelate affinity support for cytochrome c adsorption. *International Journal of Biological Macromolecules*. 38, 126-133, **2006**.
- [198]Çimen, D and Denizli, A. Immobilized metal affinity monolithic cryogels for cytochrome c purification. *Colloids and Surfaces B: Biointerfaces*. 93, 29-35, **2012**.
- [199]Tamahkar, E, Bereli, N, Say, R and Denizli, A. Molecularly imprinted supermacroporous cryogels for cytochrome c recognition. *Journal of Separation Science*. 34, 3433-3440, **2011**.

- [200]Yang, H-H, Zhang, S-Q, Yang, W, Chen, X-L, Zhuang, Z-X, Xu, J-G and Wang, X-R. Molecularly Imprinted Sol-Gel Nanotubes Membrane for Biochemical Separations. *Journal of the American Chemical Society*. 126, 4054-4055, **2004**.
- [201]Yan, C-L, Lu, Y and Gao, S-Y. Coating lysozyme molecularly imprinted thin films on the surface of microspheres in aqueous solutions. *Journal of Polymer Science Part A: Polymer Chemistry*. 45, 1911-1919, **2007**.
- [202]Zhang, M, Huang, J, Yu, P and Chen, X. Preparation and characteristics of protein molecularly imprinted membranes on the surface of multiwalled carbon nanotubes. *Talanta*. 81, 162-166, **2010**.
- [203]Chen, H, Kong, J, Yuan, D and Fu, G. Synthesis of surface molecularly imprinted nanoparticles for recognition of lysozyme using a metal coordination monomer. *Biosensors and Bioelectronics*. 53, 5-11, **2014**.
- [204]Xie, C, Liu, B, Wang, Z, Gao, D, Guan, G and Zhang, Z. Molecular Imprinting at Walls of Silica Nanotubes for TNT Recognition. *Analytical Chemistry*. 80, 437-443, **2007**.
- [205]Tang, H, Zhou, W and Zhang, L. Adsorption isotherms and kinetics studies of malachite green on chitin hydrogels. *Journal of Hazardous Materials*. 209-210, 218-225, **2012**.
- [206]Wu, C-H. Adsorption of reactive dye onto carbon nanotubes: Equilibrium, kinetics and thermodynamics. *Journal of Hazardous Materials*. 144, 93-100, **2007**.
- [207]Kuo, C-Y, Wu, C-H and Wu, J-Y. Adsorption of direct dyes from aqueous solutions by carbon nanotubes: Determination of equilibrium, kinetics and thermodynamics parameters. *Journal of Colloid and Interface Science*. 327, 308-315, **2008**.
- [208]Turner, NW, Jeans, CW, Brain, KR, Allender, CJ, Hlady, V and Britt, DW. From 3D to 2D: A Review of the Molecular Imprinting of Proteins. *Biotechnology Progress*. 22, 1474-1489, **2006**.
- [209]Larsericdotter, H, Oscarsson, S and Buijs, J. Thermodynamic analysis of lysozyme adsorbed to silica. *Journal of Colloid and Interface Science*. 276, 261-268, **2004**.
- [210]Min, M, Shen, L, Hong, G, Zhu, M, Zhang, Y, Wang, X, Chen, Y and Hsiao, BS. Micro-nano structure poly(ether sulfones)/poly(ethyleneimine) nanofibrous affinity membranes for adsorption of anionic dyes and heavy metal ions in aqueous solution. *Chemical Engineering Journal*. 197, 88-100, **2012**.
- [211]Andaç, M, Baydemir, G, Yavuz, H and Denizli, A. Molecularly imprinted composite cryogel for albumin depletion from human serum. *Journal of Molecular Recognition*. 25, 555-563, **2012**.
- [212]Baydemir, G, Andaç, M, Perçin, I, Derazshamshir, A and Denizli, A. Molecularly imprinted composite cryogels for hemoglobin depletion from human blood. *Journal of Molecular Recognition*. 27, 528-536, **2014**.
- [213]Liu, J, Yang, K, Deng, Q, Li, Q, Zhang, L, Liang, Z and Zhang, Y. Preparation of a new type of affinity materials combining metal coordination with molecular imprinting. *Chemical Communications*. 47, 3969-3971, **2011**.
- [214]Fu, G, He, H, Chai, Z, Chen, H, Kong, J, Wang, Y and Jiang, Y. Enhanced Lysozyme Imprinting Over Nanoparticles Functionalized with Carboxyl Groups for Noncovalent Template Sorption. *Analytical Chemistry*. 83, 1431-1436, **2011**.
- [215]Sharma, S and Agarwal, GP. Interactions of Proteins with Immobilized Metal Ions: A Comparative Analysis Using Various Isotherm Models. *Analytical Biochemistry*. 288, 126-140, **2001**.

- [216]Gai, Q-Q, Qu, F, Zhang, T and Zhang, Y-K. The preparation of bovine serum albumin surface-imprinted superparamagnetic polymer with the assistance of basic functional monomer and its application for protein separation. *Journal of Chromatography A*. 1218, 3489-3495, **2011**.
- [217]Li, F, Li, J and Zhang, S. Molecularly imprinted polymer grafted on polysaccharide microsphere surface by the sol-gel process for protein recognition. *Talanta*. 74, 1247-1255, **2008**.
- [218]Maneerung, T, Tokura, S and Rujiravanit, R. Impregnation of silver nanoparticles into bacterial cellulose for antimicrobial wound dressing. *Carbohydrate Polymers*. 72, 43-51, **2008**.
- [219]Özgür, E, Yılmaz, E, Şener, G, Uzun, L, Say, R and Denizli, A. A new molecular imprinting-based mass-sensitive sensor for real-time detection of 17 β -estradiol from aqueous solution. *Environmental Progress & Sustainable Energy*. 32, 1164-1169, **2013**.
- [220]Sener, G, Ozgur, E, Yılmaz, E, Uzun, L, Say, R and Denizli, A. Quartz crystal microbalance based nanosensor for lysozyme detection with lysozyme imprinted nanoparticles. *Biosensors and Bioelectronics*. 26, 815-821, **2010**.

APPENDIX

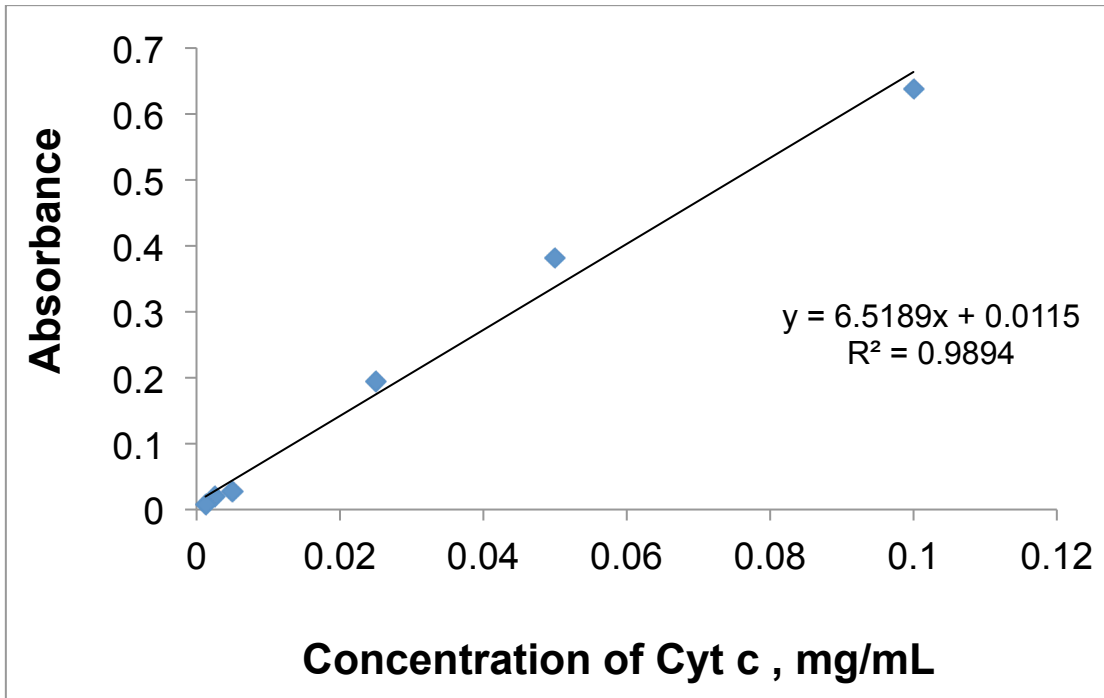


Figure 1. Calibration curve for spectrophotometric analysis of cytochrome c.

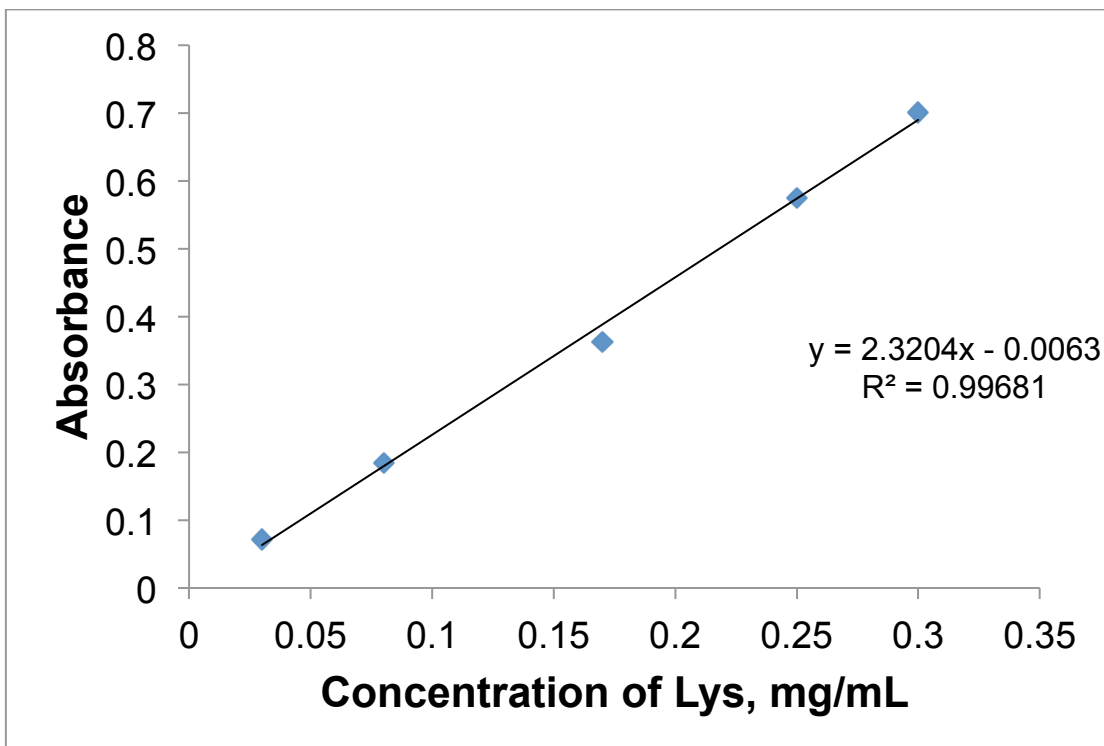


Figure 2. Calibration curve for spectrophotometric analysis of lysozyme.

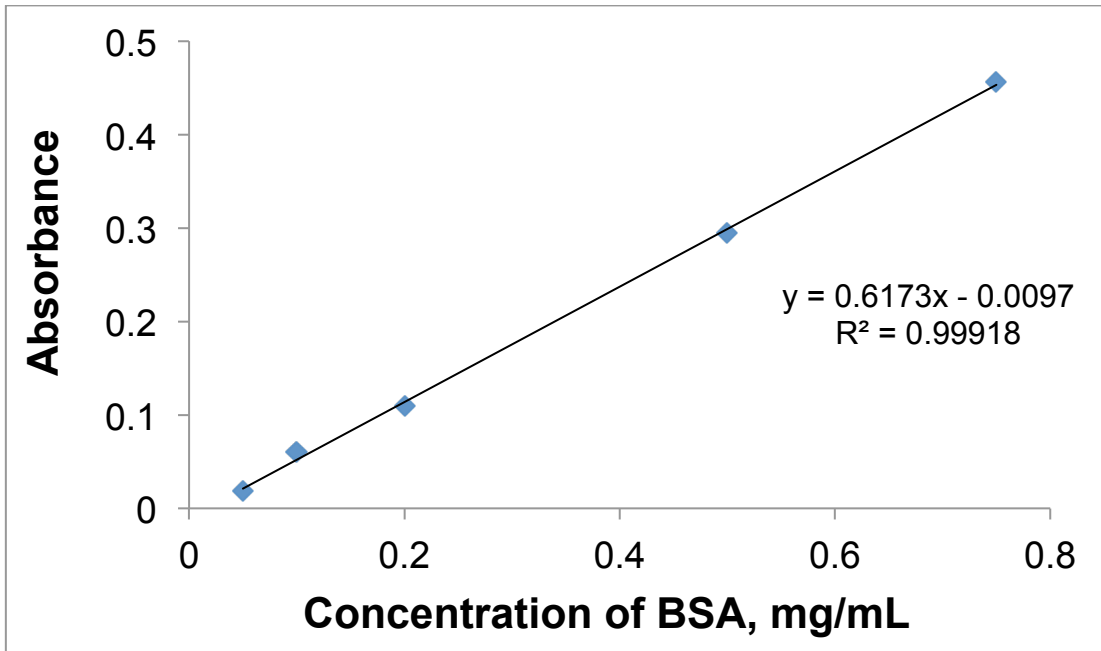


Figure 3. Calibration curve for spectrophotometric analysis of BSA.

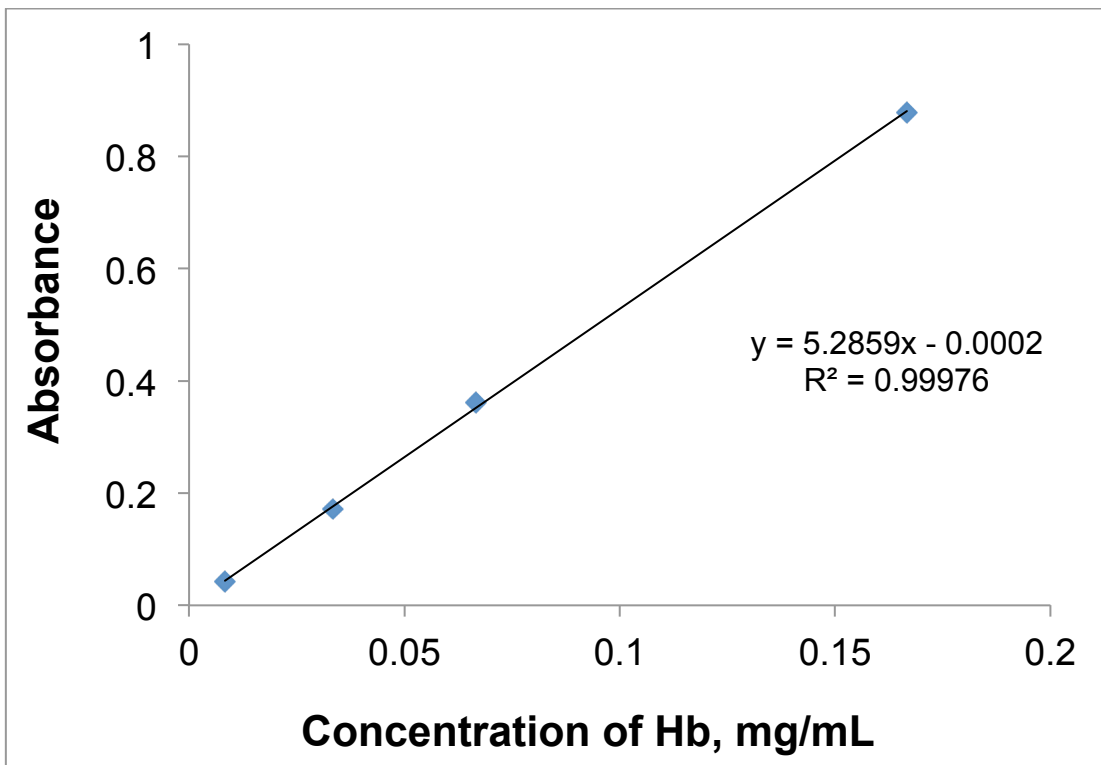


Figure 4. Calibration curve for spectrophotometric analysis of Hb.

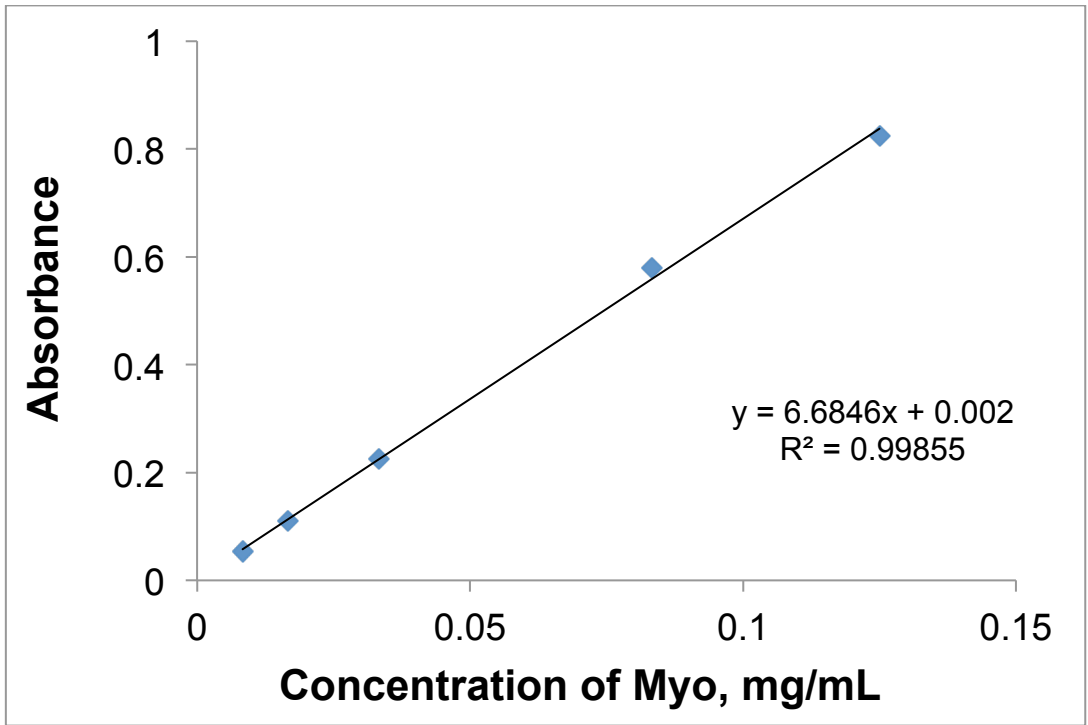


Figure 5. Calibration curve for spectrophotometric analysis of Myo.

CURRICULUM VITAE

Credentials

Name, Surname : Emel Tamahkar Irmak
Place of Birth : Edirne
Marital Status : Married
E-mail : emeltamahkar@gmail.com
Adress : Hitit University, Faculty of Engineering,
Department of Chemical Engineering

Education

High School : 1999-2002 Edirne Anadolu Lisesi
BSc. : 2003-2007 Hacettepe University, Department of Chemical
Engineering, Ankara
MSc. : 2007-2009 Hacettepe University, Graduate School of
Science and Engineering, Bioengineering Division, Ankara
PhD. : 2009-2014 Hacettepe University, Graduate School of
Science and Engineering, Bioengineering Division, Ankara

Foreign Languages

English (fluent), French (beginner).

Work Experience

2009- Research Assistant,
Hitit University, Faculty of Engineering, Department of
Chemical Engineering, Çorum

Areas of Experiences

Molecular imprinting, protein imprinting, bacterial cellulose nanofibers

Projects and Budgets

-

Publications

1. E. Tamahkar, C. Babaç, T. Kutsal, E. Pişkin, A. Denizli 'Bacterial Cellulose Nanofibers for Albumin Depletion from Human Serum' *Process Biochemistry*, 2010, 45, 1713.
2. V. Karakoç, D. Türkmen, E. Tamahkar, T. Kutsal, A. Denizli 'Bacterial Cellulose Nanofibers for Dye-Affinity Adsorption of Recombinant Human Interferon- α ' *Protein Purification*, Ed: Benitez M., Aguirre V. 2011.
3. E. Tamahkar, N. Bereli, M. Andaç, R. Say, A. Denizli 'Molecularly Imprinted Supramacroporous Cryogels for Cytochrome c Recognition' *Journal of Separation Science*, 2011, 34, 3433.
4. C. Weber, T. Neuwirth, K. Kempe, B. Özkahraman, E. Tamahkar, H. Mert, R.C. Becer, U.S. Schuber '2-Isopropenyl-2-Oxazoline: A Versatile Monomer for Functionalization of Polymers Obtained via Raft' *Macromolecules*, 2012, 45, 20.
5. E. Tamahkar, A. Denizli 'Metal Ion Coordination Interactions for Biomolecule Recognition' *Hittite Journal of Science and Engineering*, 2014, 1, 21.

Oral and Poster Presentations

1. E. Tamahkar, M. Baksphour, M. Andaç, A. Denizli, Molecularly Surface-Imprinted Nanofibers for Hemoglobin Depletion. ASPM 2013, Bled, Slovenia, 3-5 April 2013. (Poster presentation)
2. E. Tamahkar, T. Kutsal, A. Denizli, Yüzey baskılanmış bakteriyel selüloz nanofiberler ile sitokrom c saflaştırılması. 7. Ulusal Afinite Teknikleri Kongresi. İzmir, Turkey, 13-15 September 2013. (Poster presentation)
3. E. Tamahkar, T. Kutsal, A. Denizli, Surface Imprinted Cellulose Nanofibers. 13th Mediterranean Congress of Chemical Engineering. Barcelona, Spain, 30 September-3 October 2014. (Poster presentation)